TRANSIENT LIQUID PHASE BONDING OF DISSIMILAR SINGLE CRYSTAL SUPERALLOYS

By

OLUWADAMILOLA AKANDE OLATUNJI

A thesis submitted to the faculty of Graduate Studies of the University of Manitoba
in partial fulfillment of the requirements for the degree of

MASTER OF SCIENCE

Department of Mechanical and Manufacturing Engineering,
University of Manitoba, Winnipeg
Canada

ACKNOWLEDGEMENT

First and foremost, I want to thank my supervisor, Professor M.C Chaturvedi for giving me the privilege to work under his advisement. I am extremely grateful to him for his intellectual guidance and support towards the success of this thesis project. I also want to express my sincere appreciation to my co-supervisor, Professor O.A Ojo. His support, guidance, encouragement and inspiring contributions have been precious throughout the entire period of this research program.

I gratefully acknowledge the funding sources that made my research program possible. Thanks to the University of Manitoba for the award of the International Graduate Student Entrance Scholarship, and NSERC for their financial support.

Special Thanks to my departmental colleagues, Niyousha Esmaeil, Dr. Lina Zhang, Guilherme Damaceno, Gbenga Asala and Arjun. I thank God for giving me the opportunity to meet and work with great people like you. Thank You Dr. Lina for helping me with some analyses. I also want to appreciate Mike Boskwick and Trevor Smith for their technical assistance in the use of some facilities at the Material Characterization Laboratory of the University of Manitoba.

I thank my dad, mum and brother for their tender loving care and unceasing prayers. Above all, I am forever grateful to God for giving me wisdom, knowledge and understanding to complete this program.

DEDICATION

I dedicate this master's thesis to

My parents for all their support and love and putting me through the best education possible

.

LIST OF ACRONYMS

TLP: Transient Liquid Phase,

TG: Temperature Gradient,

SX: Single Crystal,

LSD: Liquid-State Diffusion,

SSD: Solid-State Diffusion,

HAZ: Heat Affected Zone,

MPD: Melting Point Depressant,

DS: Directionally Solidified,

FCC: Face Centered Cubic,

OAW: Oxyacetylene Welding,

SMAW: Shielded Metal Arc Welding,

PAW: Plasma Arc Welding,

GTAW: Gas – Tungsten Arc Welding,

GMAW: Gas – Metal Arc Welding,

FCAW: Flux Cored Arc Welding,

SAW: Submerged Arc Welding,

ESW: Electro Slag Welding,

EBW: Electron Beam Welding,

LSB: Laser Beam Welding,

RT: Room Temperature,

TG-TLP: Temperature Gradient Transient Liquid Phase,

PTLP: Partial Transient Liquid Phase,

EDM: Electro – Discharge Machine,

EDS: Energy Dispersive Spectrometer,

EBSD: Electron Backscattered Diffraction,

OIM: Orientation Image Microscopy,

SEM: Scanning Electron Microscope,

OM: Optical Microscope,

AEW: Average Eutectic Width

FEM: Finite Element Model,

DAZ: Diffusion Affected Zone,

ISZ: Isothermally Solidified Zone,

ISW (CMSX-4): Isothermal Solidified Width adjacent to the CMSX-4 substrate,

ISW (IN738): Isothermal Solidified Width adjacent to the IN738 substrate,

IPF: Inverse Pole Figure.

ABSTRACT

Transient liquid phase (TLP) bonding has proven to be the preferred method for joining extremely difficult-to-weld advanced materials, including similar and dissimilar superalloys. In this work, an approach that combines experiments and theoretical simulations are used to investigate the effect of temperature gradient (TG) in a vacuum furnace on the temperature distribution in TLP bonded samples. When joining similar materials by this technique, the simulated results with experimental verifications show that, irrespective of where the samples are placed inside the vacuum furnace, a TG in the furnace can translate into a symmetric temperature distribution in bonded samples provided the diffusion direction is parallel to the source of heat emission. In addition, the effects of TLP bonding parameters on the joint microstructure were investigated during the joining of nickel-based IN738 and CMSX-4 single crystal (SX) superalloys. An increase in holding time and reduction in gap size reduces the width of eutectic product that forms within the joint region. It was also found that Liquid-state diffusion (LSD) can occur and have significant effects on the microstructure of dissimilar TLP bonded joints even though its influence is often ignored during TLP bonding. The occurrence of LSD produced single crystal joint when a SX and polycrystal substrate were bonded. This formation of a SX joint which cannot be exclusively produced by solid-state diffusion has not been previously reported in the literature.

TABLE OF CONTENTS

TABLE OF FIGURES

LIST OF TABLES

CHAPTER 1 – INTRODUCTION

1.1 Background information

Superalloys are widely used in high temperature applications. These high performance alloys offer excellent mechanical strength, stress rupture, resistance to creep, corrosion and oxidation, as well as microstructural stability [1] [2] [3] [4]. They have austenitic FCC structure, and are all classified in terms of Nickel, Cobalt and Iron base alloy elements [3]. When manufacturing these alloys, a variety of strengthening mechanisms such as solid-solution strengthening and precipitation hardening are used [5].

In the hot sections of aero and industrial gas turbine engines, Nickel (Ni) - based superalloys are developed to meet stringent demands and ensure increased performance. Joining is necessary when manufacturing these alloys, and a significant amount of work has been done on a number of different types of techniques that can be used to successfully fabricate them. Notwithstanding the high temperature capabilities of these alloys, the parts are prone to damage during service, therefore, considering the high cost of newly manufactured superalloy components, it is generally more economically sensible to also repair the damaged parts rather than completely replacing them. Welding is one of the most commonly applied techniques for joining structural materials. Unfortunately, the high susceptibility to cracking, predominantly in the heat affected zone (HAZ) has been a major weldability problem when using this technique to join superalloy parts containing high contents of Aluminum and Titanium. As such, these superalloys are generally considered as difficult-to-weld materials. However, a process known as Transient Liquid Phase (TLP) bonding has evolved as a preferred technique that is capable of joining several difficult to weld alloys due to a number of technological and economic advantages. This joining technique, which was developed by Duval et al. [6] combines the added advantage of

brazing and diffusion bonding. It involves sandwiching an interlayer material containing a melting point depressant (MPD) element such as Boron, Silicon, Hafnium or Phosphorus between the substrate materials; such that, after subjecting the assembly to a high temperature, the interlayer melts and forms a liquid phase. Thereafter, a bond region is formed as the liquid disappears isothermally and solidifies as a result of interdiffusion between the interlayer and base materials. This solidified bond zone can exhibit matching chemistry with the substrate. Thus, the problem of weld cracking can be avoided by using the TLP bonding for difficult-to-weld superalloys. In aero-engines (Figure 1.0) and power generation turbines, the desire to join dissimilar superalloys either during manufacturing or repair becomes increasingly important. However, it is generally more difficult to join dissimilar materials than joining similar materials (or superalloys with minor differences in compositions). When joining dissimilar superalloys, welding methods face significant problems due to a number of factors including the differences in the composition and melting temperatures of materials to be joined. Consequently, this limitations among others can be overcome by using TLP bonding. Microstructure controls the properties of engineering materials, however, the influence of various TLP bonding process parameters on the joint microstructure of dissimilarly bonded superalloys is not adequately understood.

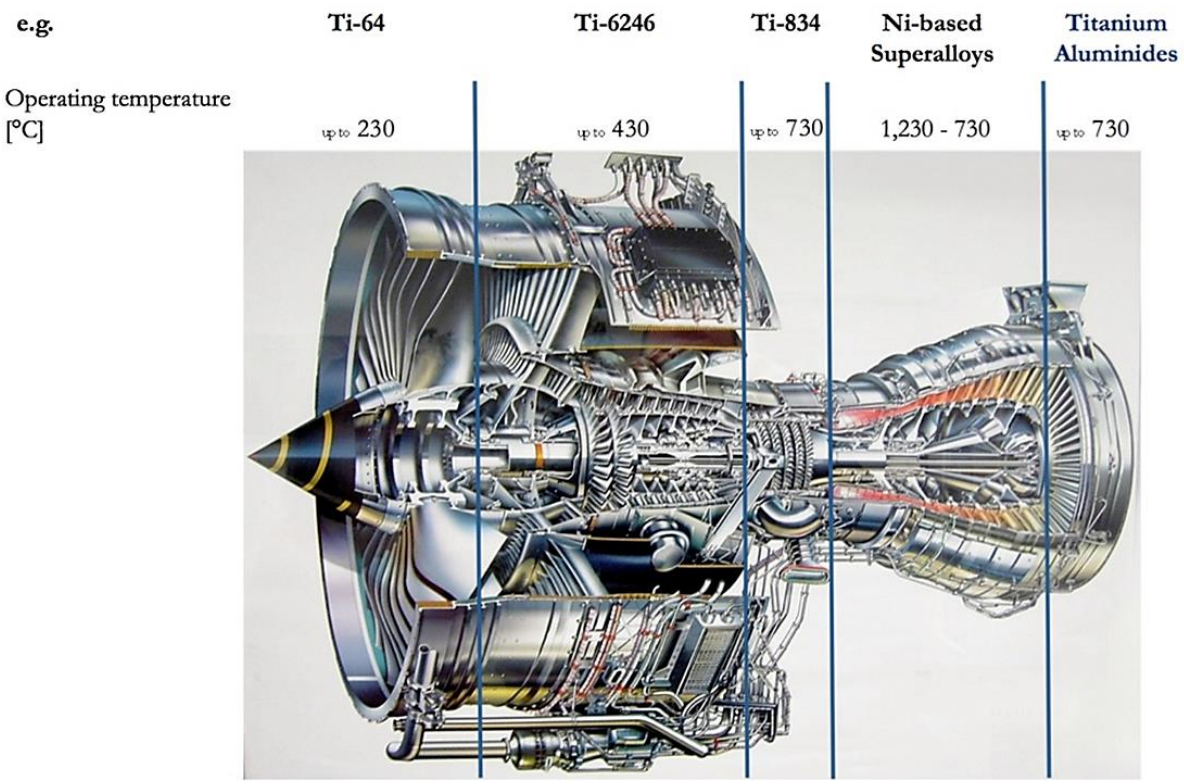

Figure 1.0 - Jet turbine engine [7] M. France, FRANCE-METALLURGIE, 2015

1.2 Research objective

The objective of this research work is to study the effect of bonding parameters such as gap size, bonding temperature and holding time on the joint microstructure of TLP bonded dissimilar Ni-based IN738 & CMSX-4 SX superalloys.

1.3 Major findings

To achieve the objective of this work, since the joint microstructure is also dependent on the temperature distribution in the sample, simulated thermal analysis by ANSYS workbench is carried out to understand the effect of temperature gradient in a vacuum furnace on the temperature distribution in TLP bonding samples. The results show that, irrespective of where the samples to be bonded are placed inside the vacuum furnace, the formation of a symmetrical temperature distribution along the joint region can be obtained provided the sample is oriented such that the solidification direction is parallel to the emitting sources. However, in order to minimize temperature gradient in TLP bonded samples, the results of the simulation also show that the best position to place samples inside the vacuum furnace is at the centre of the furnace where limited temperature gradient in the sample can be achieved.

Subsequently, experimental investigations on the influence of various bonding temperature, holding time and gap size on the joint microstructure of IN738 and CMSX-4 SX superalloys is carried out. The results showed that, longer holding time and reduced gap size decreases the eutectic width within the joint region. The isothermal solidification rate initially increases with an increase in bonding temperature up to a certain temperature beyond which it start to decrease. Furthermore, an important factor that affect the microstructure of TLP joint is the use of composite powder composition. It is found that a composite powder mixture (combination of

base alloy and filler alloy powder) in the ratio 3:7 resulted in the formation of a complete isothermally solidified joint within a shorter time frame relative to 100% filler powder used in conventional TLP bonding.

When joining dissimilar superalloys by this technique, contrary to conventional TLP bonding mechanism which assumes that the influence of liquid-state diffusion (LSD) can be generally ignored; LSD is found to affect joint microstructure. The occurrence of LSD results in the formation of a SX joint between a SX substrate bonded to a polycrystalline substrate, which cannot be obtained exclusively by solid-state diffusion. However, in the presence of LSD, the rate of isothermal solidification is still controlled by diffusion taking place in the solid-state.

1.4 Thesis structure

- Chapter 1 provides the introduction, which consists of the background information, research objective, major contributions, and thesis structure.
- Chapter 2 provides a literature review on the chemical, physical and mechanical properties of the IN738/CMSX-4 alloys, as well as the advantages and disadvantages associated with the various joining and repairing techniques applied onto metals and alloys. The TLP bonding process and the bonding parameters used for the bonding process are also discussed.
- In Chapter 3, the materials and metallographic equipment for analysis purposes used in this research work as well as the sequence of the sample preparation prior to and after bonding are described in details.

- Chapter 4 is divided into two parts. Part 1 contains the result and discussion of the simulated thermal analysis with the use of ANSYS Workbench program. Part 2 is the result and discussion on the effects of the bonding parameters and LSD on the joint microstructure.
- Finally, the summary and conclusions of this research work, along with recommended future work are presented in Chapter 5.

CHAPTER 2 - LITERATURE REVIEW

Single crystal (SX) superalloys have been commonly utilized in high pressure turbine sections of aero turbine engines as well as in industrial gas turbine engines due to their exceptional performance and properties. Improvements in SX superalloys have mostly been on increasing creep resistance, higher temperature capability and improved fuel-use efficiency of turbine engines. Therefore, with the current trend of the use of Ni–based SX superalloys for critical components in aerospace and other related industries, there is the demand and need to develop the right techniques for joining dissimilar SX superalloys, so as to further increase their usage in aerospace applications.

This review begins by discussing the metallurgy of superalloys in terms of the primary constituent phases of the most novel Ni-based superalloys, followed by the disparity in chemical composition between two different types of superalloys, IN738 and CMSX – 4, as well as the roles of some the main alloying elements used in these two Ni-based superalloys. Thereafter, since the economic rationale relating the costs for repair or replacement of superalloy materials suggests that it is generally more reasonable to repair damaged superalloys rather than completely replacing them, the joining techniques that can be used for dissimilar metals and alloys are discussed. The various joining methods will be exemplified in terms of the strengths and weaknesses of each technique that had been previously employed in joining metals and alloys; either to themselves or to others. Finally, a general overview of the concept and use of TLP bonding as an alternative means and promising approach of joining superalloys will be discussed in this chapter.

2.1 Physical metallurgy of superalloys

Superalloys are undeniably outstanding materials. For some decades, their usage has been popular in the aircraft industry and industrial gas turbines due to the fact that they are considered reliable and cost effective materials that have high temperature capability and withstand stress conditions. They can be further categorized into three different forms, namely; 1) polycrystalline, 2) directionally solidified (DS) polycrystalline and 3) SX superalloys. For example, the alloys used for turbine discs are often manufactured in poly-crystal form while it is typical to cast blades in the DS or SX form due to their increased creep properties. Iron Ni-based superalloys are used at lower temperatures, while cobalt (Co)- based superalloys may be used in place of Ni-based superalloys depending on the substantive strength that is needed as well as the type of corrosive attack that is expected [8]. However, among these three groups of superalloys, namely, Co-, Ni- and iron Ni-based, the Ni-based superalloys are the primary high temperature alloys most often used in the critical hot sections of aircraft engines. The chemical, physical and mechanical properties in terms of high temperature strength, oxidation resistivity and high fatigue among others are the optimal properties of this class of superalloys. These alloys are described with a gamma matrix, which accommodates a significant amount of solid solution strengthening elements, such as Co, chromium (Cr), molybdenum (Mo), Al and tantalum (Ta). Also, the large volume fraction of gamma prime (**Ni_3 (Al, Ti)**) precipitates coherently bond the matrix and results in the hardening of most Ni – based superalloys, thereby, acting as the main strength provider [9] [10]. Besides the gamma matrix and gamma prime phases, the microstructure of an ideal Ni-based superalloy also consists of a gamma-gamma prime eutectic phase, carbides (typically MC, M_6C and $M_{23}C_6$ – due to high carbon contents of combinations

with refractory elements like Ti, Ta, niobium (Nb) or tungsten (W)), as well as borides which basically form as a result of the segregated boron particles [10].

2.2 Review of the base materials

2.2.1 IN738 superalloy

IN738 is a vacuum melted and cast precipitation hardened Ni-based superalloy with excellent high temperature creep-rupture strength combined with hot corrosion resistance. This alloy is largely used in industrial gas turbine engine components such as blades, guide vanes and integral wheels [8]. Two versions of the cast IN738 alloy are produced: a low carbon version designated as IN738LC (C ~ 0.09 – 0.13 wt %) and a high carbon version (C ~ 0.15 – 0.20 wt. %). Low carbon is needed in this alloy for improved castability in larger sections. Tensile and stress-rupture properties are not affected by the lower carbon content [11]. Changes in certain variables, such as the composition of the alloying elements, service exposure and final heat treatment can affect the complex microstructure of IN738 superalloys. This superalloy, just like other common Ni-based superalloys, consists of an Ni-based austenitic face-centered cubic (FCC) gamma phase matrix (with a random distribution of different species of atoms) plus a collection of secondary phases. The polycrystalline form of this alloy has well serrated grain boundaries which makes it distinct, unlike the SX IN738 superalloys which have no grain boundaries.

2.2.1.1 Strengthening mechanisms for IN738

The high strength of this alloy is due to the following mechanisms:

1. solid-solution strengthening from Cr, Mo, W, Ti, Al, Nb and Co;
2. precipitation hardening from a gamma prime phase that consists of **Ni_3 (Al, Ti);** and

3. grain boundary strengthening by carbides.

2.2.1.1.1 Solid- solution strengthening

Co, Cr, Mo, Ti, Al, Nb and zirconium are all solid-solution strengtheners in IN738 superalloys. These elements vary with Ni composition in atomic diameter and concentration. As such, the changes in the lattice parameter depend on the atomic diameter of different species which can be related to the hardening observed in the IN738 alloy.

2.2.1.1.2 Gamma prime

Gamma prime precipitation is the primary high temperature strengthening phase in IN738. The composition of this phase in IN738 [12] has been suggested to be given by: $(Ni_{.922}Co_{.058}Cr_{.017}Mo_{.002}W_{.0020})_3(Al_{.518}Ti_{.352}Ta_{.046}Nb_{.41}W_{.014}Cr_{.027})$. The gamma matrix has an FCC crystal structure, and the gamma prime is a Ni_3 **(Al, Ti)** type of intermetallic phase with an ordered FCC structure with lattice parameters close to those of gamma. Yet, the mismatch due to the differences in lattice parameters between the gamma and the gamma prime phases is widely known to have indicative importance on the morphology of the gamma prime precipitates as well as the mechanical strength of the alloy phase. Figure 1.1 shows the structures of the γ and γ' phases. A gamma prime phase in an IN738 alloy, just like any other Ni-based superalloy, is generally cuboidal in shape. With increasing γ'' mismatch, the shape changes in the order of spherical (0 to +/- 0.2% mismatch), globular, blocky, and cuboidal (mismatch of about +/- 0.5% to 1%) [13]. Besides the lattice mismatch between γ and γ', the precipitation strengthening due to the γ' particles also depends on the precipitate order, precipitate size as well as volume fraction [8]

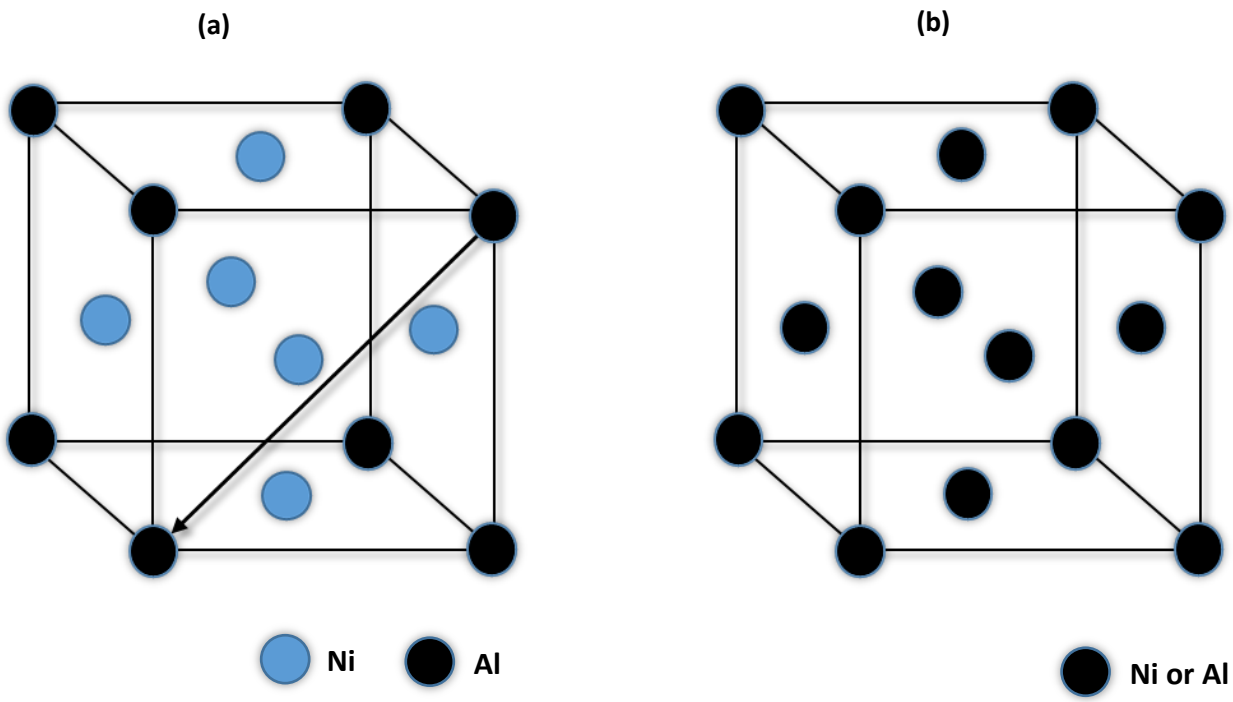

Figure 1.1 - The crystal lattice structures of: a) Ni3Al (ϒI phase) and b) NiAl (ϒ phase)

2.2.1.1.3 Carbides

Characteristically, carbides tend to have high hardness, good electrical and thermal conductivities, as well as high stability. IN738 superalloys with high and low carbon contents are known to have nominal carbon compositions of 0.17 wt. % and 0.11 wt.% respectively. Therefore, a significant amount of carbides, the majority of which are the MC type, are formed both transgranularly and intergranularly in as-cast structures. It has been suggested by Garosshen et al [12] that MC carbides have the following formula: $(Ti_{0.5},Ta_{0.2},Nb_{0.2},W_{0.04},Mo_{0.03},Cr_{0.02})C$. However, any free carbon that is not used in the formation of MC type carbides either during heat treatment or service will tend to precipitate out as free $M_{22}C_6$ and/or M_6C carbides [11]. In addition, carbides tend to increase IN738's strength by stabilizing the grain boundaries contrary to excessive shear, but the principal strengthening precipitate phase in this superalloy is gamma prime. Table 1.1 shows the compositional ranges of the primary alloying inclusions in Ni – based superalloys, as well as the nominal chemical composition of IN738 and CMSX – 4 superalloys [14] [15] [16]**.**

2.2.2 CMSX – 4 superalloys

SX CMSX – 4 is a second generation Ni-based superalloy which has been broadly reviewed and reported in the literature [17] [18] [19] [14] [20]. This alloy is hardened by a gamma prime particle content of about 70 vol% and contains approximately 3 wt.% Re. Generally, the inclusion of Re has a profound effect on superalloy properties because it causes the formation of a directional and incompressible Ni – Re bond that impedes vacancy migration [14].

Table 1.1 - a) Compositional ranges of primary alloying additions in Ni-based superalloys [15]; b) Nominal composition in Wt. % of Inconel 738 and CMSX-4 base alloys [14] [16]

a)

ELEMENTS	Cr	Mo, W	Al	Ti	Co	Nb	Ta	Re	Ni
RANGE, %(Ni-based)	5 - 25	0 - 12	0 - 6	0 - 6	0 - 20	0 - 5	0 - 12	0 - 6	- - -

b)

ELEMENT	High Carbon IN-738C	Low Carbon IN-738LC	CMSX-4
Carbon	0.17	0.11	—
Cobalt	8.5	8.5	9.6
Chromium	16	16	6.5
Molybdenum	1.75	1.75	0.6
Tungsten	2.6	2.6	6.4
Tantalum	1.75	1.75	6.5
Niobium	0.9	0.9	—
Aluminum	3.4	3.4	5.6
Titanium	3.4	3.4	1
Boron	0.01	0.01	—
Zirconium	0.1	0.05	—
Iron	LAP	LAP	—
Manganese	LAP	LAP	—
Silicon	LAP	LAP	—
Hafnium	—	—	0.1
Rhenium	—	—	3
Sulfur	LAP	LAP	—
Nickel	Balance	Balance	Balance

LAP: Low as possible

This Re bearing alloy has been widely employed in the rotating blade section following the combustion chamber in aircraft engines as well as in industrial gas turbine applications. Their exposure to notable combinations of increased temperature strengths as well as increased creep, fatigue and corrosion has been extensively examined based on the aforementioned applications of this material [21] [22]**.**

CMSX – 4 has a two phase gamma/gamma prime microstructure. This microstructure is segregated into core regions with gamma/gamma prime eutectics and dendritic patterns. In addition, the CMSX-4 superalloy has a complex microstructure, and is characterised by high levels of refractory metals (Mo + Ta + W + Re) greater than 10 wt. %. The solid solution strengthening elements have a slow diffusion rate, and for this reason, the diffusion rate of other alloying elements is reduced during solution heat treatment [14].

The roles of the existing alloying elements in IN738 and CMSX – 4 superalloys are summarized in Table 1.2.

2.3 Joining and repair techniques

Joining techniques refer to the methods used to combine materials for specific applications. In some of the advanced materials (e.g. superalloys), joining is economically feasible due to the high cost of replacements (e.g. $5K USD per blade [23]). Therefore, commercially damaged joints are preferred to be repaired rather than replaced in the aerospace industry.

Table 1.2 - Roles of major alloying elements in IN738 & CMSX-4 superalloys [4]

Effects	Ni - based IN738 & CMSX - 4 super alloys
Solid solution strengtheners.	Co, Cr, Fe, Mo, W, Ta and Re.
Carbide formers.	W, Ta, Ti, Mo, Nb and Cr.
Gamma prime (**$Ni_3(Al,Ti)$**) formers.	Al, Ti.
Raising the solvus temperature of gamma prime.	Co.
Hardening precipitates &/or intermetallics.	Al, Ti and Nb.
Oxidation resistance.	Al, Cr.
Improved creep resistance.	Re.
Grain boundary refiners.	B, Cr and Zr.

Besides, it is also essential to note that joining techniques are employed for the primary fabrication of high performance components. Consequently, a significant number of researchers have been making advances in terms of the techniques that could be utilized for the welding of SXs [24] [25] [26]**.** However, the creation of crack free welds in superalloys could be very challenging. Therefore, the joining of similar or dissimilar high performance alloys in any industrial frame of reference requires carefully determining the joining techniques. Since these kinds of alloys are known to be utilized at elevated temperatures where they should maintain most of their physical and mechanical properties room temperature properties, the joining techniques must be precisely tailored for them to withstand the operating temperatures and environments. Among the various kinds of joining techniques, fusion welding, brazing and diffusion bonding are the most common methods utilized in the industry for adhering materials that need to function at high temperatures. As mentioned in Chapter One, these popular bonding techniques have their respective strengths and weaknesses when applied to superalloys. Here, the advantages and drawbacks associated with various joining techniques are reviewed below.

2.3.1 Adhesive bonding

The use of adhesive technology has been known to provide a large degree of flexibility in designing because it can easily bond virtually all types of thermoplastic and thermosetting materials. Adhesive technology has various advantages, such as lack of susceptibility to crevice corrosion, possibility of joining large surfaces, uniform stress distribution, as well as high dynamic strength among others [27]. The procedure for this technique is structured such that, surface preparation is required prior to the application of an adhesive/glue material which is

always in the form of a liquid, after which the final strength of the adhesive bond is not gained immediately because it requires a period of time for curing.

There is the possibility of adhesively joining metal to metal because little or no heat is required to create the joint. As a result, an added advantage of this technique is that, "the material structures of the adherents to be joined are not macroscopically affected" [27] – which can generally be related to the fact that the application of heat rarely occurs. Ultimately, the disadvantage associated with the use of adhesives is the relatively poor heat resistance of the joint [27] [28]. Therefore, adhesive joints are not known to be suitable for use in service temperatures above 300^0C, thereby making its application as a means for joining either similar or dissimilar superalloys impracticable.

2.3.2 Fusion welding

Fusion welding uses the process of coalescence to make a weld. By using the heat derived from various energy sources, this joining technique involves the melting and subsequent solidification of the joint region during bond creation. As such, it is one of the most important and extensively used welding approach for joining metallic materials. However, this method applies to superalloy materials, especially those that have high Ti and Al contents (> 6% Al + Ti), and result in the development of different zones; namely, the HAZ, weld pool zone and a chill (unaffected base metal) zone within the joint region [29] as shown in Figure 1.2. The unaffected base metal zone that surrounds the HAZ is likely to be in a state of high residual stress due to the shrinkage in the fusion zone. Nonetheless, the microstructure of this zone does not undergo any changes.

In the interest of achieving more optimal joints with greater strength, the use of filler materials with lower melting point temperatures than the components to be joined, as well as the application of pressure, are in some cases effective when using fusion welding [29]**.** The three major types of fusion welding processes are as follows:

1. Gas welding
    - Oxyacetylene welding (OAW)
2. Arc welding
    - Shielded metal arc welding (SMAW)
    - Plasma arc welding (PAW)
    - Gas-tungsten arc welding (GTAW)
    - Gas-metal arc welding (GMAW)
    - Flux-cored arc welding (FCAW)
    - Submerged arc welding (SAW)
    - Electro slag welding (ESW)
3. High-energy beam welding
    - Electron beam welding (EBW)
    - Laser beam welding (LBW)

2.3.2.1 Limitations of fusion welding

Fusion welding is unfavorable for joining superalloy components as the joint microstructure changes when a steep TG develops from the liquefied weld pool in the zone of the colder base metal, as well as the induced residual stress in which the effects indicate micro – fissures in the HAZ region. Even though the chemical composition of the weld filler is carefully determined to

incorporate solid solution strengthening elements like Al and Ti, and then prolonged pre and post bond heat treatments are usually carried out so that the aforementioned problems are avoided, the high heat input which is one of the prerequisites for fusion welding has been reported to have a key role in the detrimental modification of the microstructure of the parent materials in terms of the formation of grains in the fusion zone, grain size coarsening, micro-voids, and mechanical property degradation (especially fatigue resistance) inside the joint region [30] [29]. This prevents the welding of many modern superalloys like IN738 and CMSX – 4. Besides, an inherent limitation which invariably confines the use of fusion welding as a repair process is the difficulty that is mostly related to repair components that have complex geometries since the joint surfaces might not be easily exposed to the heat source. This method is specially problematic when joining dissimilar superalloys due to differences in their melting points. For this reason, fusion welding is also not the right approach for joining IN738 and CMSX – 4 superalloys.

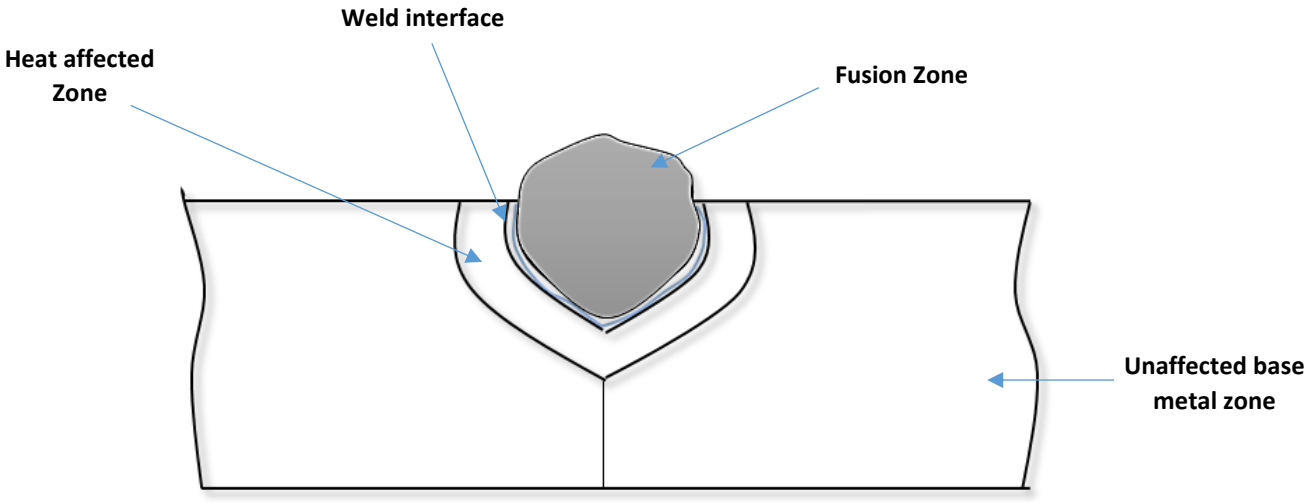

Figure 1.2 - Schematic presentation of several zones in a fusion welded joint.

2.3.3 Soldering and brazing

Soldering of metal pieces is done with the help of filler metal (also called solder), which is melted and distributed through capillary action between the faying surfaces of the parts to be joined. In this case, only the filler metal melts, as there is no melting of the workpiece material. The filler material usually has a melting temperature below 450^0C.

Brazing has the same principle as soldering, but the major difference lies in the fact that the filler material has a melting temperature that is higher than 450^0C. Brazing is one of the most widely accepted techniques for joining materials for over 5000 years [31]**.** There are two different types of brazing processes: 1) conventional brazing used for commercial products and 2) diffusion brazing used for bonding and repairing of gas turbine components. Besides, brazing can take place with little or no dissolution of the parent materials, but the major disadvantage associated with soldering and brazing is that the resultant joints commonly have low strength as compared to welded joints.

Brazing can be advantageous if considered from the viewpoint that components with complex geometries as well as a combination of narrow and wide sections can be consistently brazed together. Also, since brazing can allow the entire assembled part to be increased to the same operating temperature, localized heating which causes distortion in some sections will be avoided, unlike those produced during fusion welding.

2.3.3.1 Diffusion brazing

Conventional brazing among other joining procedures like adhesive bonding and soldering do not have the issues as found in the use of fusion welding since the parent materials as well as their microstructure remain in a solid – state. But such technique can lead to poor mechanical properties within the joint region. As such, high temperature brazing or diffusion brazing has been considered as the most preferable technique for joining Ni-based alloys as well as other high temperature materials. Diffusion brazing consists on joining two substrates such that there is the interdiffusion of atoms across the mating surfaces, which will result in bond formation. The main techniques used to melt braze alloys involve either localized heat application by using a flame torch, through electrical resistance, electrical induction, or the general heat treating of the entire component in a furnace [32] [33] [34] [35]**.** This general heat treating technique is usually conducted under a vacuum of 10^{-3} – 10^{-5} torr or in an inert atmosphere (commonly, with argon, dry hydrogen or helium) so as to avoid the oxidation of the substrates. However, there is the added cost of vacuum brazing equipment, but this can often be justified by the improved joint quality [31].

Therefore, joints with high integrity and the least amount of detrimental effects on the substrates of superalloy materials, without metallurgical discontinuity nor porosity across the interface, as well as an optimal joint when bonding dissimilar materials, are the advantages associated with diffusion brazing. Also, the possibility of the use of automation to control the basic variables of diffusion bonding such as temperature, time, pressure, and filler alloy selection is one of the greatest assets of this technique.

Thus far, some of the limitations linked to the diffusion brazing of materials is the possibility of the incomplete elimination of residual oxides on substrates, lack of reliable data on joint

behavior e.g. fatigue life or fracture toughness; and inadequate methods for non-destructive testing of the quality of joints. However, it is expected that these constraints will be addressed in the future. For instance, brazing defects such as second phase precipitation which is one of the significantly negative effects resultant of Ni-based brazes in high temperatures that arise from excessive gaps or insufficient brazing time have already been addressed by considering TLP diffusion brazing as an alternative to diffusion brazing.

2.3.4 Transient liquid phase bonding

Of particular importance in joining both similar and dissimilar superalloys is TLP bonding, which has been greatly improved and used in practice nowadays. It is an age – old technique in which liquid that fills a joint is due to the transient liquid phase that is produced from the reaction between the filler and the base material. Consequently, TLP bonding has been used to carry out post service repairs of difficult to weld aerospace materials and land – based power generation turbines, which use Ni-based superalloys, metal alloys and composite materials among other types of high temperature materials. This joining process has been applied to the bonding of similar and dissimilar superalloys [6] [36] [37] [38], similar and dissimilar metal alloys [39] [40] [41] as well as composites [42]. TLP bonding was patented by Paulonis et al. in 1971 [43] so as to address the deficiencies identified in the then known bonding techniques that were utilized on Ni – based superalloys since some of the conventional joining techniques such as the laser and tungsten inert gas welding processes in fusion welding have always resulted in the susceptibility of superalloy materials to cracking due to the material brittleness in the fusion zone and HAZ, therefore limiting their applications in the repair of damaged components [44] [30].

2.3.4.1 Advantages and disadvantages of TLP bonding

Generally, difficult to weld alloys including Ni-based superalloys which contain high amounts of Al and Ti have been successfully joined by employing TLP bonding. In essence, this technique is a diffusional induced isothermal solidification process that results in a thin interlayer, which consists of MPD element(s) sandwiched between the faying surfaces of the substrates to be bonded. However, the added advantage of this technique over other joining techniques such as conventional brazing is that the solid – state homogenization following the isothermal solidification of TLP bonded joints can result in joints with mechanical properties and compositions similar to those of the base metal due to a wide range of inter-diffusion of elements between the substrates and the interlayer. As such, the re-melting temperature of the joints will exceed the initial bonding temperature. This technique is suitable for joining dissimilar materials; at the same time, the high thermal stresses associated with fusion welding can be avoided, thereby reducing the susceptibility of the formation of HAZ cracking in the joint region [6] [45]. Since the processing parameters and interlayer design can be tailored for the specific application requirement of a given alloy, TLP bonding also influences the presence of secondary phase precipitates which can reduce the mechanical properties as well as the corrosion and oxidation resistance of the joint. In addition, wide gap TLP bonding allows repair of defects up to 0.1 mm in width. Theoretically, TLP bonded joints have no interface [46]. Yet there is the possibility of the formation of brittle phases within the joint region which have deleterious effects on the chemical and mechanical properties of a joint if complete solidification of the liquid interlayer is not carried out. As such, the brittleness of this phase would make it an undesirable situation especially under design considerations of creep strength and toughness. There are also requirements for long holding times (hours), restriction of high temperatures, and rapid heating

up, which are some of the key weaknesses associated with this technique [46]. Besides these key disadvantageous factors, joints bonded by using TLP bonding can often times perform below expectations due to inappropriate sample configuration/set-up, inadequate filler material in the joint region as well as poor vacuum conditions.

2.3.4.2 TLP bonding setup and cycle

During the setup of TLP bonding, jigs may be used to ensure that sample alignment is maintained during bonding [32]. The setup conventionally focuses on obtaining a thin interlayer with a melting point lower than that of the substrates to which it has been enclosed. One of the widely employed approach in TLP bonding practices is the placement of the interlayer material outside the joint region so that it flows in through capillary action. Although the interlayer materials can have diverse configurations, such as brazing foils (thin/amorphous foils) and brazing pastes, the most utilized materials are those in the powder form.

Based on descriptions in [47] [48] [46], a TLP bonding cycle can be divided into four steps as shown in Figure 1.3. The first step is the bond set-up which is carried out at room temperature (RT). The assembled sample is then heated (on rare occasions in open, nitrogen, hydrogen or nitrogen and hydrogen atmospheres, but in most cases, inside a vacuum furnace) to a specific bonding temperature which is always above the liquidus temperature (T_1) of the interlayer, but below the solidus temperature of the base materials under consideration, so as to produce a liquid in the bond region. At the bonding temperature, the interdiffusion process starts to take place (Step 3). By holding this assembly at the bonding temperature (Step 4), a brazed joint is obtained through isothermal solidification (due to diffusion), which could be with or without the precipitation of unwanted phases depending on the holding time and bonding temperature. After

solidification, the TLP bonding process concludes with the homogenization of the bonded sample which can be obtained at the bonding temperature, or at another suitable heat-treating temperature.

2.3.4.3 TLP bonding kinetics

Based on the preceding steps of the TLP joining process, it has been found that in previous studies, there are inconsistent description of the kinetics (Table 1.3).

Therefore, by building on the different stages reviewed by various researchers as well as using a phase diagram (schematic) of binary eutectic alloy systems as shown in Figure 1.4, the kinetics behind the defined TLP bonding processes by and large include the following.

- **Heating-up stage**

Prior to the heating up stage, Figure 1.5 shows the concentration profile and binary eutectic phase diagram representative of a TLP bonding set-up initially at RT. As illustrated by this figure, the filler alloy has an initial thickness of W_o and initial MPD (boron atoms) composition of $C_{F.}$

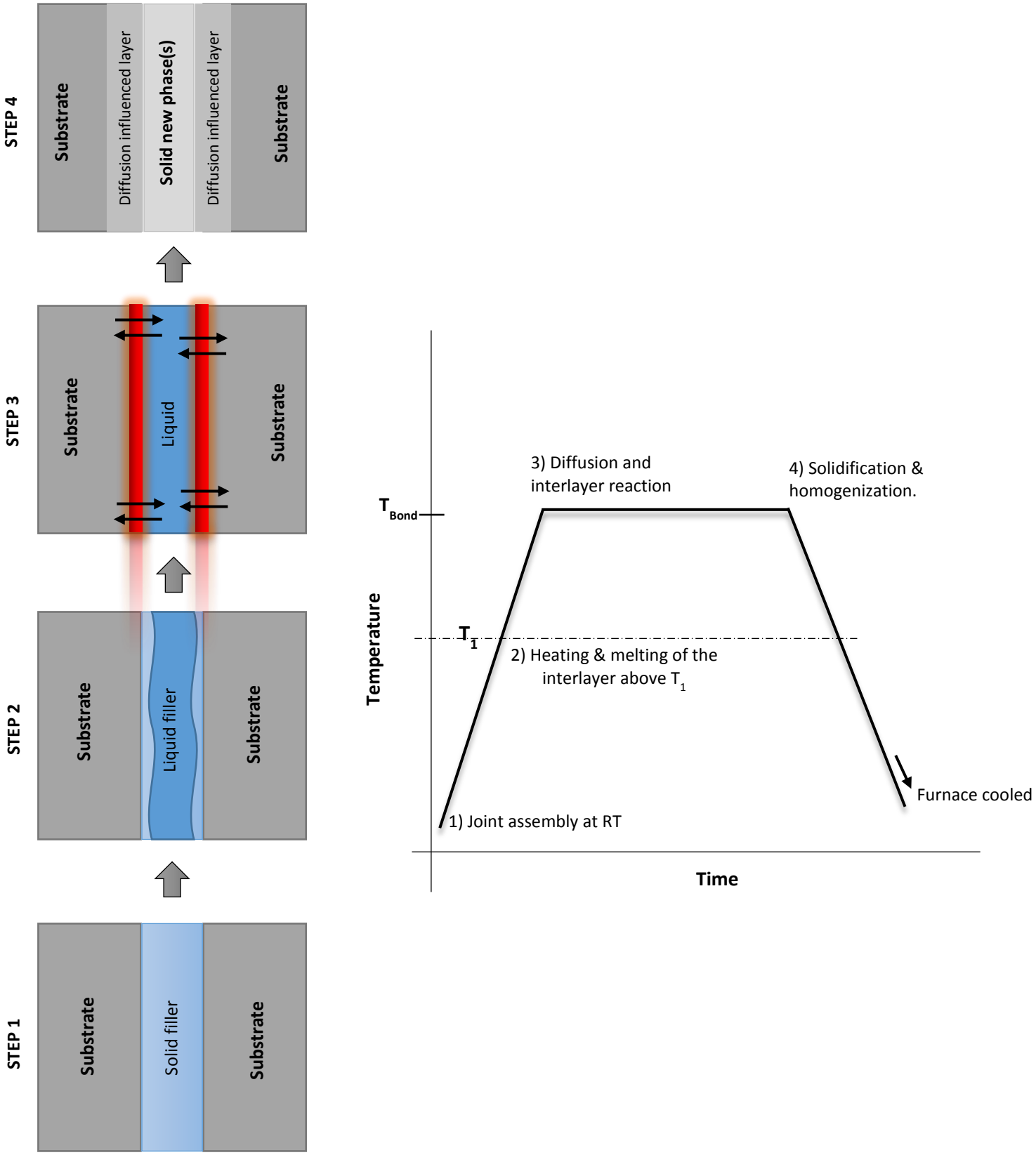

Figure 1.3 - Temperature profile and corresponding steps of joint formation for a TLP bonding brazing cycle

Table 1.3 - TLP bonding kinetics in previous experimental investigations by various research

Authors	Heating up	Substrate Dissolution	Joint widening	Isothermal Solidification	Homogenization
Duvall et al [6]		●		●	●
Tuah-poku et al **[33]**		●	●	●	●
MacDonald & Eager **[46]**	●	●	●	●	●
Zhou et al **[47]**	●	●	●	●	●
Gale & Butt **[61]**		●		●	●

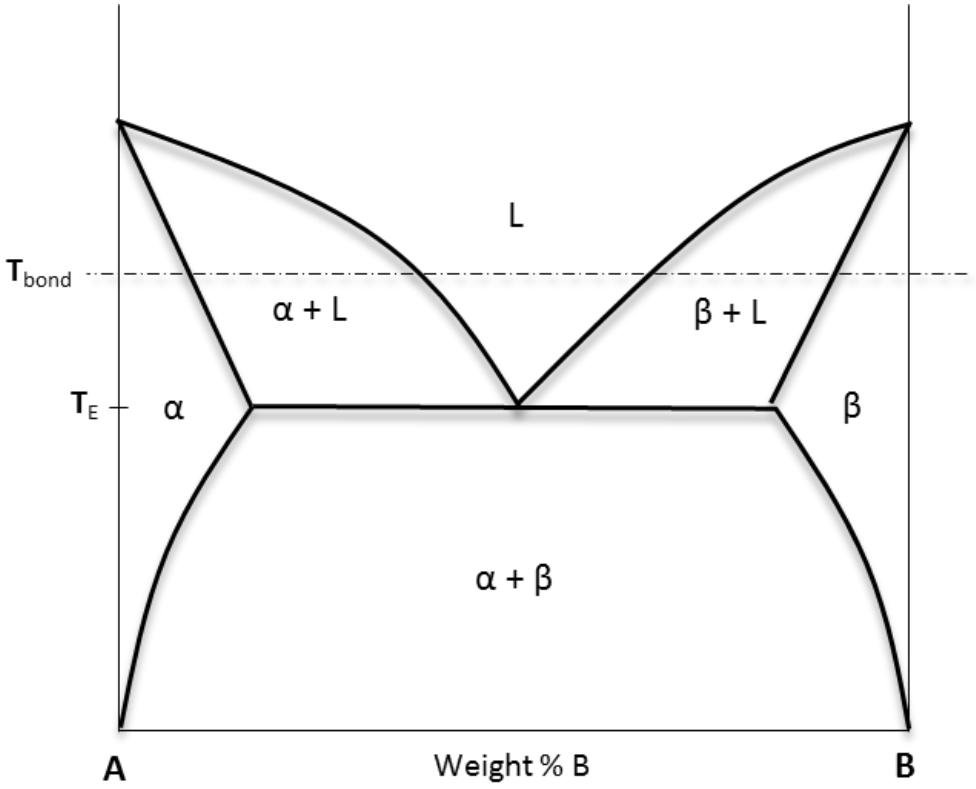

Figure 1.4 - Binary eutectic phase diagram

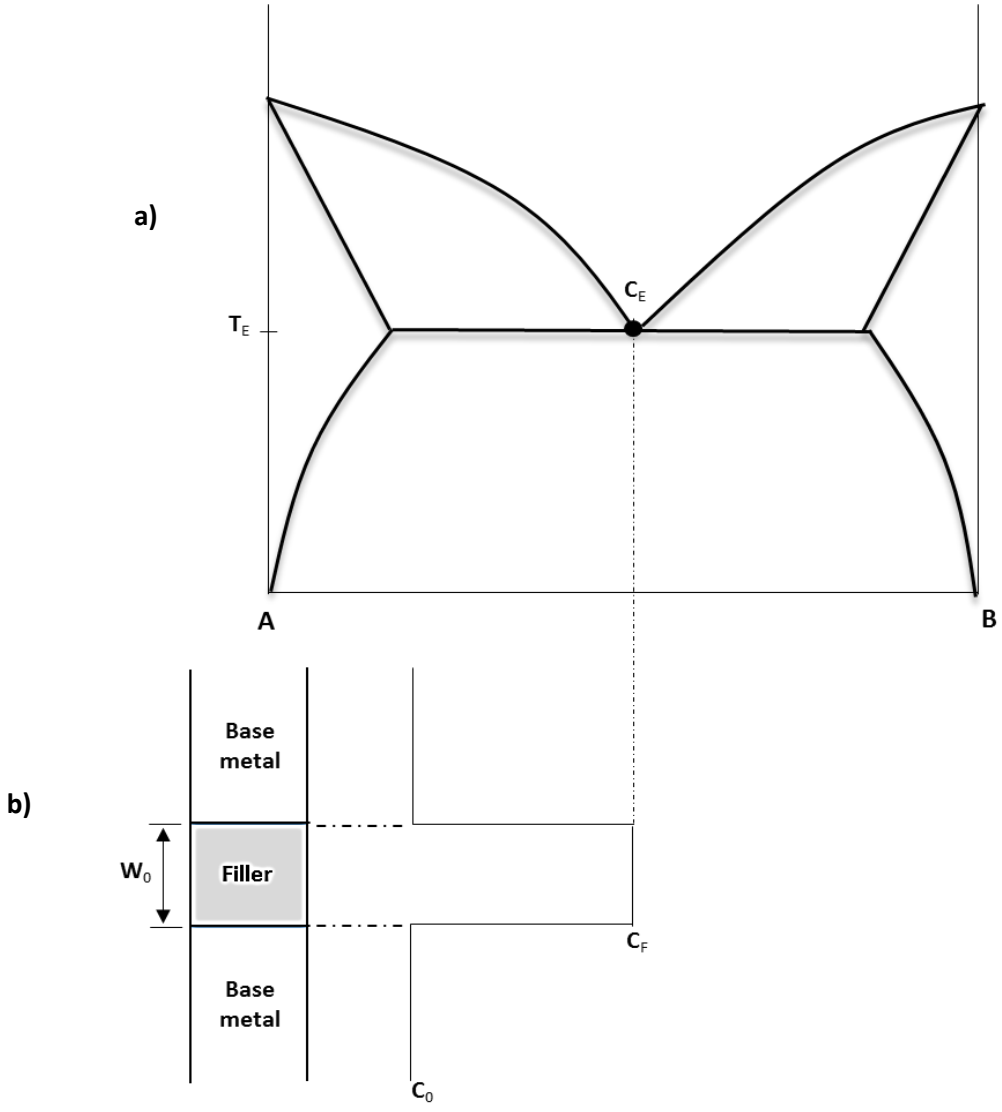

Figure 1.5 - Kinetics of TLP bonding: - initial condition of joint assembly a) Phase diagram schematic, b) bond schematic and composition profile across the joint [61, 50]

However, by simply heating this bond assembly from RT, solid-state inter – diffusion takes place between the substrates and the interlayer material. This causes changes in the elemental concentrations at the joint region as well as added-on changes in the solute concentration at the substrate/filler material interface. Nonetheless, the diffusion coefficient between the substrates and filler material in the solid state along with the heating rate and eutectic temperature influence the amount of elemental diffusion during this stage. Deficient solute concentration in the filler may result from slow rates of heating, thereby causing the solute concentration to be lower than the solidus composition at the bonding temperature. As a result, no liquid will form upon reaching the joining temperature. This problem becomes more critical with very thin filler alloys and low solute concentrations [35]**.**

- **Base metal dissolution and widening stage**

During the TLP bonding process, the total portion of the interlayer is expected to have completely liquefied due to reaching the melting point of the interlayer material. However, in order to ensure that there is complete melting of the interlayer, the bonding temperature is always above the melting point of the interlayer (Figure (1.6a)). As the heating continues to increase from the melting temperature to the bonding temperature, dissolution continues as more of the MPD interlayer or eutectic forming interlayer element diffuse into the base metal. This tends to dissolve (melt back) the substrate, thereby causing widening of the joint region. The aftermath of this dilution and widening of the interlayer brings the compositions of the interlayer and the substrate into local equilibrium. As illustrated in Figure 1.6, W_{MAX} is the maximum dissolution width obtained at a specific bonding temperature, while Cs and C_L represent the equilibrium

solidus and liquidus concentrations of the solutes which equal the solute concentrations in the solid and liquid at the interface.

The dissolution stage becomes very significant in aerospace applications such as honeycomb structures, rocket fins as well as thin foil structures where large base metal dissolution can lower the load bearing capability of thin sections. The extent of base metal dissolution depends on many factors including the initial concentration of the MPD element in the filler ($\mathbf{C_F}$), initial gap size ($\mathbf{W_o}$) and the solubility of the MPD solute in the base material.

- **Isothermal solidification stage**

The isothermal solidification stage is when solidification of the liquid zone occurs because subsequent to the liquid interlayer reaching its maximum width, isothermal diffusion takes place between the substrate and the interlayer materials. It is often considered as the most decisive stage with a completion process that depends on the time needed for the liquid in the joint region to solidify. By that, the duration of this stage is determined by the diffusion of the MPD into the base metal, which is directly influenced by the bonding temperature, as well as the initial thickness of the interlayer. In other words, isothermal solidification occurs until the liquid interlayer is completely dissolved as the solid/liquid interface reverses its direction, with the solidus composition Cs being the governing composition required for the completion of this stage. Figures 1.7a and 1.7b show the schematics of the concentration profiles and binary phase diagrams during and after the isothermal solidification stage.

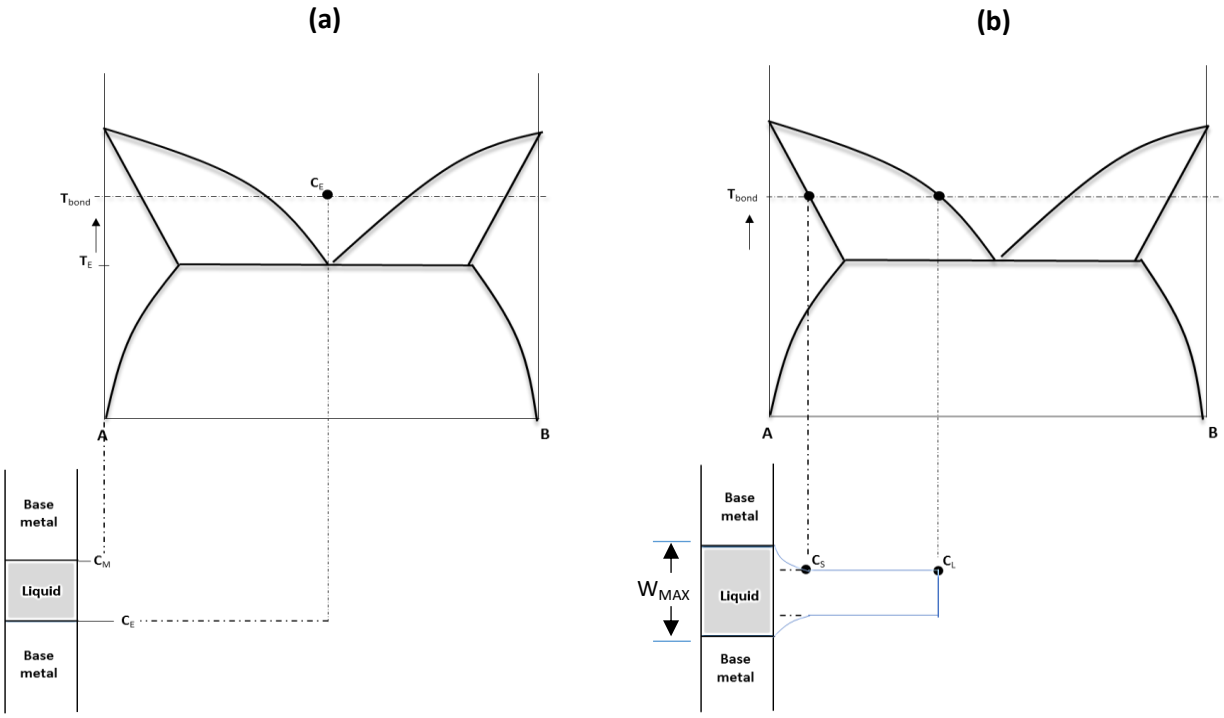

Figure 1.6 - Kinetics of TLP bonding a) Melting of the interlayer, b) Substrate dissolution [61, 50]

Terminologies:-

C_M = Composition of substrates; C_E = Initial (eutectic) composition of the liquid interlayer;

T_B = Bonding temperature; C_S = Solidus composition; C_L = Liquidus composition;

MPD = Melting point depressant; T_a & T_b = Homogenization temperatures above and below T_B

However, during TLP bonding, if sufficient time is not allowed for the liquid in the joint to completely solidify, the residual liquid during cooling will result in detrimental microstructural phases along the joint region.

- **Homogenization stage**

TLP bonded joints undergo homogenization for some predetermined period of time (be it above or below the bonding temperature) so as to cause the solid state redistribution of the solute peaks that prevail at the end of the isothermal solidification stage. Consequently, homogenizing TLP bonded joints for an ample period of time could possibly result in a concentration profile with no gradient on the entirety of the bonded sample (fig 1.7c). Upon cooling, due to the formation of a uniform solute concentration and elimination of secondary phases at the bond line, the added advantage of solid-state homogenization during a TLP bonded process is that the re-melting temperature of a homogenized bond of a TLP joint is always above the initial bonding temperature. Hence, the microstructural and mechanical properties of TLP bonds can approximate those of the substrate materials, unlike brazing [49]. Thus, the result is notably high bond strength since there is the homogeneous distribution of the solute concentration throughout the entirety of the bonded sample.

2.3.4.4 Processing parameters for transient liquid phase bonding

To determine the applicability of the use of TLP bonding is to gauge whether it will work for a period of reasonable operating time.

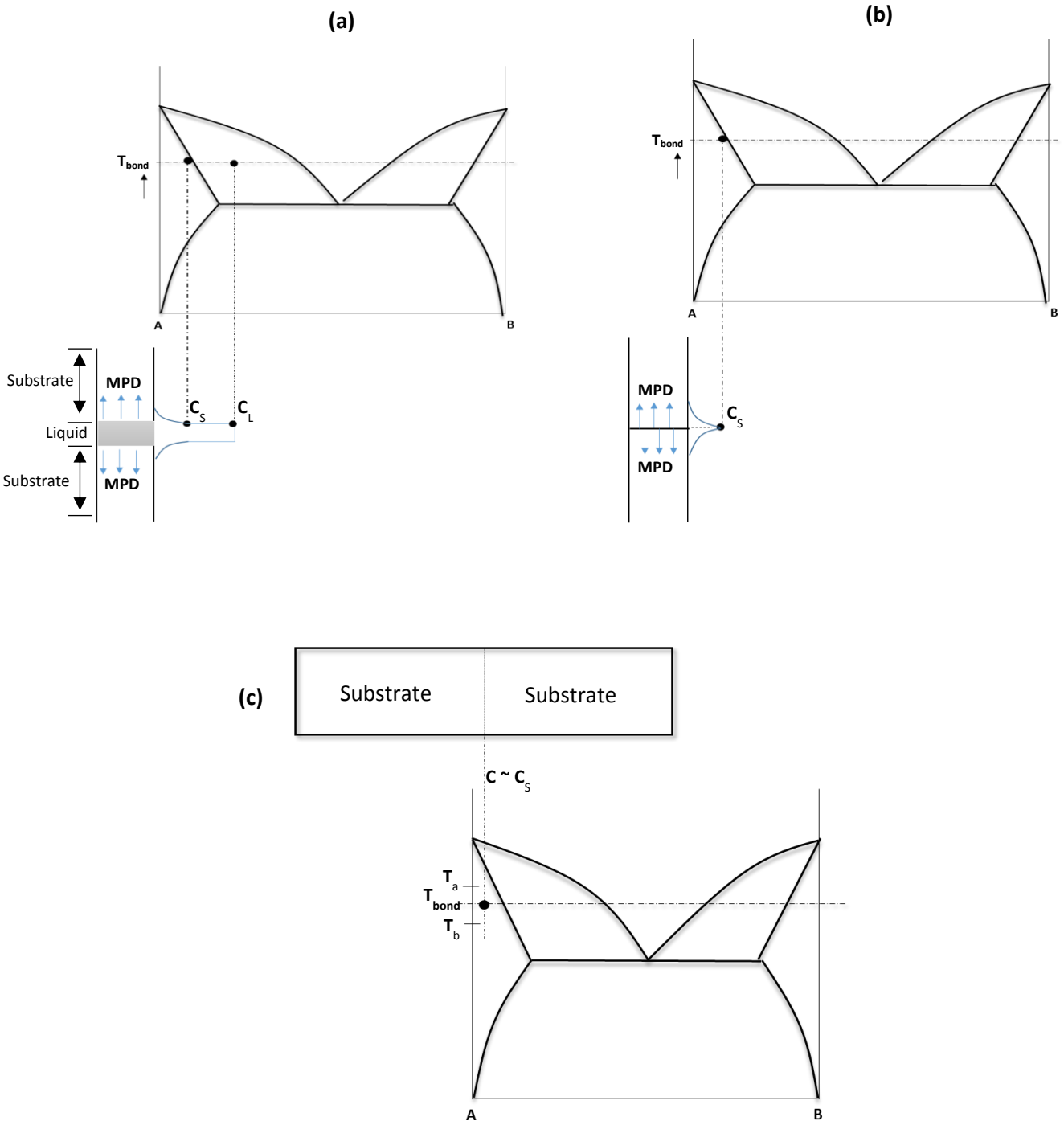

Figure 1.7 - Kinetics of TLP bonding a) During isothermal solidification, b) End of isothermal solidification c) Solid-state homogenization

(Terminologies are the same as shown in figure 7)

From this point of view, the literature shows that proper understanding of the consequences of applicable TLP bonding process parameters in order to obtain joints with qualities similar to the substrate materials, as well as creating joints free of detrimental intermetallic micro - constituents is significant for the optimization of this joining technique for industrial applications. The process parameters include the applied pressure, surface roughness, and most importantly, the bonding temperature, time, surface preparation and interlayer characteristics (composition, thickness and the filler form).

1. Bonding temperature

Bonding temperature has been considered as one of the most essential processing parameters in TLP bonding because it actively influences isothermal solidification and homogenisation. The bonding temperature (T_B) is selected such that it stays above the liquidus temperature of the interlayer material, but below the solidus of the parent material. Increases in the bonding temperature is expected to greatly reduce the time required to complete isothermal solidification (t_{IS}) which prevents the formation of intermetallic micro constituents (eutectic phase) within the brazed region as long as there is an increase in the MPD diffusion coefficient. However, there have been indications that relatively high temperatures can also have a negative impact on the rate of solidification and result in undesirable changes in the substrate material such as grain coarsening [50][60]. This means that increasing the bonding temperature above a critical temperature has negative effects on the time required to complete solidification. This decrease in rate of isothermal solidification at high temperatures can be due to the possible reduction in the MPD (example – boron) flux that has been utilized for the bonding operation, due to a decrease in its solubility as temperature increases [51] [52] [53] [54].

2. Surface preparation

Surface preparation is also a key factor that determines the quality of a brazed joint. A rougher faying surface of the materials means more residual voids on the bonding interface which adversely affects the quality of the joint. Therefore, the mating surface of the substrates to be TLP bonded must be thoroughly processed so as to avoid an uneven surface finish. This can be basically achieved through grinding, grit blasting, hydrogen gas cleaning, fluoride ion cleaning or a combination of these treatments [55]. Although grinding is commonly used to easily remove surface oxides, complete eradication of surface oxides can be accomplished by using gas blasting. Hydrogen gas has been considered satisfactory for the cleaning of Ni-based alloys with low Ti and Al contents, whereas Ni-based alloys with high Al and Ti contents contain significant amounts of Al and Ti oxides which cannot be easily broken down in hydrogen gas. For this reason, hydrogen fluoride has proven to be efficient for removing such embedded oxides that appear on the surface of Ni-based superalloys [55].

3. Holding time

The time needed to form a TLP bonded joint is also considered as a decisive parameter that dictates the strength and microstructure of the joint region. The amount of residual liquid at the joint will decrease with an increase in holding time, thereby resulting in a decrease in the eutectic phase within the joint region which is known to be detrimental to the properties of the bonded materials. Costs can be reduced by determining the least possible amount of holding time that is required to achieve a completely solidified joint. However, the influence of the characteristics of the materials to be joined, gap size, characteristics of the interlayer material and bonding

temperature among other factors have significant roles in altering the time required to form a joint. As stated earlier, as the bonding temperature increases above a critical value, the time required to completely eliminate the eutectic phase will increase with a fixed initial gap size. As such, one of the most effective approaches that is used in the literature to reduce the time required to complete isothermal solidification during TLP bonding is by using a composite powder mixture of a gap-filler alloy and a brazing alloy instead of the convention 100% brazing alloy powder.

4. Interlayer characteristics

When considering TLP bonding as the means for repair or fabrication, the interlayer characteristics which embodies the thickness of the interlayer (gap size) as well as the interlayer makeup (foils, powders, pastes, etc.) and interlayer composition not only influence the optimization of the process, but are also crucial for prescribing the efficiency of the joint in terms of the strength and ductility relative to the parent materials. The interlayer can be a pure material, an alloy, or even a combination of interlayers of different metals [6] [56] [57] [58]. Alterations to the gap size and interlayer material chemical composition have been broadly researched for the TLP bonding of Ni-based superalloys. In TLP bonding, out of all the MPD elements, such as silicon, phosphorus or their combinations, boron is the most favored because it has the highest diffusivity and very little is needed to reduce the melting point of Ni. Besides, the gap tolerance is always setup in such a way that the gap is narrowly sufficient for the braze interlayer to flow through by capillary action. In some cases, silicon and boron can both be considered as the braze filler material because the addition of the former has been found to increase the corrosion resistance of a TLP bonded assembly. Also, phosphorus acts as a good MPD element. Yet

despite its satisfactory brazing characteristics and an extremely low melting point, the low ductility, strength and greater fluidity of phosphorus in the molten state are some of its disadvantages in comparison to boron and silicon [34]. Likewise, recent research has examined the practicability of using hafnium as an MPD element [59]. Hafnium is attractive as an MPD element because it provides a more ductile joint than with the conventional use of silicon or boron. In addition, it also provides some resistance to high temperature corrosion [59].

With an increase in initial gap size, the rate of joint solidification at a constant bonding temperature and time remains the same, but the volume of the liquid within the joint increases. Hence, the time required to achieve completely solidified joint increases with increase in initial gap size.

2.3.5 Influence of base alloy composition on isothermal solidification rate

Ghoneim and Ojo [50] used numerical modeling to show that TLP bonded joints produced by using composite interlayers with various base alloy compositions (without MPD elements) and various filler powder compositions (with MPD elements) can be effective in increasing the isothermal solidification rate than with the conventional use of entirely filler materials. They showed that, depending on a combination of parameters, such as: 1) the type of MPD solute, 2) the ratio of the volume of filler alloy powder to the base alloy powder, and 3) the concentration of the MPD element in the filler alloy, the composite powder mixture can be successfully used during the TLP bonding of SX superalloys without the formation of stray grains.

This method was implemented for the TLP bonding of an SX intermetallic alloy, IC6 [60]. They joined two SX IC6 substrates together by using two different types of interlayer materials;

namely, 1) 100% Nicrobraz 150 powder, and 2) a mixture of Nicrobraz 150 powder and IN738 gap filler powder at a ratio of 7:3. Their results, in which the same initial gap size and bonding temperature were used proved that the application of a composite powder mixture (in that ratio) as a substitute to only filler powder, can significantly reduce the isothermal solidification time, reduce the erosion of the SX substrate materials, and also produce a SX joint.

2.3.6 Modelling of TLP diffusion bonding

Based on the increasing usage of TLP bonding for the joining of advanced materials in recent years, some attempts have been made by a number of researchers to separately model the discrete stages (namely heating, dissolution, widening, isothermal solidification and homogenization) with numerical and analytical approaches. Since TLP bonding relies on the diffusion of the MPD element(s) out of the joint region, the models were all generated by applying Fick's first and second laws of diffusion.

At the steady state condition, Fick's first law is given by:

$$J = -D\frac{\partial c}{\partial x} \qquad (1)$$

where J is the diffusion flux. Accordingly, Fick's second law is also relevant for the kinetics of the TLP transient phase, such that the concentration profile (change in concentration with time) of the MPD element in the substrate is denoted by:

$$\frac{\partial c}{\partial t} = D\frac{\partial^2 c}{\partial x^2} \qquad (2)$$

where $\frac{\partial c}{\partial t}$ (the rate of change in concentration of the MPD) provides an indication of the isothermal solidification rate; D (diffusion coefficient of the MPD element) strongly depends on the bonding temperature, and $\frac{\partial^2 c}{\partial x^2}$ (concentration gradient of the diffusing solute in the parent material substrates) is influenced by the solute solubility.

Equations (2) forms the basis for the analytical model derivations that describe the mass transfer in TLP bonding. Based on these equations, a general error function solution was employed for expressing the solute diffusion out of a confined interlayer into the semi-infinite parent materials given by [61]:

$$C_{(x,t)} = {}^{1}/_{2}\ C_0 \left[\mathrm{erf}\frac{[h-x]}{2Dt^{1/2}} + \mathrm{erf}\frac{[h+x]}{2Dt^{1/2}}\right] \qquad (3)$$

where C(x, t) –solute concentration as a function of the distance from the centre of the interlayer (x) and time (t),

C_0 – Initial solute concentration in the filler alloy,

D – Diffusion coefficient of the solute in the substrate,

t– Solidification time, and

2h – Width of the interlayer.

However, published works on TLP bonding models rely on principal assumptions which are provided below [61].

- The diffusion coefficient of the solute is independent of the composition.
- A state of local equilibrium is maintained at the solid/liquid interface.

- The substrate material is treated as semi-infinite because the diffusion of solute into the substrate is very low.

1. Heating-up stage

Equation (4) was applied by Niemann and Garret [62] to account for the loss of the interlayer width during the heating up cycle from RT to the bonding temperature during the TLP bonding of Al – B composites with an electroplated Cu interlayer.

$$x\rho_c = 1.1284\ \rho_a\ [C_{\infty s} - C_m]\ [Ds\ t]^{1/2} \qquad (4)$$

The copper thickness that was lost as a result of diffusion is x, and ρ_c and ρ_a are the densities of copper and the substrate respectively. Ds is the diffusion coefficient of copper in Al, C∞s is the solubility of Cu in Al, and Cm is the initial Cu concentration in the Al substrate.

Since both the solute solubility and the diffusion coefficients change with temperature, MacDonald and Eager [63] used the effective diffusion coefficient $D_{eff,}$ to compensate for the effects of changes in temperature. This is given by the equation:

$$D_{eff} = \frac{\int_0^t D(t)dt}{t_0} \qquad (5)$$

2. Substrate dissolution stage

Nakao et al. [64] estimated that a dissolution parameter (P) based on a derivation of the Nernst – Brunner theory could be used to examine the isothermal dissolution during the TLP bonding of Ni-based superalloys by using an Ni-15.5 wt. % Cr filler metal. The value of this dissolution parameter is given as:

$$P = kt = hln\left[\frac{W_0 - (Wt + ph)}{\rho h\,(W_0 - W_r)}\right] \qquad (6)$$

where ρ is the ratio of the liquid to solid interface, W_t is the width of the dissolved base metal at time t, W_0 is the equilibrium dissolution width, h is half of the initial liquid width, and K is a material constant at a temperature dictated by respective phase diagrams.

Liu et al. [65] developed an analytical model that accounts for isothermal dissolution in TLP bonding by using a general error function solution from which the time required for dissolution of the brazed interlayer with a thickness of 2h at a known temperature is given by Equation (7) which is a function of the diffusion of the MPD element into the liquid phase, D^C:

$$t_d = \frac{(2h)^2}{16{k_1}^2 D^c} \qquad (7)$$

Their result showed that, although the time required for dissolution is directly proportional to the square of the initial thickness (W_i), they concluded that the dissolution rate is chiefly dependent on the diffusion of the solute into the liquid phase (not into the solid phase), which is not the case in actual practice since the process kinetics during base alloy dissolution can also be affected by solute diffusion into the solid.

3. Isothermal solidification stage

Thus far, various analytical models on isothermal solidification during TLP bonding have been developed and proposed by a number of researchers. The interdiffusion coefficient in the solid phase base material controls the rate of solidification as the liquid interlayer starts to solidify due to the diffusion of solutes from the joint region into the solid. During this stage of the TLP

bonding process, the distribution of solutes into the liquid is assumed to be uniform, and therefore, solute diffusion into the liquid can be neglected. Additionally, the substrates can be assumed to be semi-infinite because the diffusion of solutes into the solid is relatively slow. Analytical modeling approaches are largely used in practice. As such, various models are readily available in the literature.

Stationary solid/liquid interface modeling, which is alternatively known as modeling of the single phase solution, is considered as the simplest modeling approach for predicting the time required for isothermal solidification during TLP bonding. The system is treated as a single semi-infinite phase with a fixed solute concentration, with the main advantage that the calculation of the final liquid width at the end of dissolution which basically requires extensive experimental work and/or complex model calculations in order to account for the moving boundary is not needed. Tuah-poku et al. [61] derived a method for estimating the completion time of isothermal solidification based on a stationary liquid/solid interface during TLP bonding. In their approach, an error function solution was used to explain for the solute distribution in the semi-infinite parent metal with a surface on which the concentration of the solutes was maintained at C_{oL}:

$$C_{(x,t)} = C_{oL} + (C_m - C_{oL}) \,.\, \mathrm{erf}\left(\frac{x}{2\sqrt{D_s t}}\right) \qquad (7)$$

where C_m is the initial solute concentration in the base metal, D is the solute diffusivity in the base metal and t is the solidification time.

For the isothermal solidification modeling of a moving interface solution, Lesoult [66] followed the method derived by Dankwerts [67] for mass and heat transfer. The derived solution for the

isothermal solidification stage in TLP bonding was obtained by using Fick's equations for a semi-infinite medium with a constant surface composition and a moving interface (Equation 8):

$$C_{(x,t)} = \frac{C_0 - C_{wc} - C_0}{\mathrm{erf}(k)-1} + C_{wc} - \frac{C_0}{\mathrm{erf}(k)-1} \cdot \mathrm{erf}\left(\frac{x}{2(Dt)}\right) \qquad (8)$$

This derivation was also utilized by Tuah-poku et al. [61] and Liu et al. [65]. By using the equations:

$$W_{max} = \frac{C_f . W_0}{CL\propto} \quad \text{and} \quad t_f = \frac{W_{max}^2}{16k^2\Delta} \qquad (9)$$

they gave the time required for the completion of the isothermal solidification stage as:

$$t_f = \frac{(W)^2 max}{16K^2 D^c} \qquad (10)$$

Ramirez and Liu [68] also derived this solution, which was used in a general form by other researchers like Sekerka [69], Jung and Kang [70], Li et al. [71] and Zhou [72]. However, they all used different approaches to generate the same result.

2.4 Variants of TLP bonding

2.4.1 Temperature gradient TLP bonding (TG-TLP)

Considering the fact that in TLP bonding, the equilibrium compositions at solid/liquid interface are parameters which depend on temperature, it's possible to create a composition gradient over the reaction zone by imposing a temperature gradient ΔT across it [45]**.** Due to such application, solute will start migrating from the higher solute concentration (lower temperature) region into

the lower solute concentration (higher temperature) region. And as the solute start diffusing to the hotter zone, its concentration will be reduced in the colder zone. Consequently, solidification will start from the colder side, and advance to the hotter side and stronger bonds results from this non-planar bond interface [45]**.** This indicates that a temperature gradient can change the solidification mechanism.

2.4.2 Wide-gap TLP bonding.

Wide gap TLP bonding has the advantage of traditional TLP bonding and is useful for repairing cracks which are resultant of extreme environments. Gaps more than 100 micron can be considered as wide gap. One of the main issues with wide gap brazing is the long holding time for eliminating the eutectic. Despite a fact that; in other to achieve complete isothermal solidification, MPD solute is required to diffuse into the base metal; the problem associated with wide-gap TLP bonding is mainly caused by the continual diffusion of MPD into the base material which results in the reduction of solute concentration gradient ($\partial C/\partial x$) below a critical value [73]. So a practical way to limit the reduction in ($\partial C/\partial x$) is to reduce the amount of MPD solute that is required to diffuse into the base material to achieve complete isothermal solidification [73]**.** This can be done by using composite powder mixture which contains a filler alloy powder with MPD and another powder without MPD (additive powder).

2.4.3 Active TLP bonding.

Ceramics have been widely used in structural components because of its good mechanical properties. However their inherent brittleness has limited their usage [74].This material has been

used mostly with metals; so joining of these two specimens have been an issue over time since differences in their mechanical responses and thermal expansion coefficients often causes fracture to occur within the ceramic substrate [75] [76]**.** By using an active TLP bonding technique, research has shown that metals and ceramics can be successfully joined by using ductile metal interlayer so as to relieve residual stresses [77]**.**

2.4.5 Partial TLP bonding (PTLP)

PTLP bonding is mostly used to join ceramic components. The bond set-up in PTLP bonding has the substrates to be sandwiched with a thick refractory metal/alloy between thin layers of low melting point metals/alloys as the interlayer materials; but generally, the process principles remains the same in both PTLP as well as the conventional TLP bonding technique [78]**.** One of the key advantages of PTLP is that, the twofold nature of the multi-interlayer material tends to provide some beneficial joint properties with limited or avoidable deleterious intermetallic reactions.

2.5 Application of transient liquid phase bonding to dissimilar alloys

The joining of two dissimilar alloys that have different physical and mechanical properties is a great challenge. A review of related research works shows that various attempts have been made to bond dissimilar superalloys by considering different joining techniques. However, the advantages of TLP diffusion bonding, as discussed earlier in Section 2.3.5, has so far demonstrated appreciable potential to join these types of complex alloys. As such, the possibility of bonding dissimilar superalloys with TLP bonding has been previously reported by a few

researchers after investigating the bonding behavior in terms of the microstructural and mechanical properties. Some of these works on TLP bonding of dissimilar superalloys are as follows.

Liu at al**.** [79] successfully used TLP bonding to join a Ni-based superalloy, SX DD98 and a poly-crystal superalloy, M963 by using an interlayer foil of Ni-15Cr-3B amorphous alloy. The bonds obtained were characterised in terms of their microstructural evolution, crystallographic orientation and stress rupture. Their result showed that insufficient holding time results in the formation of eutectic micro constituents within the joint region, and at a constant temperature, and gap size, the width of the eutectic phase decreases as the holding time increases. This observation can be generalized to all TLP bonded joints. Differences in the crystallographic orientation, dissymmetry of the bonding line, along with gamma prime particles were detected within the joint region. The dissymmetry of the bonding line was attributed to the difference in the diffusion of the MPD element as a result of the difference in the isothermal solidification rate of the two substrates.

Ghoniem and Ojo [80] used TLP bonding to join a poly-crystal alloy and a SX alloy. In their study, they predicted the location of the solid/liquid interface as well as the isothermal solidification time through a finite element (FE) numerical model. Their result showed that, when joining two dissimilar superalloys, the asymmetric distribution of the residual interlayer liquid can be attributed to the mismatch in the lattice coefficient of the diffusion of the substrates or the solute solubility. In addition, their result showed that, notwithstanding the fact that solute diffusivity increases with bonding temperature, an increase in temperature can also lead to a much longer time that is required to prevent the formation of the detrimental eutectic phase during the bonding of dissimilar alloys. However, in a situation where a material is coupled with

another material that displays a better capability of accommodating the MPD element diffusing out of the liquid insert, the occurrence of this deviating behavior in eutectic size with temperature can be reduced.

2.6 Scope of the present investigation

As shown in the previous sections, different bonding techniques are available for the joining of multi-material components. Without exception, each technique has its inherent advantages and disadvantages. When joining difficult-to-weld engineering materials like superalloys, TLP bonding has certainly proven to be the most preferred technique. Unfortunately, only a few scientific investigations have studied the TLP bonding behavior on the joint properties of dissimilar superalloys in the literature. In other words, the effects of the different process parameters on the microstructure of joints produced between two dissimilar superalloy materials is not adequately understood. Therefore, the primary objective of this work is to investigate the effects of the TLP bonding process parameters and interlayer material on the microstructural changes during the bonding of IN738 and CMSX-4 SX superalloys.

The first part of this work aims to study how the TG inside a vacuum furnace will affect the temperature distribution in TLP bonded samples. This thermal analysis will be carried out by using ANSYS Workbench software. However, to complete this simulated thermal analysis of joints carried out inside a vacuum furnace, experimental verification will also be performed to affirm the validity of the information deduced from the simulation analysis.

The second part of this work focuses on studying how variations in bonding temperature, holding time, and gap size influence the microstructure of TLP bonded joints between IN738 and

CMSX-4 SX by using a Ni-Cr-B filler alloy, AMDRY 775. Overall, this thesis contributes to the characterization of the joint properties when bonding dissimilar superalloy materials by using TLP bonding.

CHAPTER 3 - MATERIALS AND EXPERIMENTAL PROCEDURE

3.1 Materials characterization

Two different Ni-based SX superalloys are used as the parent alloys for this research work. The first alloy is Inconel 738 SX, and the second alloy is CMSX-4 SX. The former was received in the as-cast plate condition, while the latter in a rod form. The bonding coupons from each of the parent alloys were cut into 5 mm x 9 mm x 11 mm dimensions. In Table 1.5, the chemical compositions of the IN738 and CMSX-4 SX superalloys are listed in detail.

For the interlayer material, AMDRY 775 filler alloy powder having an actual composition of Ni-15Cr-3.5B was used. The solidus and liquidus temperatures of this filler alloy powder are the same, and given by 1052^0C.

3.2 Sample preparation

The bonding coupons were sectioned from the parent alloys by using a numerically controlled wire electro-discharge machine (EDM). Thereafter, to remove the re-cast layers formed during the cutting process as well as producing uniform and flat surfaces from the sectioned coupons, the mating surfaces were grounded by using silicon carbide (SiC) paper to a 600 grit finish. Prior to bonding, the grounded coupons were ultrasonically cleaned in acetone for about 15 mins.

3.3 Joining process and bonding equipment

For the joining, a jig was used to keep the coupons in position and prevent them from shifting. Figure 1.8 shows the joint assembly. As shown in the figure, the sides of the samples and Al foils were coated, to serve as a guiding frame to prevent the liquefied interlayer material from flowing

out of the joint during the bonding process and also prevent a reaction between the substrate and the jig. Two different sizes of joint spacers (70 um and 127 um – Mo wires) are used in different conditions during the course of this study. In order to ensure a precise initial gap size and comparable results, a constant force was applied by using a torque wrench for all of the coupled samples. The TLP bonding operations were carried out in a LABVAC 11 vacuum furnace. The whole process was performed under a vacuum pressure of approximately 5×10^{-5} torr so as to reduce oxidation. The samples were bonded by heating them to a particular bonding temperature, holding them for specified times, and once the bonding cycle was complete, they were allowed to furnace cool to RT. The bonded specimens were sectioned perpendicularly to the bonding surfaces by using the EDM. They were then mounted on Bakelite, grounded and then polished down to a 5 um finish. Some samples were electro-etched by using 48 mL of sulfuric acid and 40 mL of nitric acid and 12 mL of phosphoric acid solution.

3.4 Microscopic examination

The microstructure of the bonded samples were preliminarily examined by optical microscopy with the use of an inverted-reflected light microscope equipped with CLEMEX Captiva vision 3.0 image processing software. The examination of the microstructure of the joint and compositional analysis of the joint were conducted by using a JEOL 5900 scanning electron microscope equipped with an ultra-thin window Oxford energy dispersive spectrometer (EDS) system. The scanning electron microscope was used in the secondary and back scattered electron modes to produce better images of the surface morphology as well as characterize the phases within the microstructure.

Table 1.4 - Chemical compositions in Wt. % of CMSX-4 and IN738 SX superalloys used for experimental studies

ALLOY	C	Cr	Co	W	Mo	Al	Ti	Ta	Nb	Fe	B	Zr	Hf	Re	Ni
IN738 SX	0.11	16	8.5	2.6	1.75	3.4	3.4	1.8	0.9	0.05	0.01	0.04	—	—	bal
CMSX-4 SX	1	6.4	9.6	6.4	0.6	5.6	1	5.8	—	—	—	—	0.1	2.9	bal

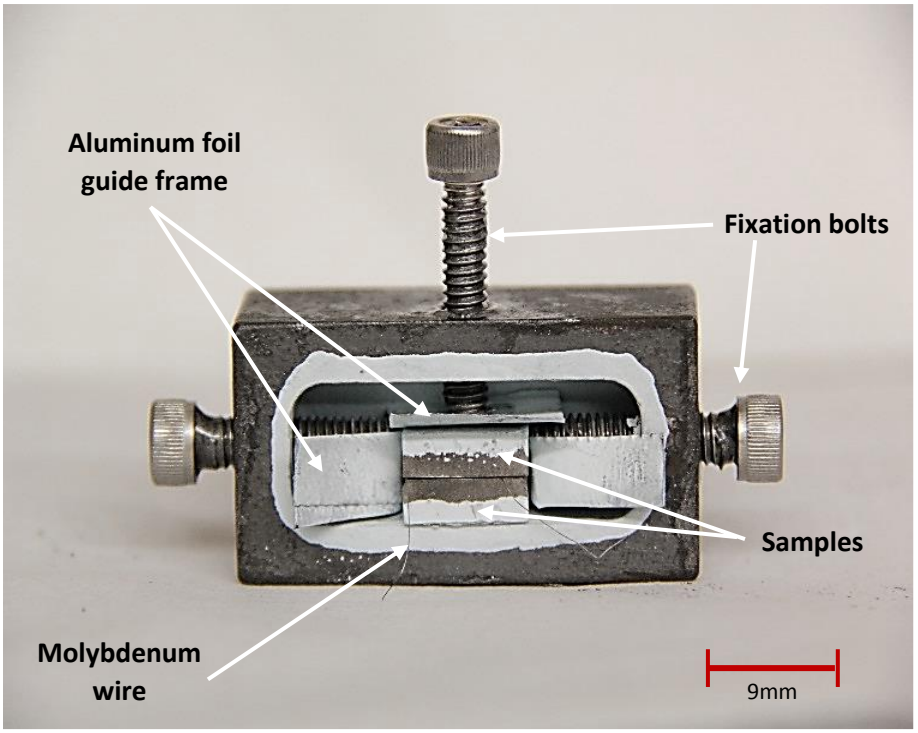

Figure 1.8 - Joint assembly

The crystallographic orientation relationships between the joint region and the SX parent alloys were examined by using electron backscattered diffraction (EBSD) based orientation image microscopy (OIM). The analysis was carried out by using an EBSD detector that was attached to a Philips XL 30 scanning electron microscope.

CHAPTER 4 - RESULT AND DISCUSSION

PART 1

4.1 SIMULATION WITH EXPERIMENTAL VALIDATION

Already noted in the literature review is that TLP diffusion bonding is a novel technique for joining certain difficult to weld advanced materials. Since this technique is known to be carried out in a vacuum furnace, a temperature gradient (TG) inside the furnace can translate to a TG in the sample, and this can affect the microstructure of TLP bonded joints. However, research on TLP bonding has not been carried out through thermal analysis simulation to understand how the TG in a furnace will affect the temperature distribution in the sample for TLP bonding. In order to carry out the simulation analysis, ANSYS Workbench was used. This study focuses on steady state three dimensional modeling, and various sample configurations in terms of orientation and position inside a vacuum furnace are considered. The simulation process is shown in figure 1.9. To verify the simulation results, experiments were also conducted.

4.1.2 MODELING AND ANALYSIS

4.1.2.1 Material property definition

Two different types of materials were used in the analysis. Structural steel was used as the vacuum furnace material, and a superalloy for the samples. The material properties of the structural steel are already incorporated in the ANSYS software program as follows (Material no. 1, see Table 1.5), while the material properties of the superalloy, IN718, used for the simulation analysis are Material no. 2, see Table 1.6.

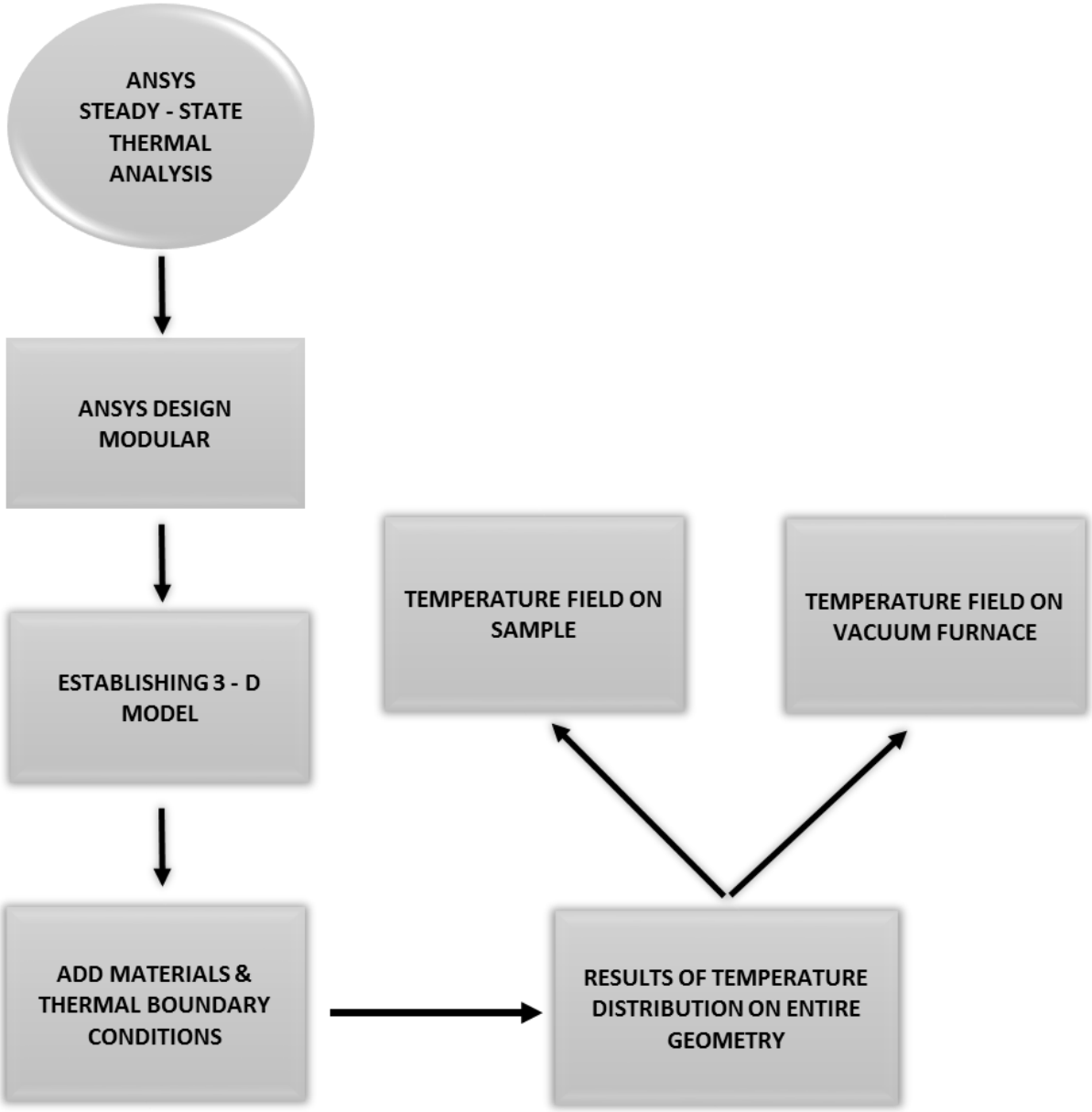

Figure 1.9 - Workflow for the overall simulation process.

Table 1.5 - Material property of structural steel.

Material properties	Unit	Structural steel
Thermal conductivity	(W/m^0C)	60.5
Density	(Kg/m^3)	7850
Specific heat capacity	(J/Kg^0C)	434

Table 1.6 - Material property of IN718 [85]

Material properties	Unit	IN718
Thermal conductivity	(W/m^0C)	11.1
Density	(Kg/m^3)	8193
Specific heat capacity	(J/Kg^0C)	435

Isotropic material properties are assumed for the FEM simulations developed in this study. All the material properties listed in tables 1.5 and 1.6 are assumed to be constant as a function of temperature in the simulations.

4.1.2.2 Vacuum furnace and sample model

ANSYS uses radiation effects only through the boundary conditions, and since the heat emitted by the vacuum furnace is caused by radiation, a heat transfer loading condition by radiation was the basis for determining the temperature distribution in the sample.

Other key assumptions that were made while modeling the process are given below.

1. The modelled vacuum furnace consisted of two vertically oriented heating elements on the sides/walls of a rectangular shell with dimensions of 50 mm x 50 mm x 100 mm.
2. In thermal analyses, ANSYS requires specifications for the ambient temperature. As such, the ambient temperature of the samples when placed in the furnace was set at 25^0C.
3. The temperature of the heating source used in the analysis was 1150^0C. It is imperative to note that the heating source was constant during the entire simulation. In other words, since the two sides of the inner shell were considered as the sources of dissipating heating, therefore the temperature distributed on the samples is only significant to the stability of the radiating source temperature (Figure 2.0). Additionally, this figure shows that there will always be a TG in the vacuum furnace.
4. The outmost cylindrical shield was 80 mm in diameter with a depth of 110 mm. Each of the two bonded samples inside the vacuum furnace was in the form of a square bar with bonded dimensions of 5 mm x 5 mm x 30 mm (Figure 2.1).

4.1.2.3 Meshed model of vacuum furnace and sample

Figure 2.2 shows the meshed solid model layout of the vacuum furnace and sample. From this figure, the mesh used in all the computations of this work contained a total of 31,496 nodes and 4592 elements, wherein 4152 nodes and 750 elements out of the total nodes and elements were attributed to the joined samples. Therefore, a comparison of the results was based on the same applied analytical procedure.

4.1.2.4 Thermal analysis of the modeled system

Figure 2.3 shows how the temperature is distributed throughout a bonded sample of the same shape and dimensions inside the vacuum furnace in a steady state condition. This figure indicates the existence of temperature variation across the sample. The highest temperature is at the joint interface of the bonded samples. With a heat source temperature of 1400^0C, the maximum temperature is around 1395^0C (T_1). The temperature has a decreasing trend further away from center of the joint in both directions. At a distance of 7 mm away from the center of the joint, the obtained temperature is 1382^0C (T_2). Thus, a change in temperature with distance from the center of the joint can be found in the bonded samples inside the vacuum furnace.

However, in the presence of a TG across a sample inside the vacuum furnace, symmetric and non-symmetric temperature distributions in the sample can be obtained. As shown in Figure 2.3, conformity to exactly the same temperature profile on each sample at the two sides of the joint implies a symmetric condition, while different temperature profiles on each bonded samples apply to the situation where symmetry is broken.

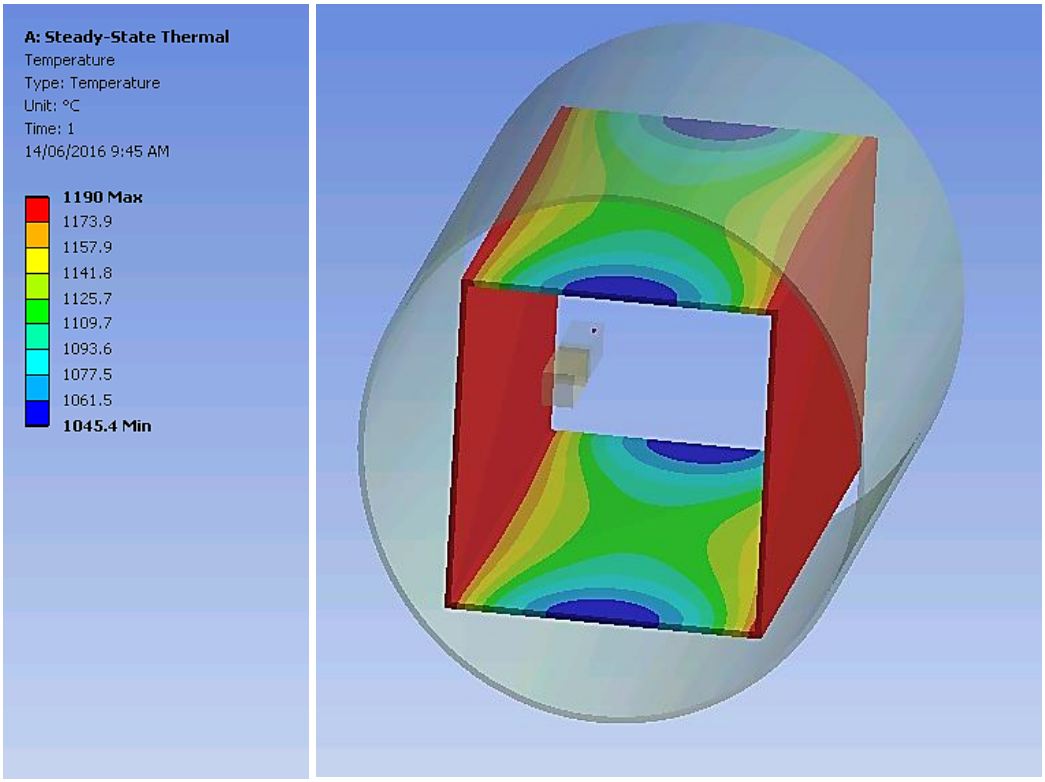

Figure 2.0 - Modeled vacuum furnace geometry from ANSYS design modular, showing temperature distribution in the rectangular shell casing.

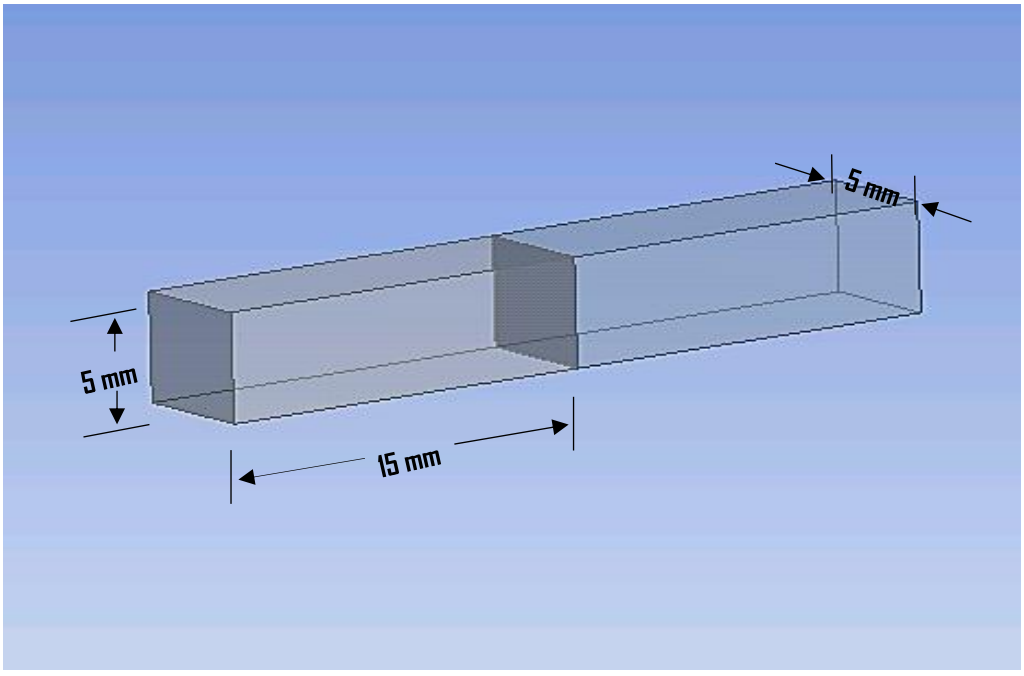

Figure 2.1 - Basic geometric dimensions for square-bar bonded samples modeled with the ANSYS design modular.

Details of "Mesh"	
Display	
Defaults	
Sizing	
Inflation	
Patch Conforming Options	
Patch Independent Options	
Advanced	
Defeaturing	
Statistics	
Nodes	31498
Elements	4592
Mesh Metric	None

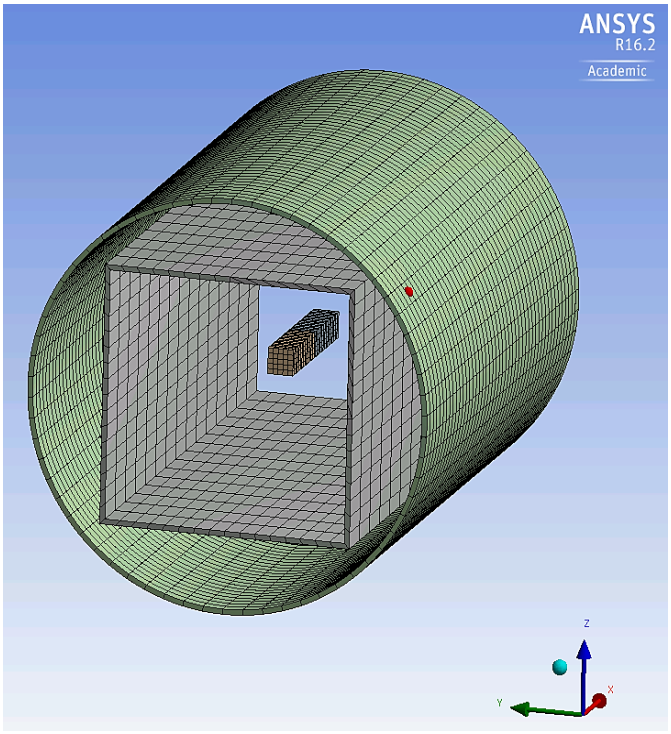

Details of "Mesh"	
Display	
Defaults	
Sizing	
Inflation	
Patch Conforming Options	
Patch Independent Options	
Advanced	
Defeaturing	
Statistics	
Nodes	4152
Elements	750
Mesh Metric	None

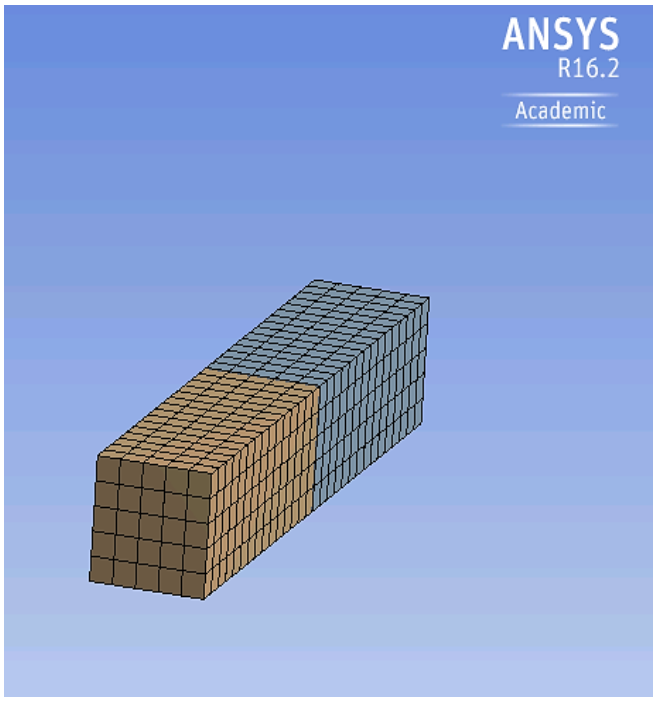

Figure 2.2 - Meshed model of the overall assembly.

For example, assume that the solid/liquid interfaces in a TLP bonded joint from which solidification proceeds inwardly as shown in Figure 2.4a are represented by equidistant positions from the centerline of the joint in Figure 2.4b of the simulated analysis with temperatures T_1 andT_2 respectively. From this thermal analysis, the average value of temperature T_1 after considering three different positions of 1, 2 and 3 is the same as that for temperature T_2 after averaging three different positions of a, b and c. Similarly, across the solid/liquid interfaces (Fig 2.4c), the average temperature from 6 differently identified positions within the face of 'ABCDA' is the same at the two substrate interfaces. In this case, symmetry exists.

Thus, the above simulation indicates that a TG in the furnace can translate into a symmetric temperature distribution in the sample.

4.1.1.5 Temperature distribution based on two different sample orientations in the vacuum furnace

It can be intuitively assumed that symmetry is mainly achieved if the sample is placed at the center of the furnace. By considering the different sample configurations in the furnace, the result of the thermal analysis at the steady state shows that symmetry can exist when samples are placed far away from the center of the furnace. To achieve this, however, it must be placed in a particular orientation as shown in Figure 2.5. In this case, the solidification direction needs to be parallel to the source of heat emission.

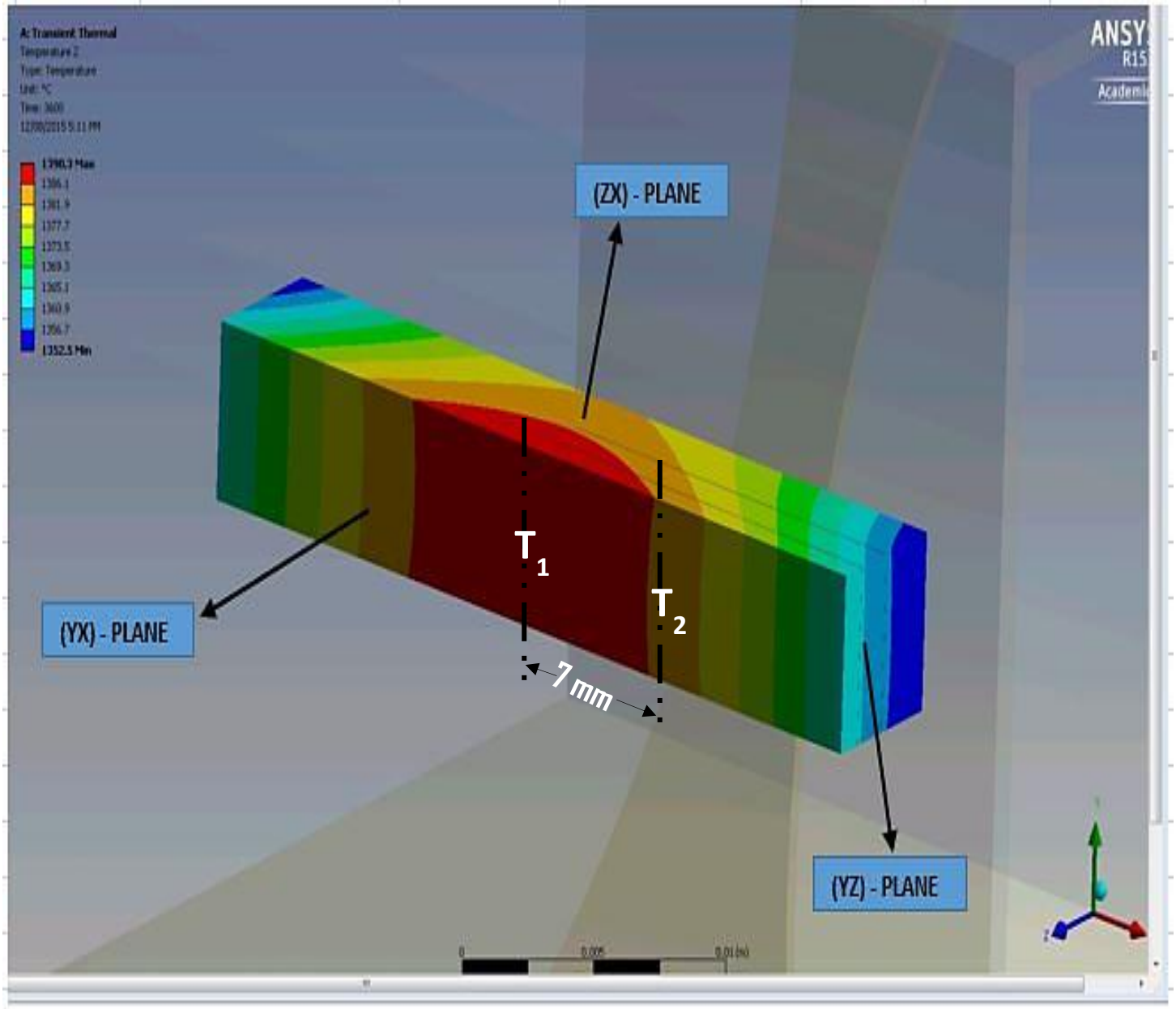

Figure 2.3 - Steady state temperature field for a bonded sample in a vacuum furnace due to the effect of radiation heat dissipation.

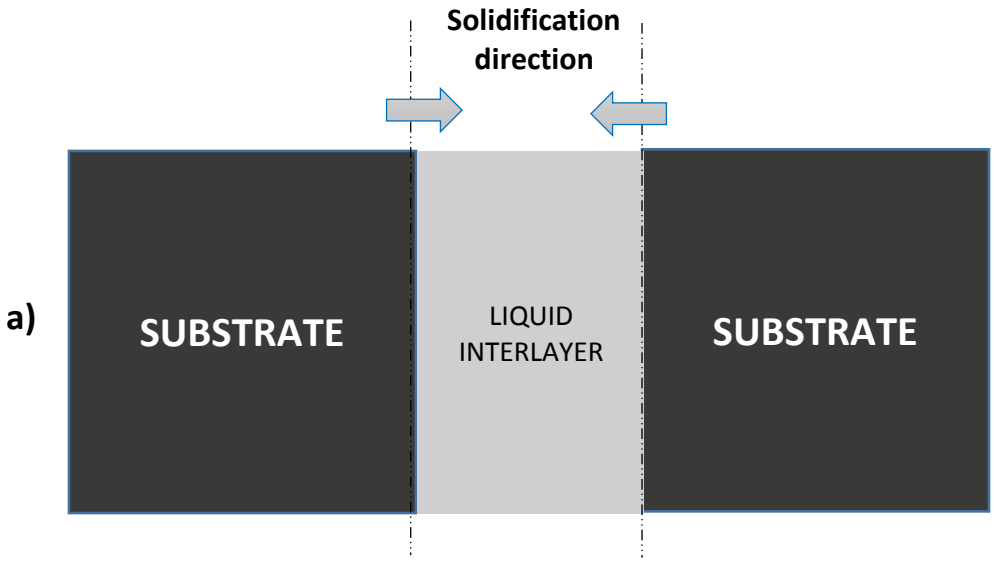

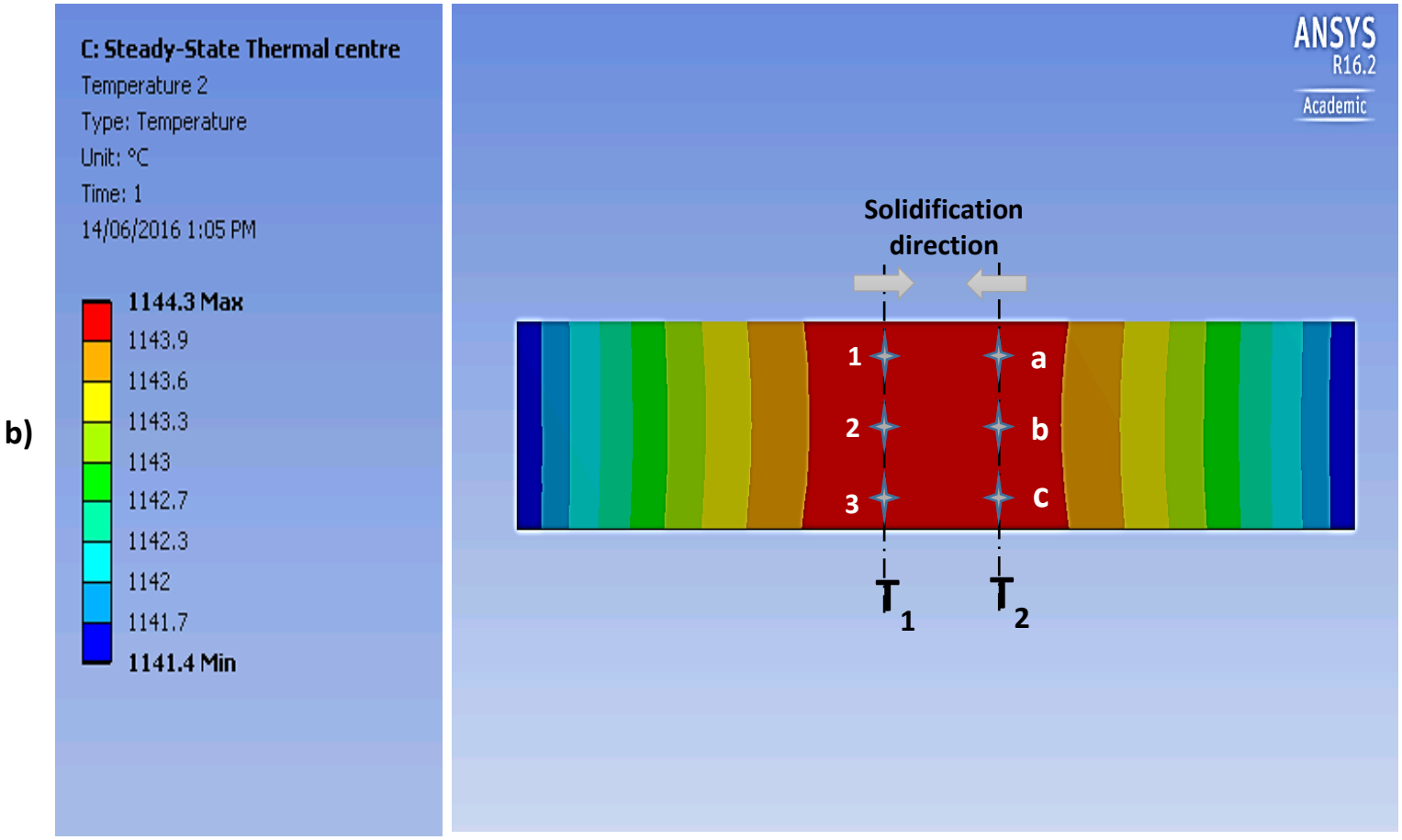

Figure 2.4 - Schematic (a), and simulated configurations (b, c) of a typical TLP bonded assembly showing the direction of joint solidification and the obtained temperature at the solid/liquid interfaces.

c)

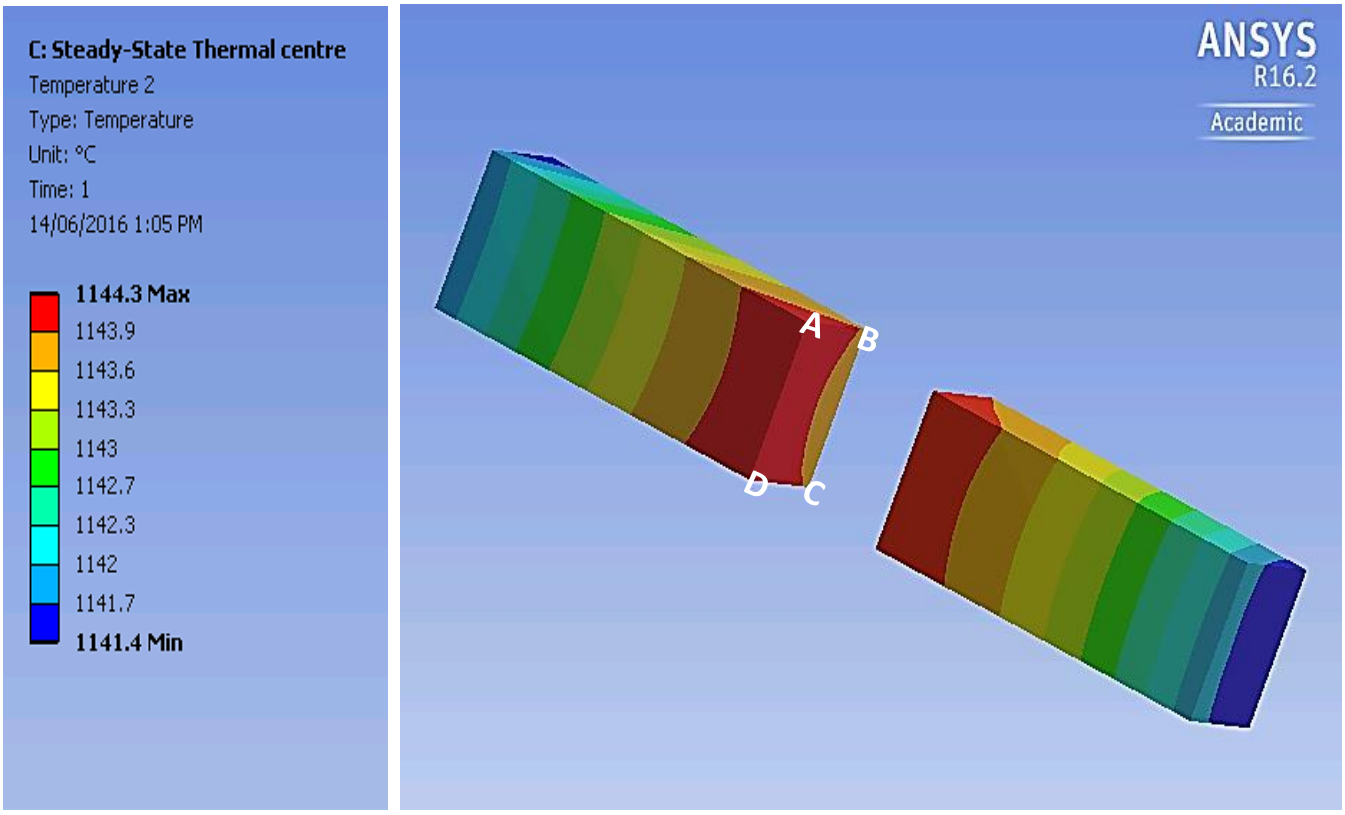

Figure 2.4 - Schematic (a), and simulated configurations (b, c) of a typical TLP bonded assembly showing the direction of joint solidification and the obtained temperature at the solid/liquid interfaces.

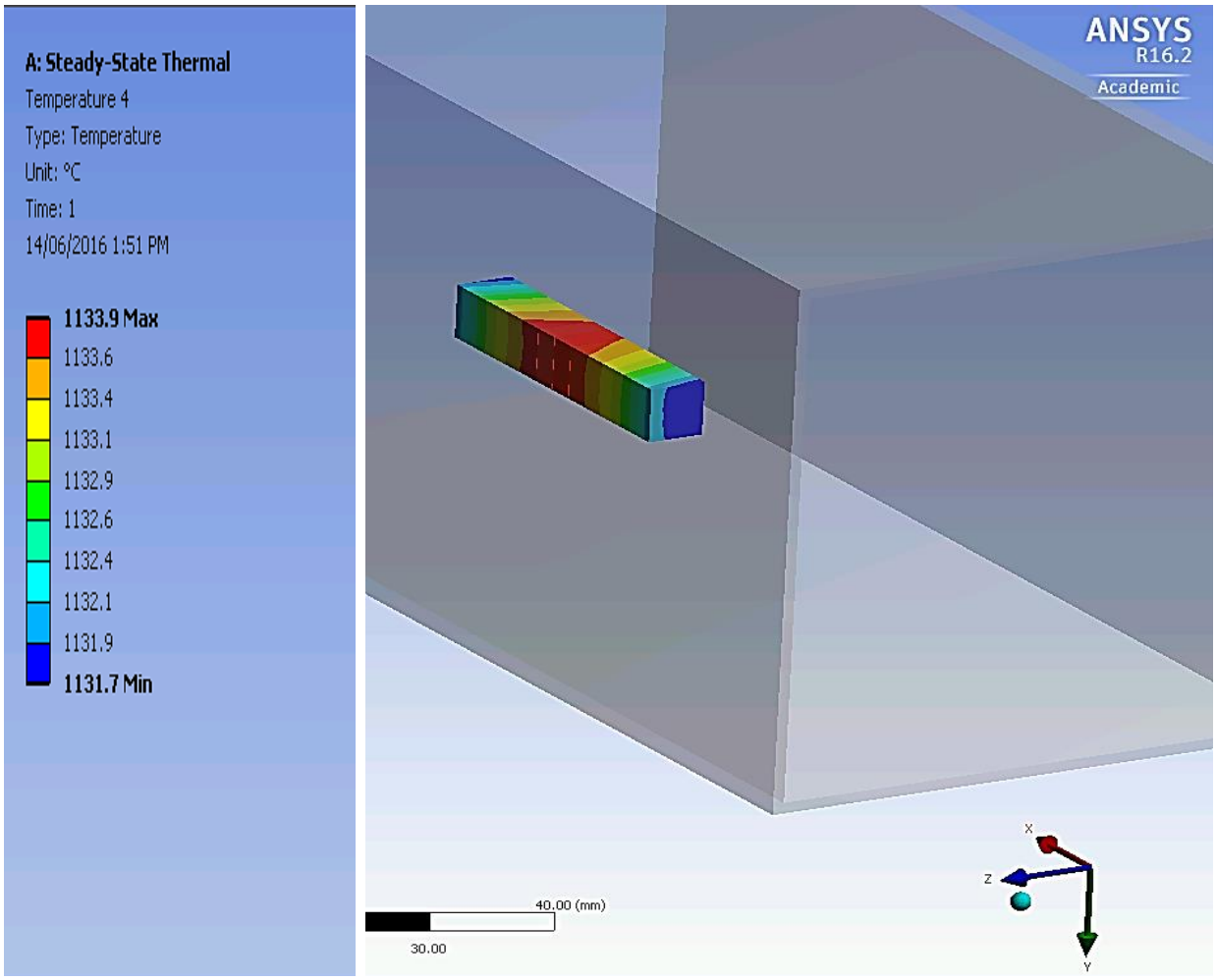

Figure 2.5 - Temperature distribution in steady state condition of a bonded sample placed far away from the furnace center, but whose direction of solidification is parallel to the emitting sources.

In Figure 2.6, the symmetry between the two bonded samples is broken when the solidification direction is perpendicular to the heat source. Therefore, an asymmetric microstructure is expected in the joint region.

4.1.3 Experimental validation

Experimental verification was carried out on two similarly coupled IN738 samples which were both placed far away from the center of the furnace. Bonding was carried out at a temperature of 1150^0C with a holding time of 4hrs 30mins. One of the coupling was oriented in such a way that the solidification direction was parallel to the source of heat emission, while the other coupling was oriented in a way that the direction of the solidification was perpendicular to the heating source (as already simulated, see Figures 2.5 and 2.6).

Figure 2.7a shows the microstructural morphology of the bonded sample when the direction of the solidification is parallel to the source of heat emission, and figure 2.7b shows the microstructural morphology of the bonded sample when the direction of the solidification is perpendicular to the source of heat emission.

The results indicate that at some distance away from the center of the furnace, there is a symmetric temperature distribution, which signifies the formation of a symmetric microstructure in the joint region (Figure 2.7a), where the eutectic (solidification product formed during cooling) is found approximately near the center of the joint. The non-symmetric temperature distribution results in an asymmetric microstructure within the joint region (Figure 2.7b), where the eutectic is shifted towards one of the substrates.

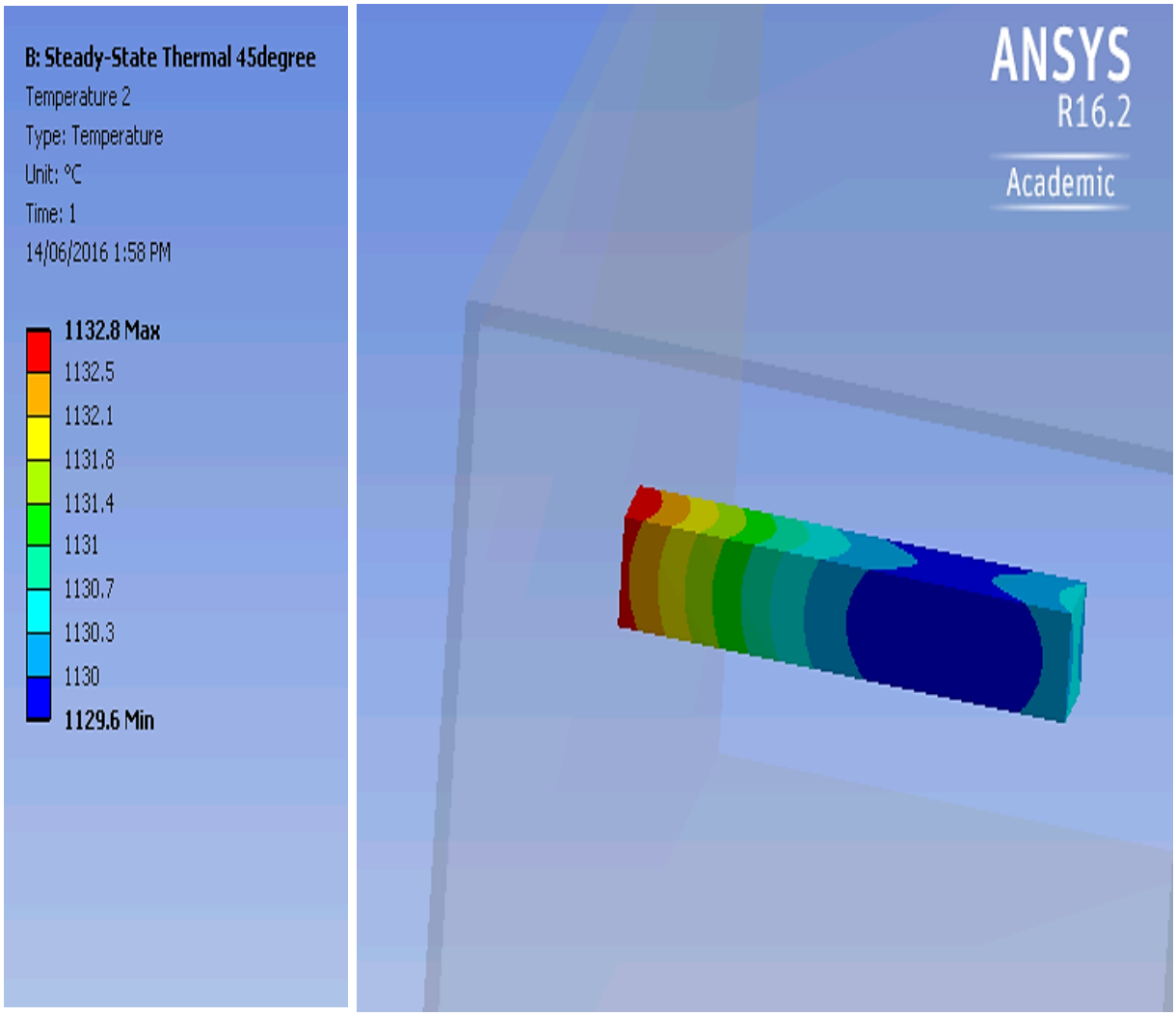

Figure 2.6 - Temperature distribution in steady state condition of a bonded sample placed far away from the furnace center, but whose direction of solidification is perpendicular to the emitting sources.

a)

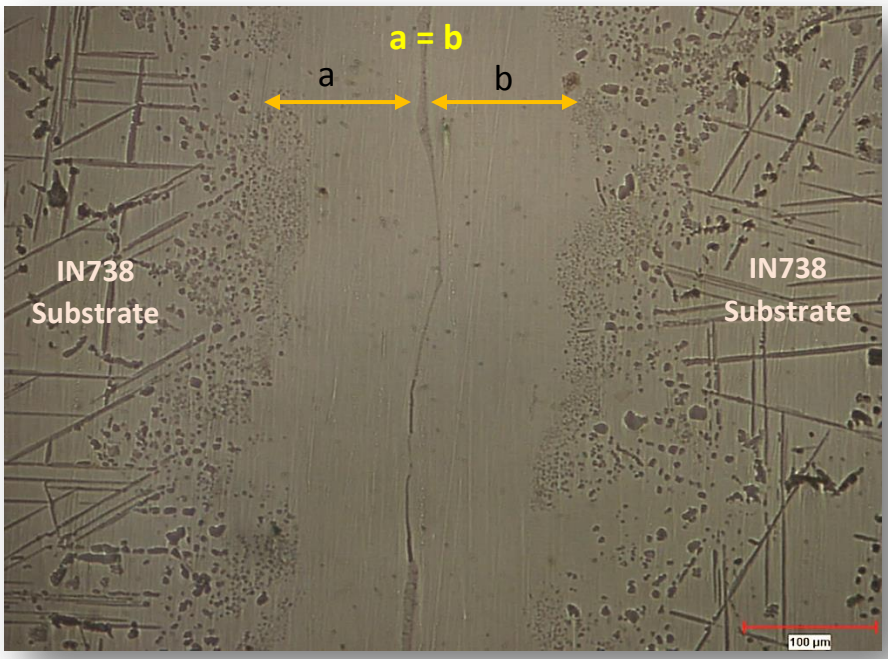

b)

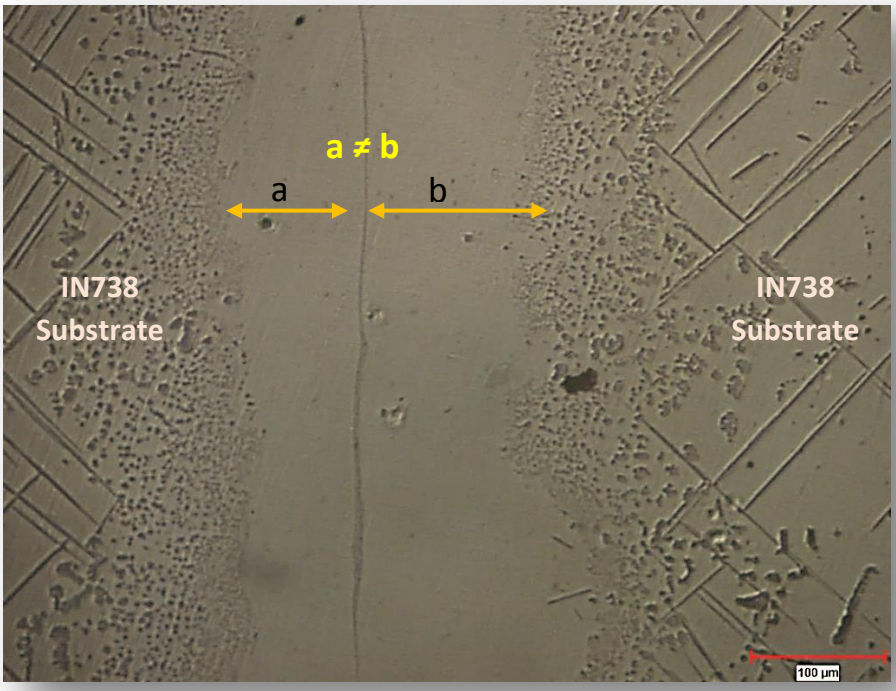

Figure 2.7 - Optical micrographs of joints prepared at 1150^{0}C for 4hrs 30mins when the direction of joint solidification is: a) parallel and b) perpendicular to the emitting sources.

Therefore, the simulated thermal analysis has been validated by the experimental observations. The key information here is that in the presence of a TG, a symmetric microstructure can be obtained anywhere away from the center of the furnace if proper orientation is used. Although, symmetrical temperature distribution may exist in a sample with TG, the magnitude of the TG is very important as this may induce residual stress in the bonded sample. Further simulations were carried out to investigate how the TG varies in a bonded sample placed inside the furnace, and with symmetric temperature distribution, by shifting it away from the center of the furnace (Figure 2.8). This figure shows that the TG increases as samples with symmetric orientations are shifted away from center of the furnace (C_F) towards one of the sources of heat emission. By placing the samples at the center of the furnace (that is, 25 mm away from one of the heat sources), the average TG from the 6 faces of the bonded sample is 0.58^0C/mm; while it is 1.39^0C /mm at 8mm to one of the heat sources. In other words, by moving the TLP bonded samples towards the center of a furnace (hot zone), the sample has the lowest temperature gradient.

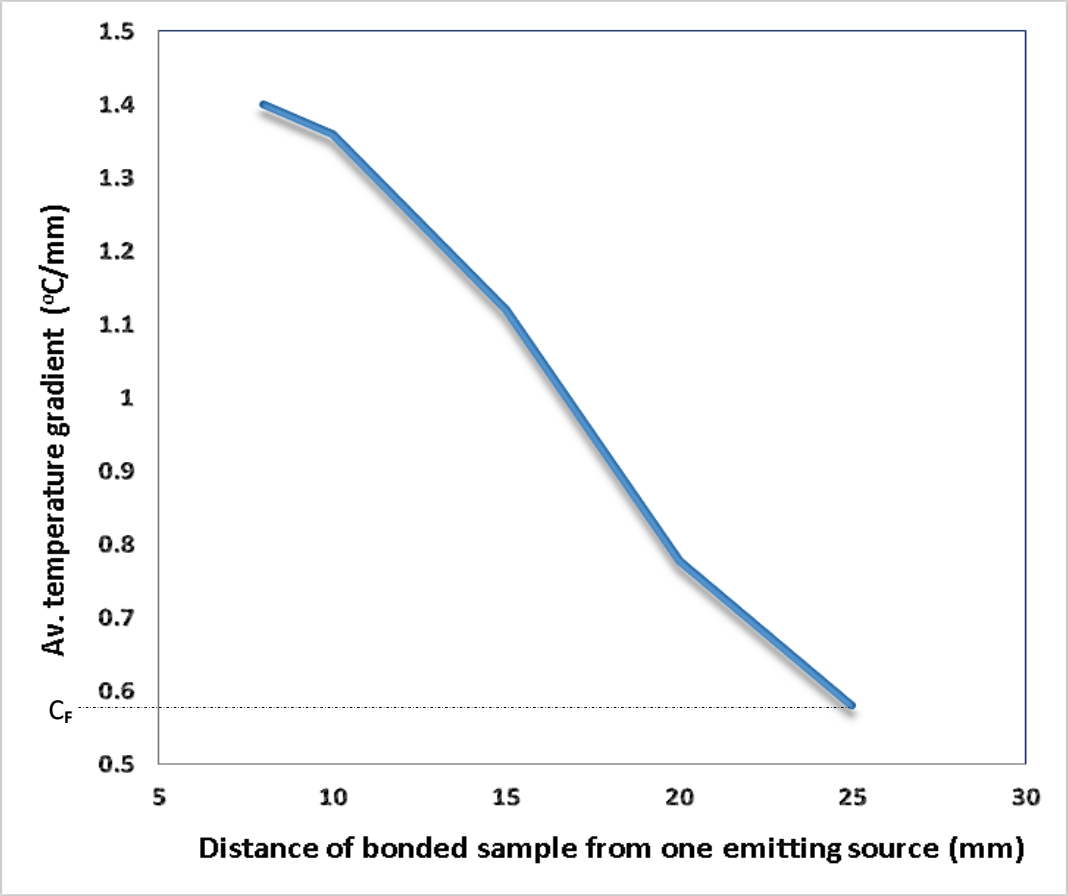

Figure 2.8 - ANSYS simulation result of the variation in temperature gradient of symmetrically oriented samples bonded at different positions from one emitting source of the vacuum furnace.

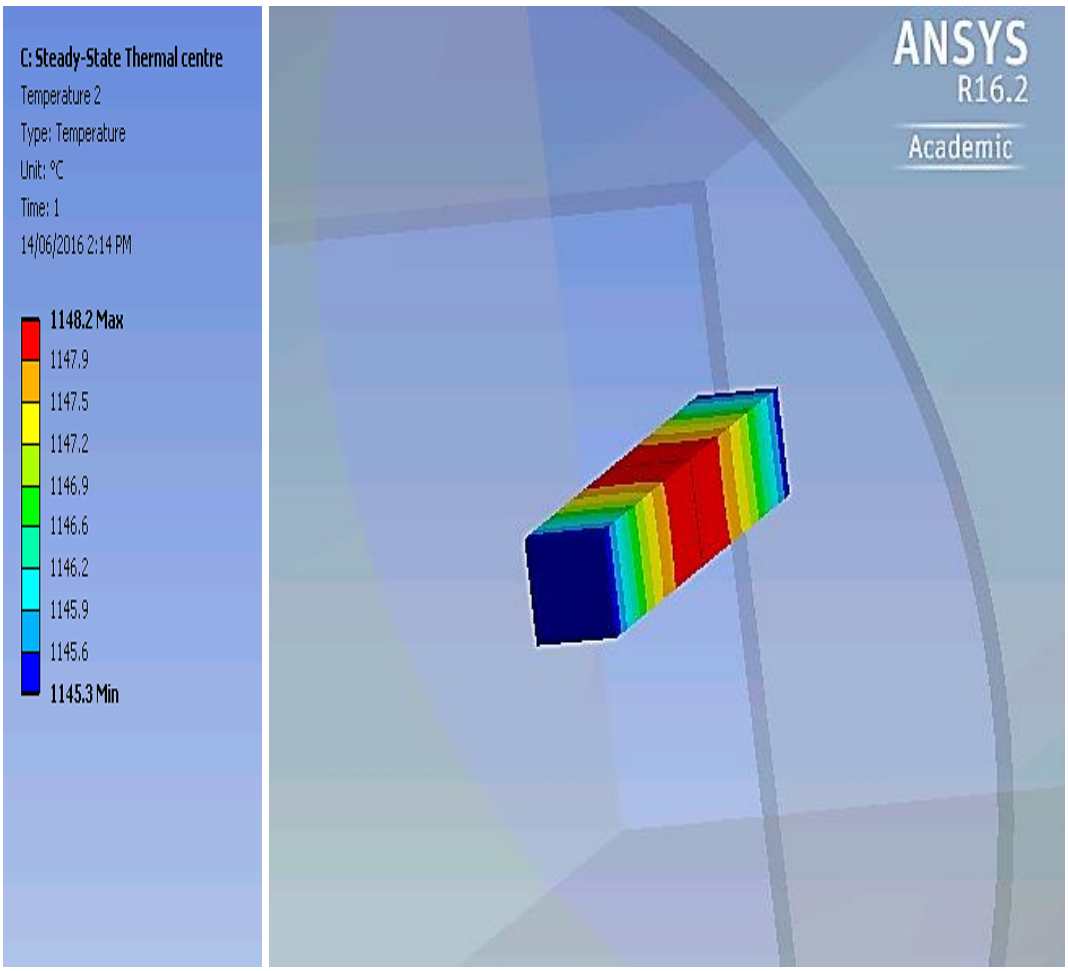

Figure 2.9 - Temperature distribution in steady state condition of a bonded sample placed at the furnace center.

Thus, this study shows that to obtain symmetry in TLP bonded samples of same material; placement anywhere inside the vacuum furnace is acceptable if the direction of solidification is parallel to the source of heat emission. However, considering the added benefit of minimizing the TG so as to minimize the inducement of residual stress, the best position to place a sample is at the center of the furnace where both symmetry as well as the lowest TG can be obtained (Figure 2.9)

However, it should be noted that when dissimilar materials are bonded, symmetry can be broken due to differences in the thermal properties of the substrate materials. Figure 3.0 shows how the temperature is distributed in the bond of two dissimilar materials (IN718 and IN625). From this figure, it can be observed that the temperature distribution in IN718 is not symmetric with that in IN625.

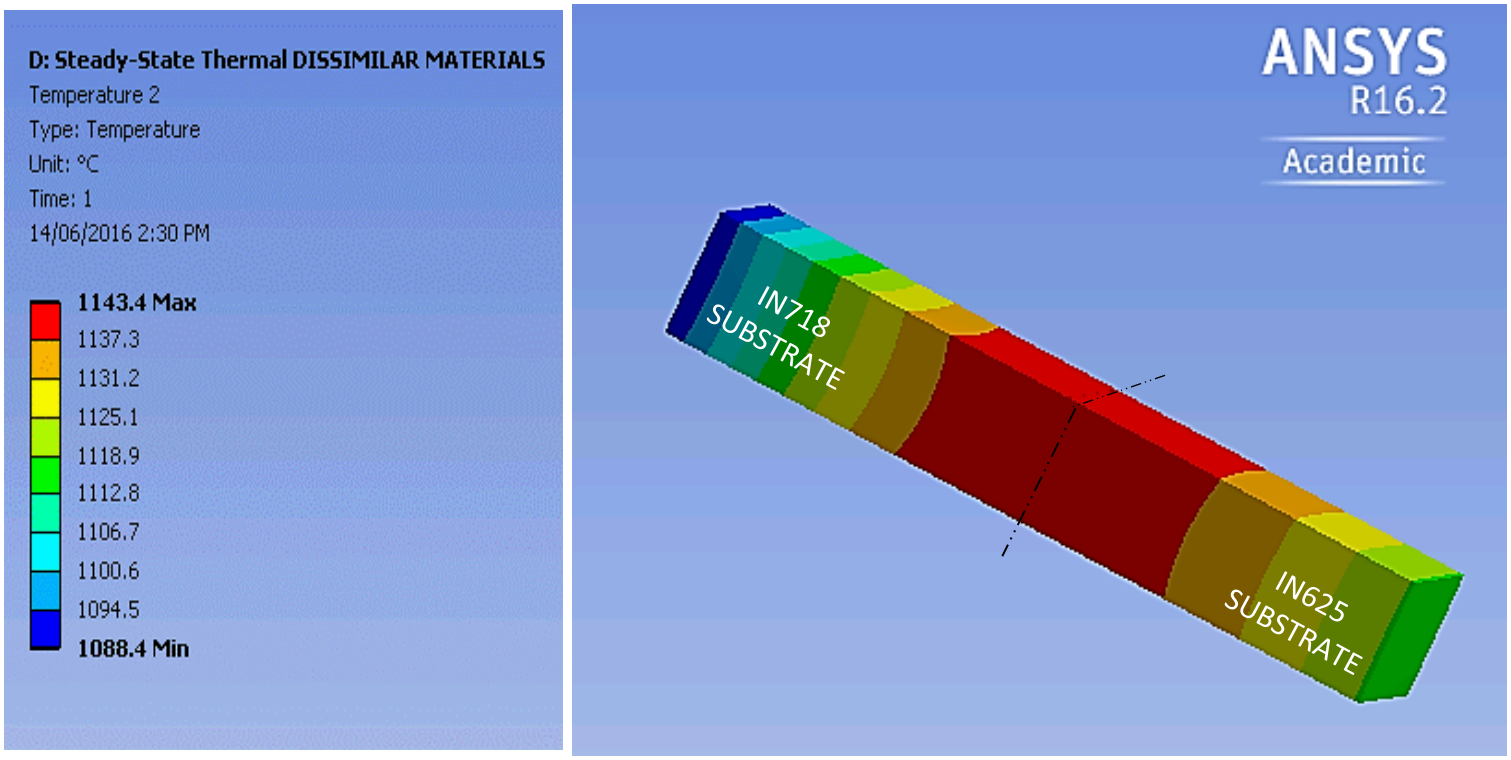

Figure 3.0 - Temperature profile due to lack of symmetry caused by difference in material properties of two bonded samples in the vacuum furnace.

PART 2

4.2 EFFECT OF TLP BONDING PARAMETERS ON DISSIMILAR SUPERALLOYS

4.2.1 Microstructural analysis

In this study, scanning electron microscopy is used to investigate the microstructure of a TLP bonded joint that consists of IN738 and CMSX-4 SX superalloys. As shown in Figure 3.1a, after bonding at 1150^0C for 3 hrs, four different microstructural zones are identified in the joint region.

Zone 1 (athermally solidified liquid zone) in this study is the eutectic that was formed during cooling of the joint. This zone can serve as a site for crack propagation (Figure 3.1c) and was formed as a result of the incomplete diffusion of the MPD element (boron) out of the joint area into the substrate materials. From the scanning electron micrograph shown in Figure 3.1b, it can be seen that three different phases are found in the eutectic. Table 1.7 which shows the results obtained from the EDS compositional analysis, suggest that they are Ni– rich and Cr – rich boride phases, and a gamma solid solution phase, based on what has been reported in the literature [81].

Zones 2a and 2b as shown in Figure 3.1a are the isothermally solidified zones in the joint region. The microstructure of this zone consists of Ni-rich gamma solid solution phase that contain some Al, Ti, Re, Mo, Nb and Ta that were not initially present in the filler alloy composition.

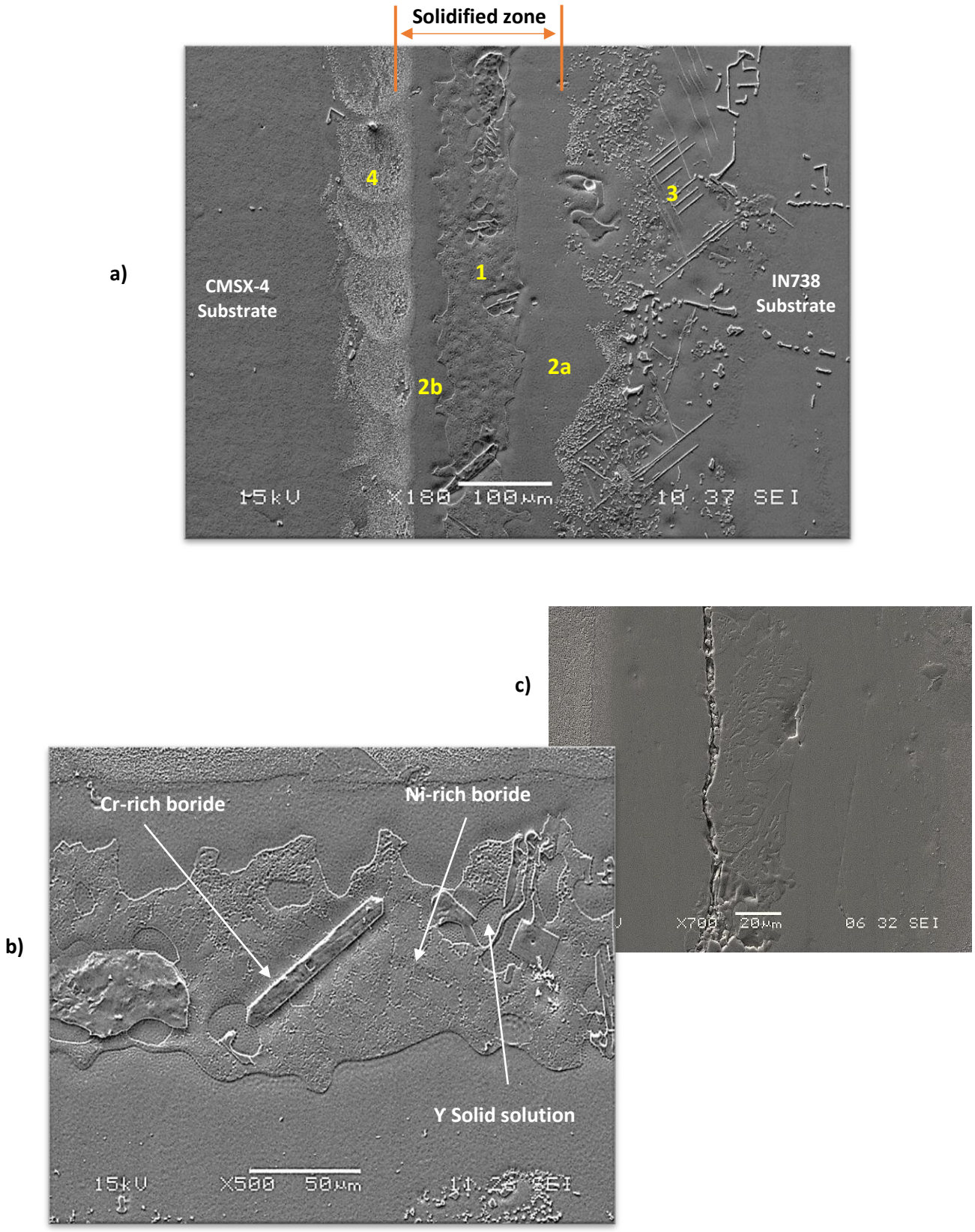

Figure 3.1 - (a) SEM Micrograph of a joint between IN738 & CMSX-4 SX's prepared at 1160^{0}C for 1hr; (b) Higher magnification of the eutectic phase formed in the joint; c) Crack propagation within the IN738/CMSX-4 eutectic phase

Table 1.7 - Compositions in at. % of eutectic constituents formed within the joint region

Element	Ni – rich boride	Cr – rich boride	Ni – based solid solution (ϒ)
Ni	70.16	4.47	71.93
Ti	3.43	1.06	2.07
Cr	9.13	87.16	13.60
Co	9.11	4.91	4.69
Al	2.86	—	5.70
Nb	*1.53*	—	0.30
Ta	2.45	0.12	0.64
W	1.33	2.10	0.53
Mo	—	0.18	0.54

Zone 3 is a region on the IN738 substrate affected by the diffusion of the MPD element (boron) from the interlayer material. The microstructure of this zone has been well-established from previous works that involve the diffusion brazing of the IN738 superalloy. This zone consists of two different morphologies of second phase particles which are blocky-like and needle-like [81]. A typical microstructure of the DAZ on the IN738 substrate in this study is shown in Figure 3.2

Zone 4 is a region on the CMSX-4 substrate that is affected by the diffusion of the MPD element (boron) from the interlayer material. There are some discretely dispersed particles in the diffusion zone near the CMSX-4 region, with a greater number of white blocky particles surrounded by the gamma prime layers (Figure 3.3). The quantitative map analysis in Figure 3.4a reveals that, particles in the CMSX-4 DAZ contain significant amounts of Cr relative to the CMSX-4 substrate. Therefore, it is likely that CMSX – 4 also has some Cr – rich particles in its DAZ just like in the DAZ of IN738 which has been vastly known to contain Cr – rich boride (Figure 3.4b).

4.2.2 Effect of initial gap size on joint microstructure

In order to examine the effect of initial gap size on the microstructure of TLP bonded IN738 and CMSX-4 SX joints, samples with a gap size of 70 μm and 127 μm were bonded at 1160^0C for various holding times, using AMDRY 775 filler powder. Figure 3.5 shows the microstructure of the samples at the considered gap widths for 5 hrs as obtained by a scanning electron microscope that was operated in the secondary electron mode.

The average eutectic width (AEW) as shown by the dashed lines in Figure 3.5a was obtained by taking at least 20 different point measurements on each bonded sample.

Measurements of the eutectic width showed that the average width increases with increase in initial gap size from 40.21 μm with an initial gap size of 70 μm, to 101.24 μm with an initial gap size of 127 um, after 5 hrs of bonding time. This observation is due to the fact that since the diffusion of the MPD element from the liquated interlayer into the CMSX-4 and IN738 substrates determines the isothermal solidification, the rate of solidification at a constant bonding temperature and holding time is expected to be comparable at different gap sizes. Thus, the increase in the volume of the residual liquid with increase in initial gap size implies an increase in the concentration of the MPD element; therefore consequently resulting in a larger eutectic and a longer time to achieve complete isothermal solidification in the sample with the larger (127 um) gap size than the sample with the smaller gap size.

Plots of the eutectic width as a function of holding time of the joints with a gap size of 70 μm and 127 μm are shown in Figure 3.6. The pattern in this figure also explains the observed increase in the eutectic width with increased initial gap size, such that a completely solidified joint, free of the deleterious eutectic phase, was achieved after 11 hrs of holding time with an initial gap size of 70 μm, but after 16 hrs of holding time with an initial gap size of 127 μm.

a)

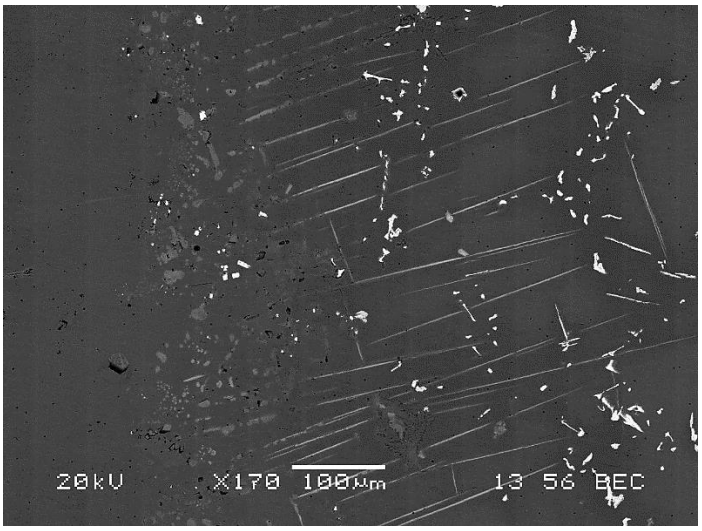

b)

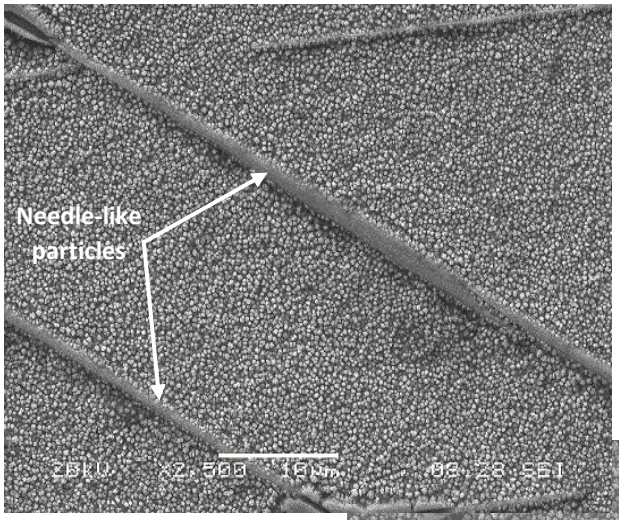

c)

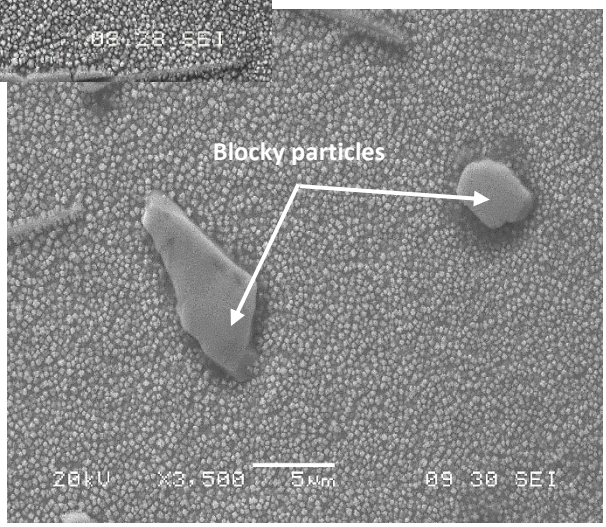

Figure 3.2 - Secondary and backscattered electron images of a) various kind of phases, b) needle-like phases and c) blocky phases formed in the diffusion affected zone of IN738.

a)

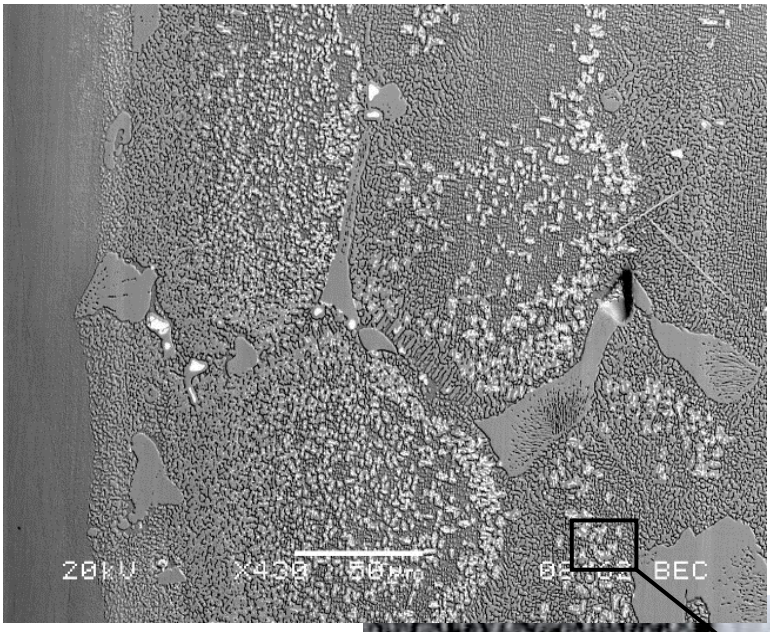

b)

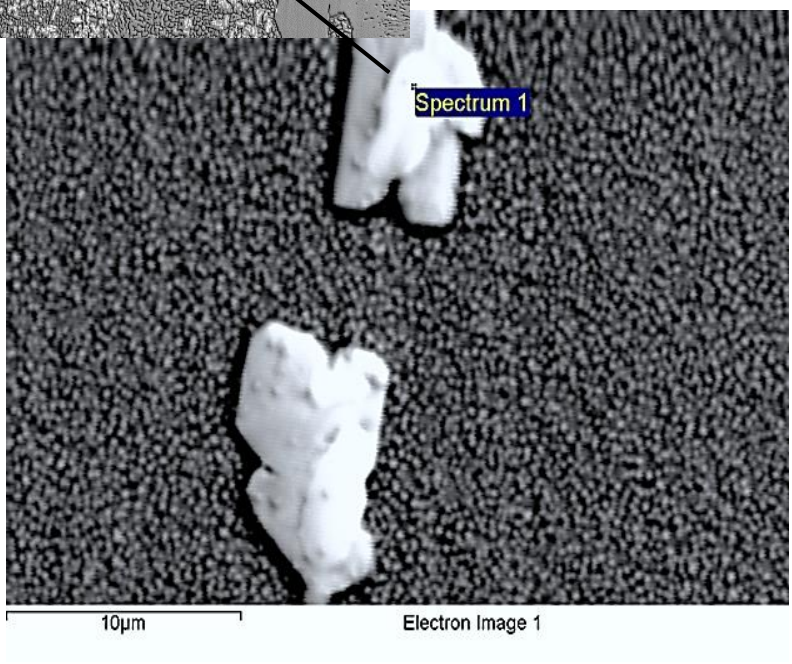

Figure 3.3 - Backscattered electron images of: a) various kind of phases and b) blocky phases; formed in the diffusion affected zone of the CMSX-4 substrate.

a)

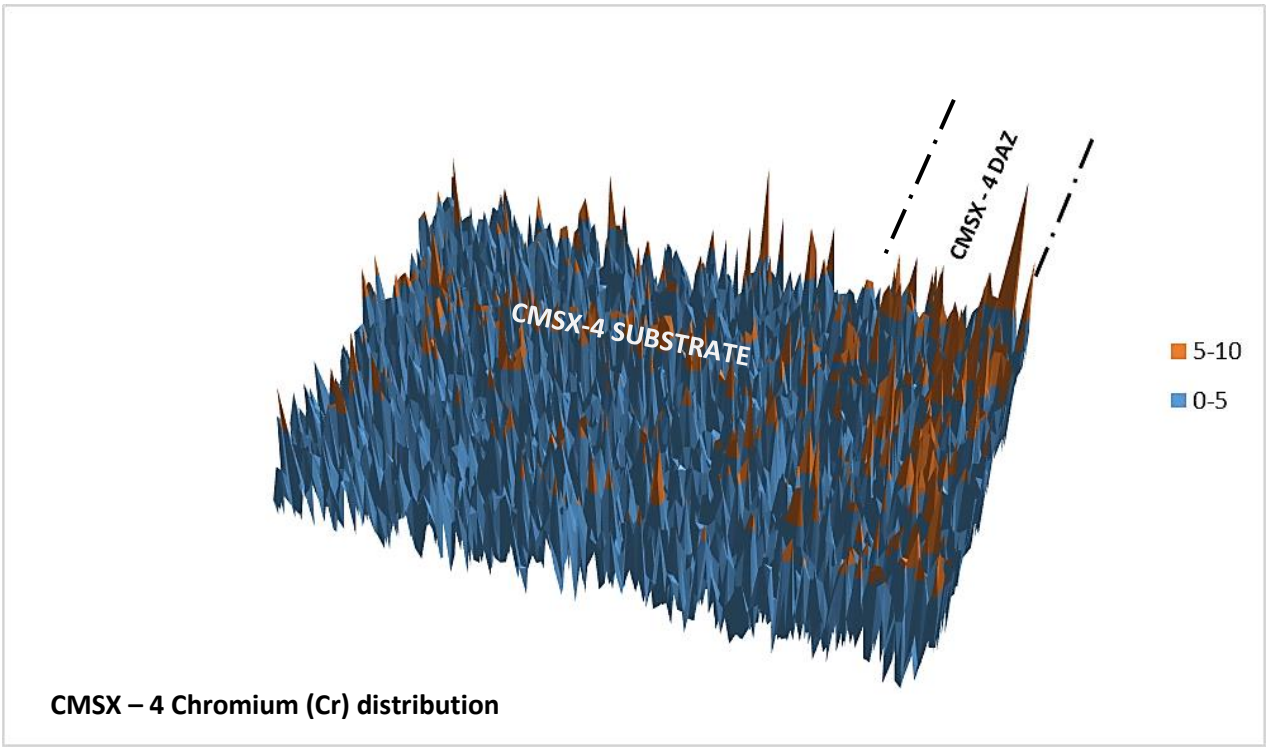

b)

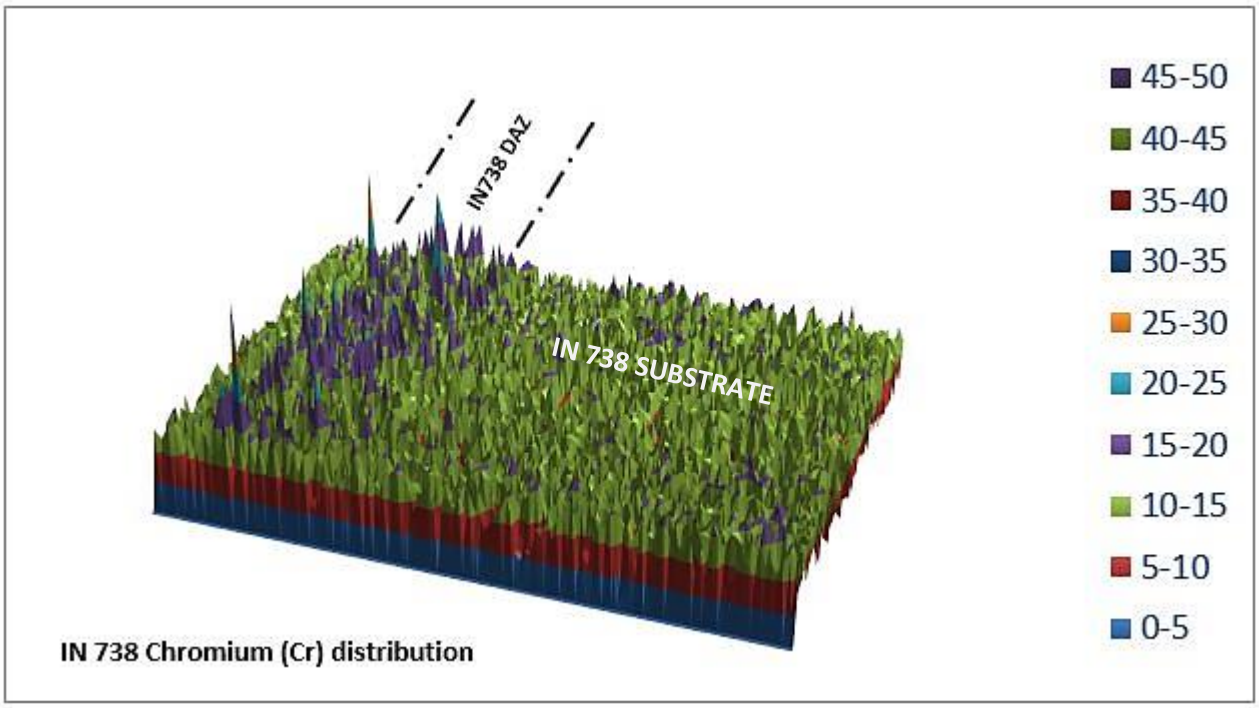

Figure 3.4 - Quant map analysis showing Chromium distribution within the: a) CMSX-4 side and b) IN738 side.

a)

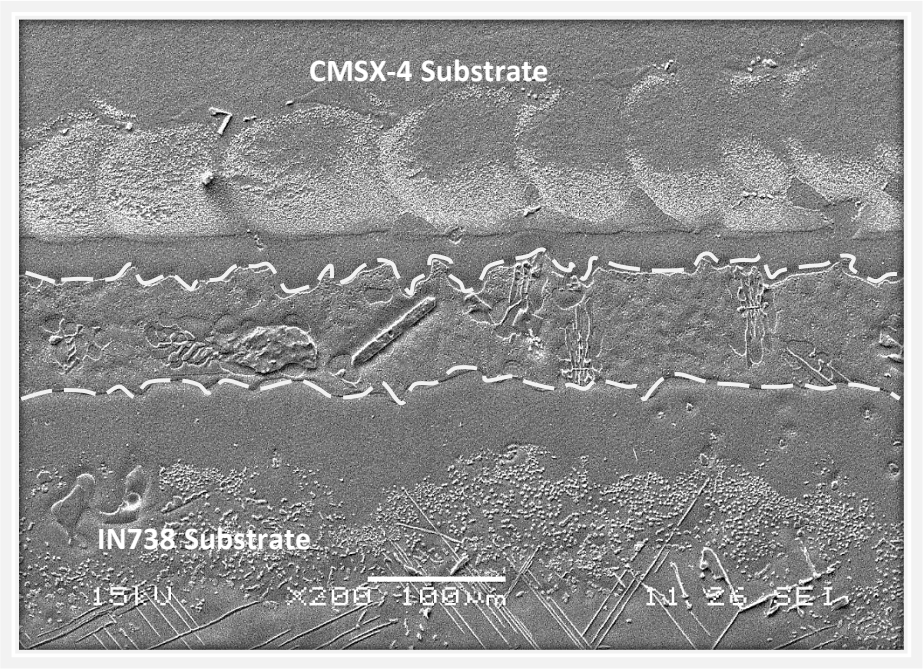

b)

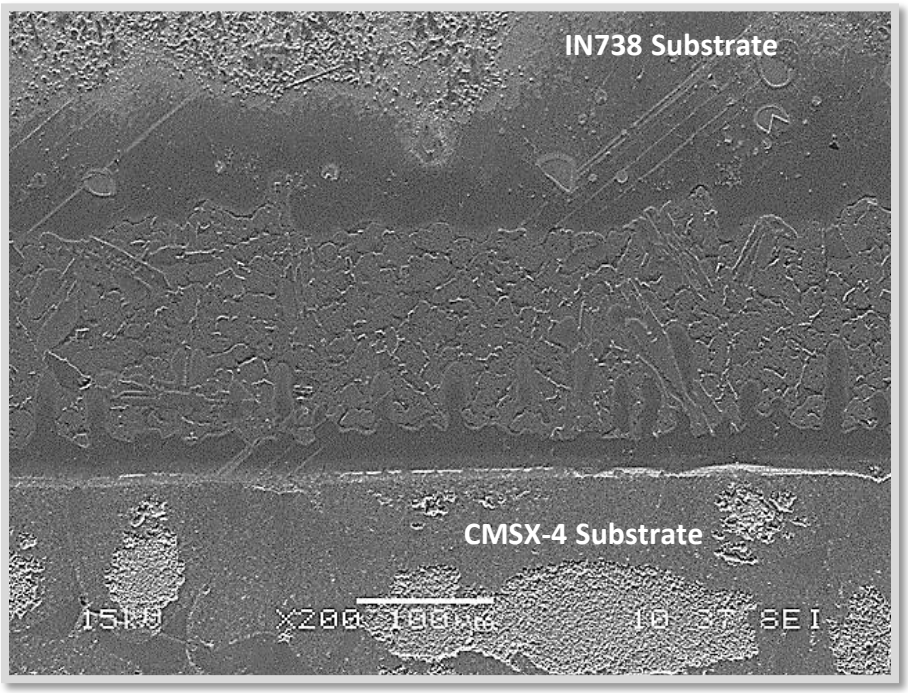

Figure 3.5 - SEM micrographs of the joints made at 1160^{0}C for 5hrs with initial gap sizes of a)70µm, and b) 120µm.

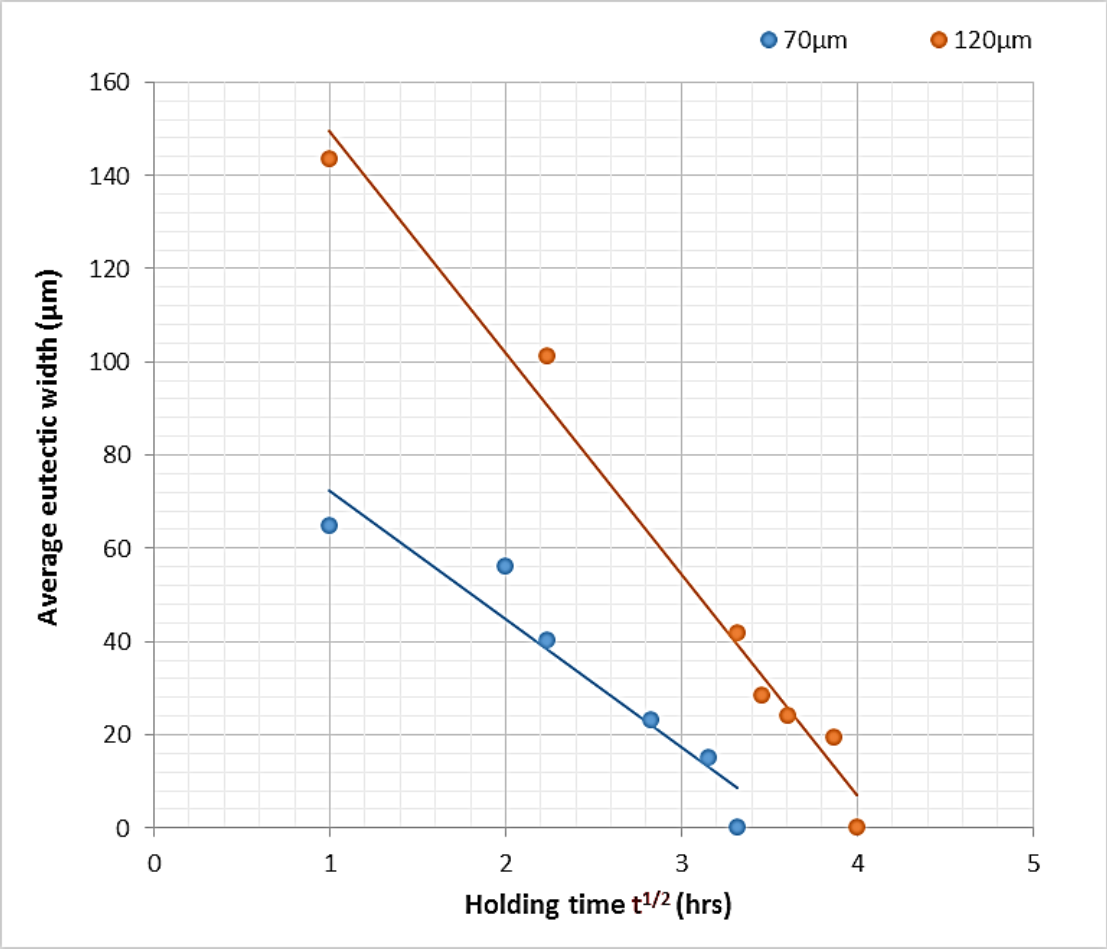

Figure 3.6 - Plot of eutectic width against square root of time in 70µm and 120µm initial gap size joints prepared at 1160^{0}C.

4.2.3 Effect of bonding temperature on joint microstructure

The effect of bonding temperature on the bond microstructure was studied during the TLP bonding of IN738 and CMSX-4 SX superalloys by using AMDRY 775 filler alloy powder. Samples with an initial gap size of 70 μm were bonded at two different temperatures: 1150^0C and 1160^0C for various holding times. The microstructure of the samples after 1 hr of bonding at the respective temperatures showed incomplete isothermal solidification of the liquid phase, thus resulting in the formation of continuously distributed eutectic constituents. The AEW at a bonding temperature of 1150^0C is 79.32 μm and 64.72 μm at 1160^0C after 1 hr of bonding.

However, complete isothermal solidification occurred within the 11 hrs of holding time at a bonding temperature of 1160^0C as the joint was entirely free of the eutectic, while continuous eutectic was observed in the joints prepared at a bonding temperature of 1150^0C after 11 hrs of bonding. This observed result as shown in figures 3.7a and 3.7b indicates that the diffusivity of boron as the MPD element into the substrates increases as the bonding temperature increased from 1150^0C to 1160^0C. Consequently, this causes an increase in the rate of isothermal solidification, which has been conventionally predicted by TLP bonding models.

a)

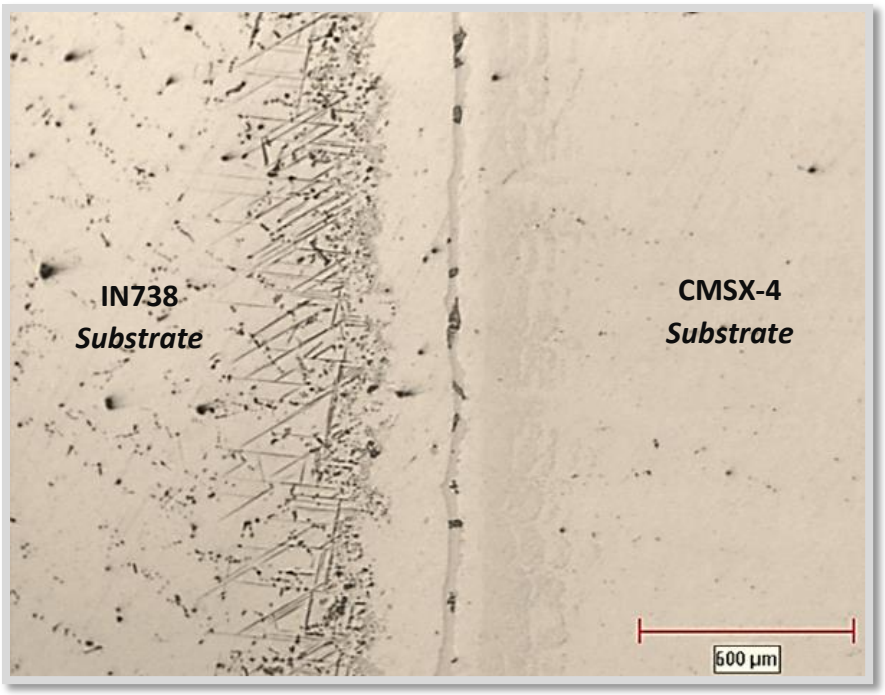

b)

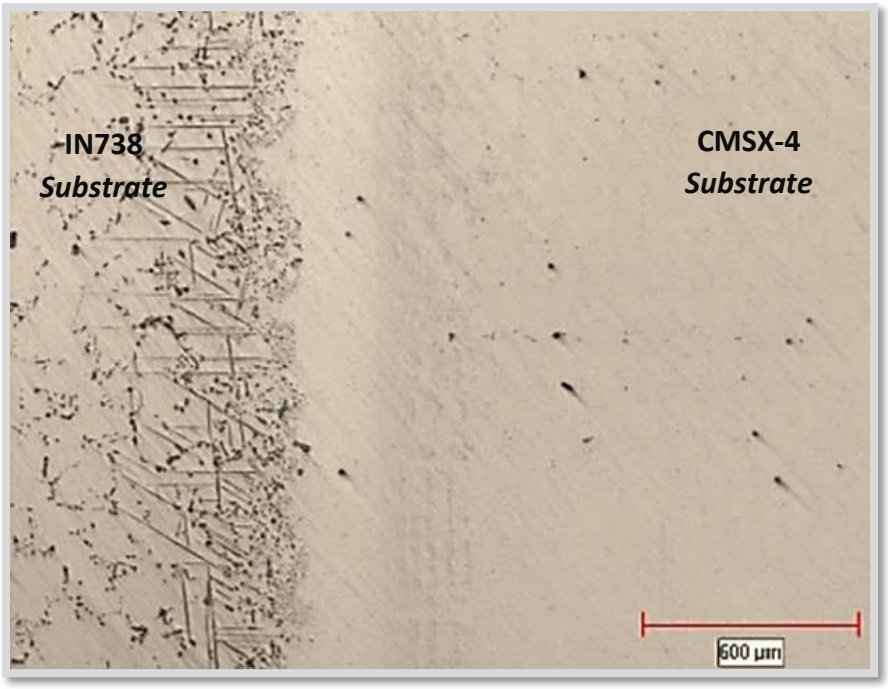

Figure 3.7 - Optical micrographs of 70µm initial gap size joints prepared for 11hr at a) 1150^0C and b) 1160^0C bonding temperatures.

However, by further increasing the bonding temperature to 1190^0C, a continuously distributed eutectic was observed after the 11hrs holding time (figure 3.7c). Therefore, increasing the bonding temperature from 1160^0C to 1190^0C increased the time needed to complete isothermal solidification. As such, there is a significant deviation from the conventional expectation in the isothermal solidification behavior that an increase in bonding temperature would produce more diffusion of MPD element into the substrate, thereby resulting in a higher solidification rate. This anomalous behavior is in agreement with previous works, in which at higher bonding temperatures, the rate of isothermal solidification decreases when the concentration gradient of the diffusing MPD element (Boron) into the substrates reach a critical value, since the use of boron as an MPD element results in a reduction in its solubility as bonding temperature increases [50] [51] [82].

According to Fick's second law of diffusion ($\frac{\partial c}{\partial t} = D\frac{\partial^2 c}{\partial x^2}$) , when the bonding temperature is lower than the critical temperature, the effect of increasing the bonding temperature on the coefficient of diffusion (D) was more significant than the decrease in solute concentration gradient ($\frac{\partial^2 c}{\partial x^2}$). Therefore increase in the bonding temperature from 1150^0C to 1160^0C increased the isothermal solidification rate. On the other hand, at higher bonding temperature of 1190^0C, the decrease in $\frac{\partial^2 c}{\partial x^2}$ was more significant than the increase in the diffusion coefficient. Consequently, the elimination rate of the deleterious eutectic constituents decreased.

c)

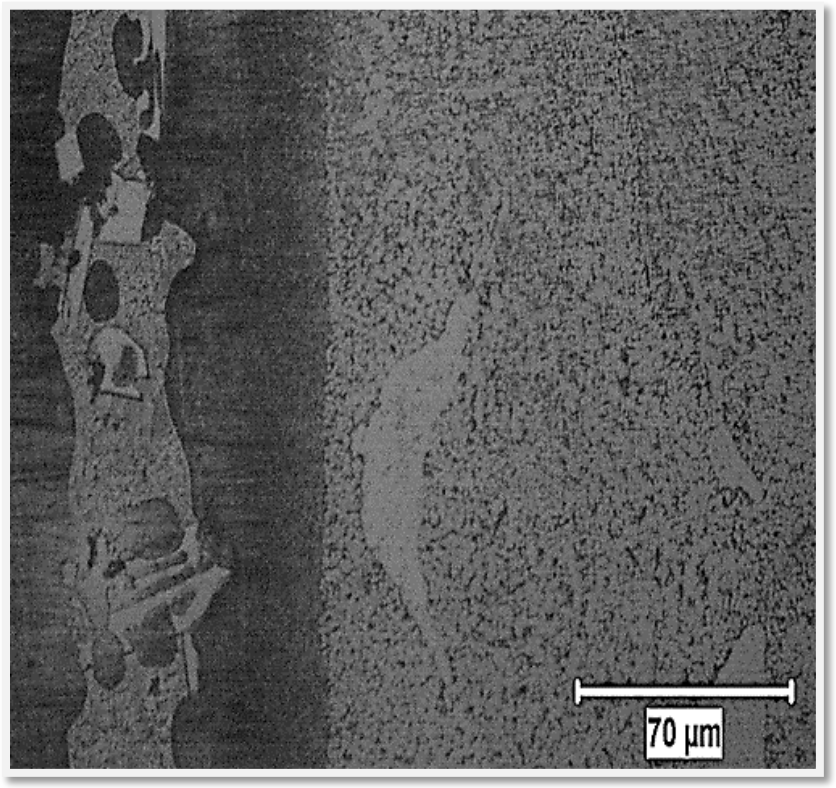

Figure 3.7c - Optical micrograph showing eutectic in bonds made at 1190^{0}C for 11hr.

4.2.4 Effect of bonding time on joint microstructure

Microstructure of a TLP bonded joint, which influences the joint performance depends on elemental interdiffusion between the substrates and the interlayer, which in turn is controlled by the bonding time. To analyze the effect of the holding time on the microstructure of the joint, bonding of the IN738 and CMSX-4 specimens with an initial gap size of 70 μm was done at 1160^0C by using AMDRY 775 filler alloy powder. Figure 3.8 shows the variation of the eutectic width with bonding time.

The microstructure of the joint produced after 4 hrs of holding time showed a continuous eutectic constituent (average of 55.92 μm), while the average eutectic thickness after 8 hrs of holding time is 23.14 μm. Thus, it can be inferred from Figures 3.8 that an increase in the bonding time reduces the width of eutectic-type micro-constituents in the joint region because more boron would have diffused into the base metals.

4.2.5 Isothermal solidification rate in similar and dissimilar Ni-based superalloys

In order to compare the time required to complete solidification when samples of same materials (IN738/IN738 SX) are bonded, to when samples of different materials (IN738/CMSX-4 SX) are bonded, a processing temperature of 1150^0C over a range of holding times and a filler alloy interlayer (Ni-15%Cr-3.5%) with an initial gap of 70 μm were chosen.

The microstructure of the joints developed at this bonding temperature for different durations are shown in Figure 3.9, while Figure 4.0 shows how the AEW varies with holding time.

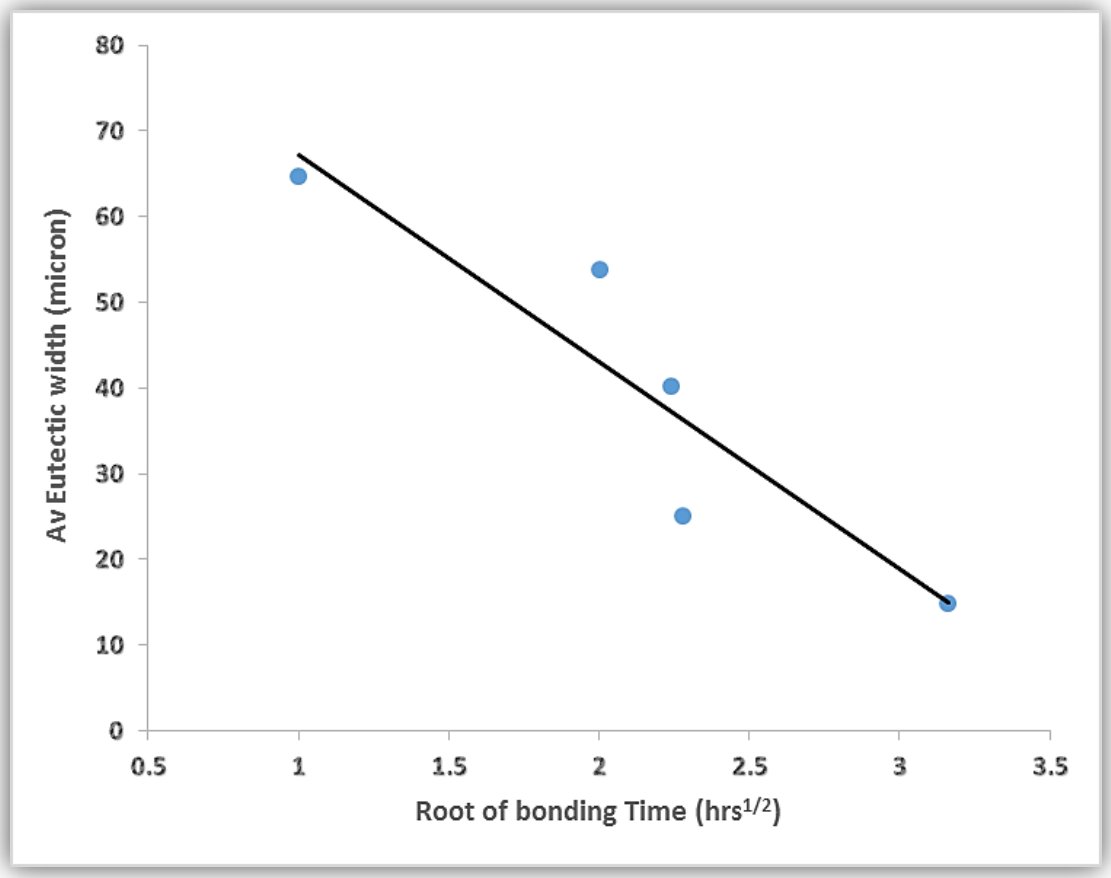

Figure 3.8 - Plot of the eutectic width as a function of holding time in 70µm joints prepared at 1160^{0}C.

The microstructure of the joints bonded for 1 hr explicitly shows the presence of continuously distributed eutectics, which is an indication that the isothermal solidification of the liquid interlayer has not been completed after bonding the samples at 1150^0C for 1 hr (Figures 6.8a and 6.8b). The AEW after the 1 hr of bonding time was found to be 27.8 μm in the IN738/IN738 sample, and 72.83 μm in the IN738/CMSX-4 sample.

However, after increasing the bonding time to 5 hrs, the similarly bonded sample was completely free of the eutectic. On the other hand, with an increase in the bonding temperature from 3 to 5 hrs, the width of the eutectic in the sample bonded with dissimilar materials continues to decrease. This observation suggests that the isothermal solidification time (t_f) is significantly less when joining similar (IN738) Ni-based superalloys than dissimilar (IN738/CMSX-4) Ni-based superalloys at the same bonding temperature, same initial gap size and with the use of the same interlayer material. A possible reason for longer time with the IN738/CMSX-4 may be due to reduced diffusion in the CMSX-4.

The inclusion of Re in Ni-based superalloys causes the formation of an incompressible Ni – Re bond which prevents vacancy migration [14]. As such, the presence of Re among other refractory elements like Mo, Ta and W in the CMSX-4 SX superalloy, which are all characterized by slow diffusion rates, can tend to decrease the rate of diffusion of other alloying elements during TLP bonding.

a)

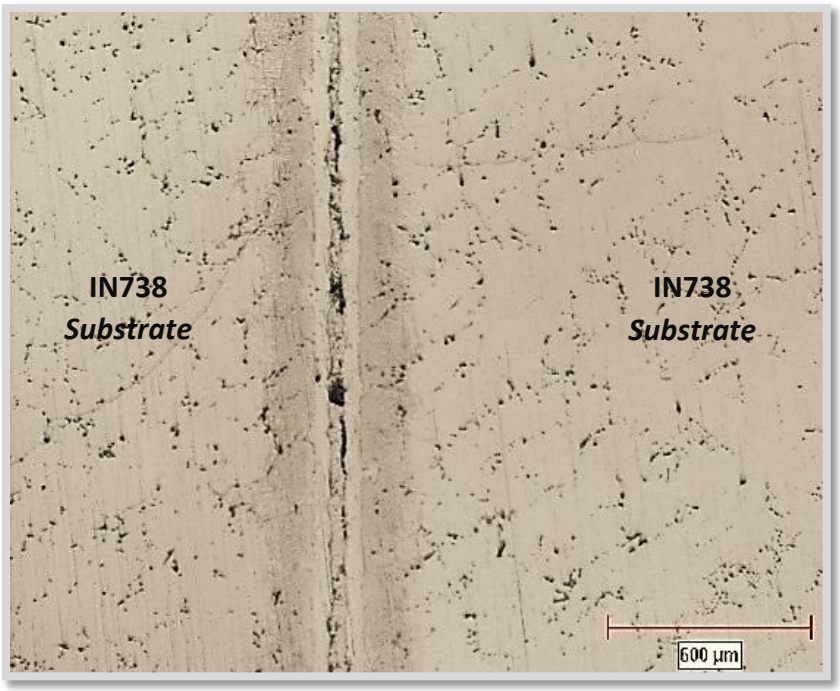

b)

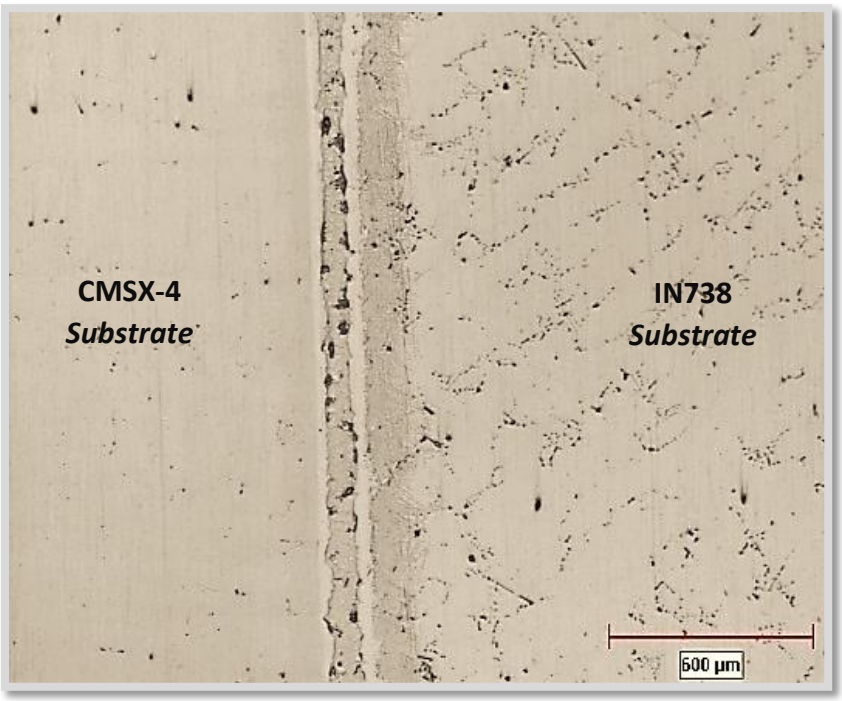

Figure 3.9 - Optical micrographs of joint prepared at 1150^{0}C for 1hr between a) IN738 & IN738 SX's, and b) IN738 & CMSX-4 SX's.

c)

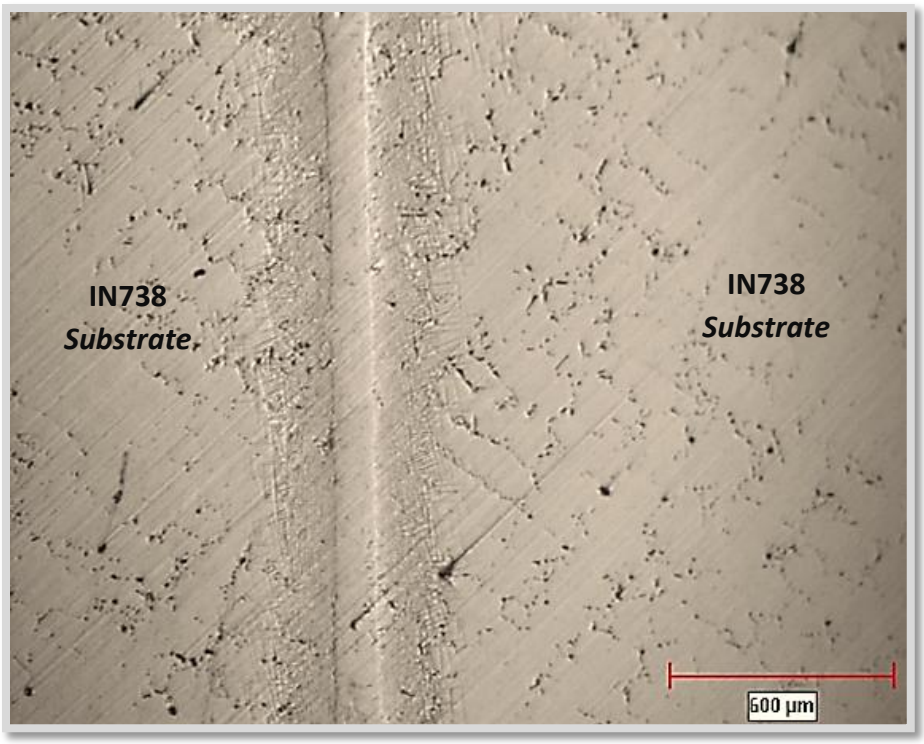

d)

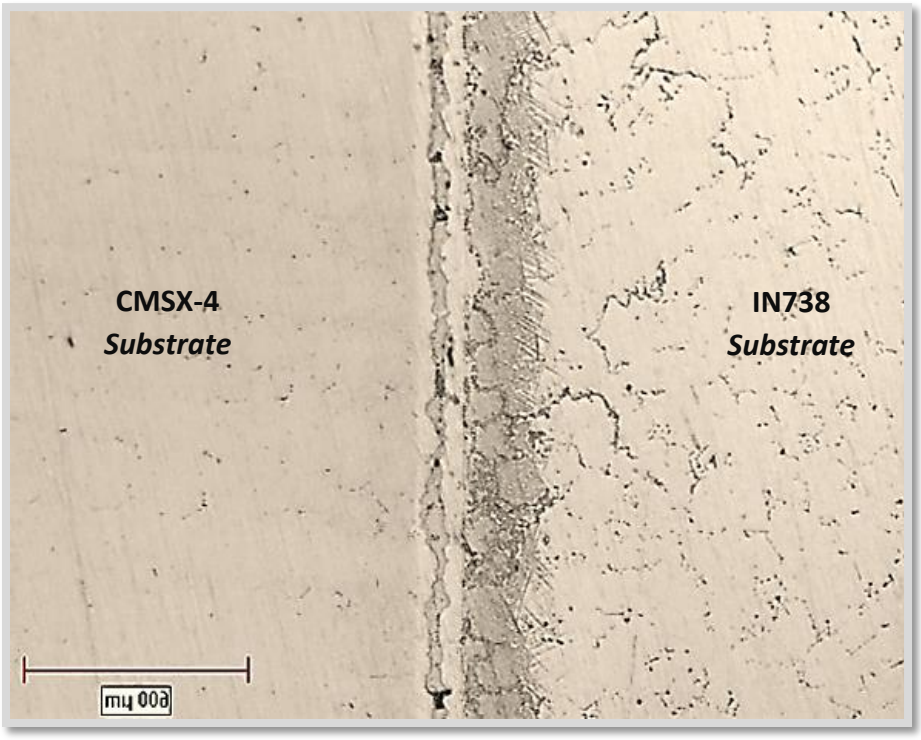

Figure 3.9c,d - Optical micrographs of joint prepared at 1150^{0}C for 5hr between c) IN738 & IN738 SX's, and d) IN738 & CMSX-4 SX's.

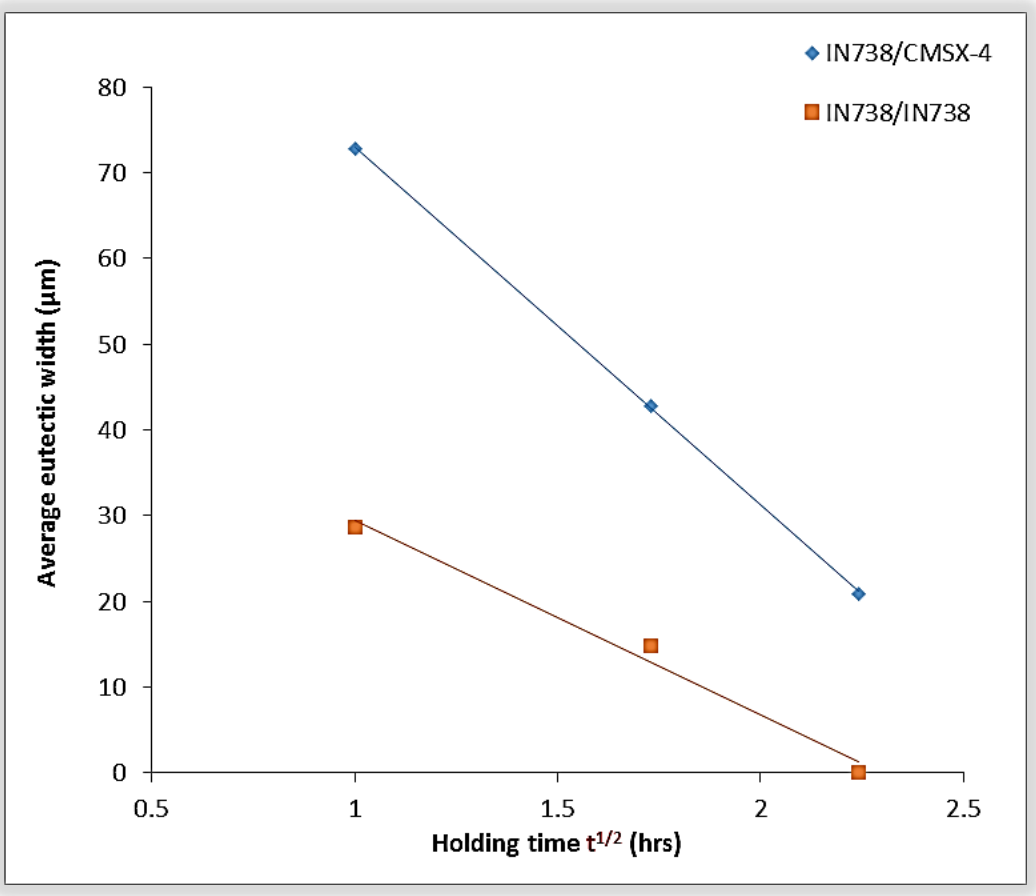

Figure 4.0 - Variation in average eutectic width with bonding time for IN738/IN738 and IN738/CMSX-4 single crystals at 1150^{0}C.

Therefore, when joining CMSX-4 SX superalloys to other Ni-based SX superalloys by TLP bonding, an increased bonding time can be required to facilitate eutectic dissolution within the joint.

4.2.6 Reduction in processing time during TLP bonding of CMSX-4 and IN738 SX superalloys.

As mentioned in the literature, a key parameter when considering TLP bonding for commercial applications is to obtain a suitable holding time in order to achieve an eutectic-free joint at a specifically operating temperature. Since the investigation above has shown that the processing time (t_f) during TLP bonding of IN738 and CMSX-4 SX superalloys is typically long, this can limit the commercial application of TLP bonding for the joining of dissimilar materials. Theoretically, $\frac{\partial c}{\partial t}$ (changes in solute concentration with time) from Fick's second law of diffusion (Equation 12) provides an indication of the isothermal solidification rate.

$$\frac{\partial c}{\partial t} = D\frac{\partial^2 c}{\partial x^2} \qquad (12)$$

where D (diffusion coefficient of boron into the substrates) strongly depends on the bonding temperature, and $\frac{\partial^2 c}{\partial x^2}$ (concentration gradient of the diffusing boron) is influenced by its solubility into the substrates. However, for a fixed bonding temperature and initial gap size, an increase in the rate of isothermal solidification is a consequent of limiting the extent at which the concentration gradient of boron diffusing into the IN738 and CMSX-4 substrates is reduced. Therefore, as already reviewed in the literature, one of the efficient ways to increase $\frac{\partial^2 c}{\partial x^2}$ is by reducing the amount of boron that might diffuse out of the joint into the CMSX-4 and IN738

substrates. This has been reported to be feasible by applying a composite powder mixture that contains a filler alloy powder and another type of powder (gap-filler powder) which is free of the MPD solute, as the interlayer material. In addition, this approach has also been reported to be extensively favorable as it causes enrichment of the joint with base metal alloying elements as well as reduces the liquid phase erosion of the substrate materials [60]. For these reasons, the influence of a composite powder mixture of commercial- and gap filler alloys as the interlayer material, which has been used by different researchers for wide-gap TLP bonding, and particularly on similarly based materials [73] [60] [84] [85] [86], was also examined on the joint microstructure of bonded IN738/CMSX-4 SX substrates. However, it has been reported from previous experimental studies that, complete melting of a composite powder mixture with a volume ratio of commercial Ni-Cr-B filler alloy powder to that of IN738 base alloy powder ($R_{CF/B}$) of 7:3 occurred at 1150^0C [60].

In this study, IN738 and CMSX-4 SX samples were bonded and compared at a bonding temperature of 1160^0C for various holding times by using:

1. a composite powder mixture of filler alloy (AMDRY 775) and gap-filler alloy (IN738) ratio ($R_{CF/B}$) of 70:30, and
2. a 100% filler powder.

Figure 4.1 shows the variation in AEW with [holding time] $^{1/2}$ for both the composite powder interlayer and the 100% filler powder. As shown in this figure, a comparison between the average values of the eutectic width shows that the use of the composite powder mixture has the advantage of producing smaller eutectic width compared to the 100% filler powder. This would therefore imply that the time required to complete solidification will be less when using a composite powder interlayer as opposed to only filler powder. As such, Figure 4.2 shows that

while a continuous eutectic is formed within the brazed region of the joint prepared with only AMDRY 775 powder at 1160^0C after a holding time of 7 hrs and 30 minutes, a joint that was prepared with the composite powder mixture at the same initial temperature, gap size and bonding time was found to be completely free of the eutectic.

Crystallographic orientation by electron backscattered diffraction (EBSD) technique was performed on the completely solidified joint produced from the composite powder mixture. The EBSD pattern within the joint region, as shown in figure 4.2c reveals the formation of a joint free of grain boundaries. Therefore, in addition to reducing the time required to complete solidification during the TLP bonding of dissimilar SX substrates, the use of the composite powder mixture also produced a single crystal joint.

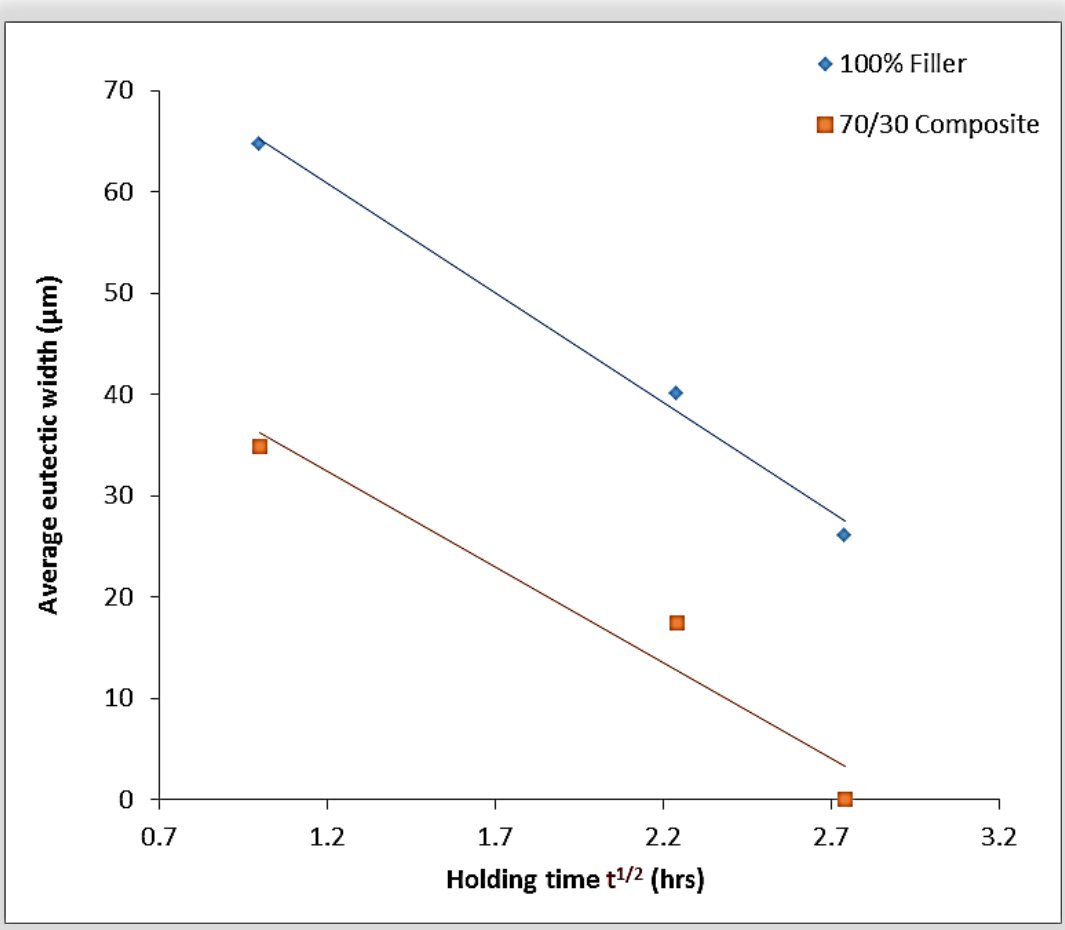

Figure 4.1 - Variation in average eutectic width with square root of bonding time for IN738/CMSX-4 SX's at 1160^{0}C by using the 100% filler powder and composite powder mixture.

a)

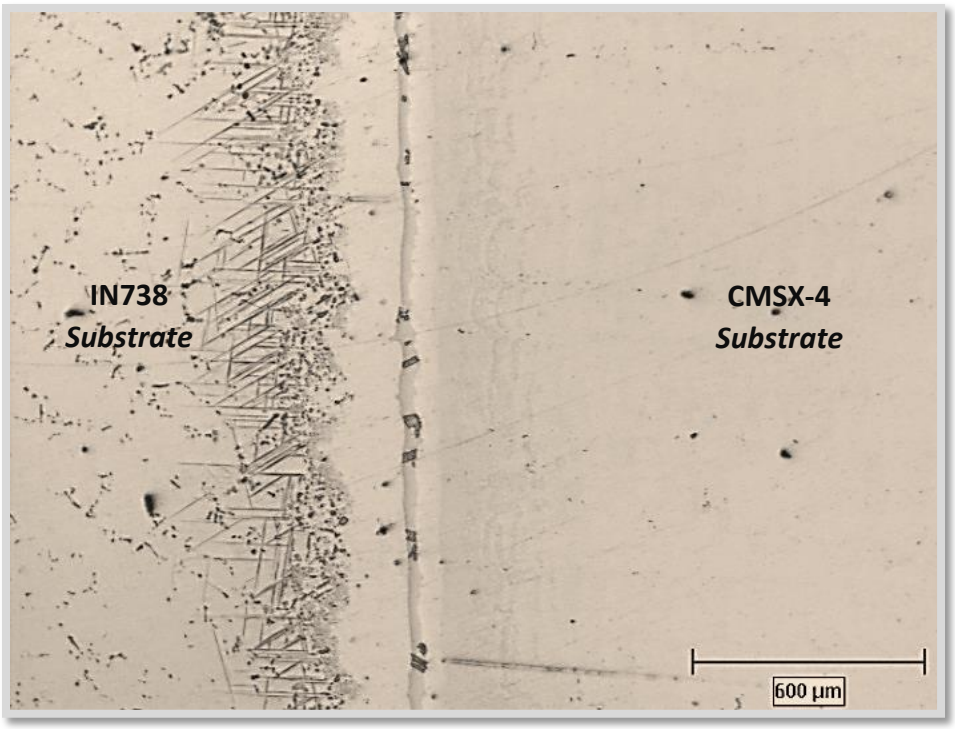

b)

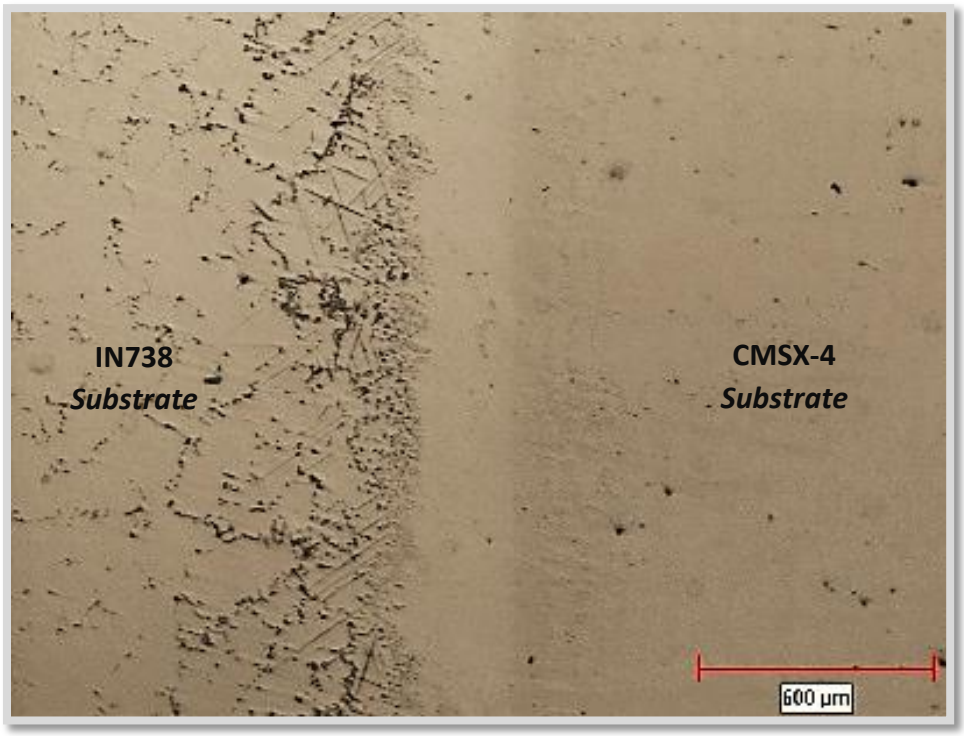

Figure 4.2 - Optical micrographs of joint between IN738/CMSX-4 SX are prepared at 1160^{0}C for 71/2hrs using: a) 100% filler powder and b) 70/30% composite powder mixture.

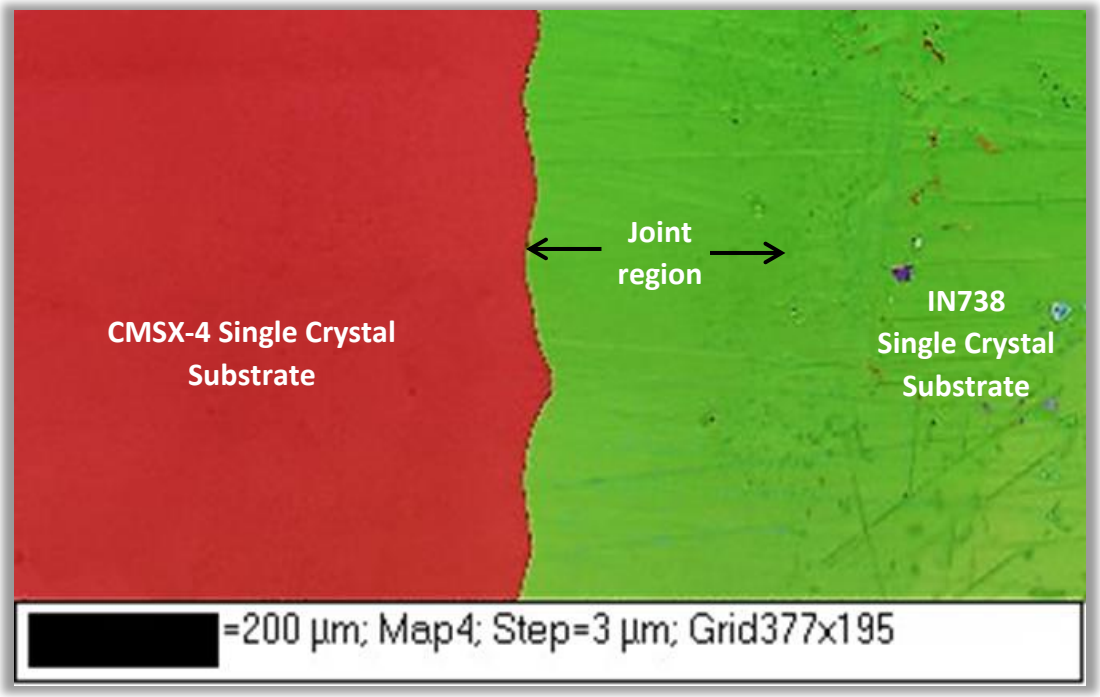

Figure 4.2c – OIM map of IN738/CMSX-4 SX TLP bonded joint prepared with a composite powder mixture that comprises of 70% filler and 30% base alloy powder.

4.2.7 Influence of liquid-state diffusion on microstructure

One of the main advantages of TLP bonding is the elimination of cracks that plagues welded superalloys. However, inadequate TLP bonding time leads to incomplete isothermally solidified joint that is unfavorable for the joint strength. Nevertheless, the joining of two dissimilar superalloys together by TLP bonding can induce Liquid-state diffusion (LSD), but its influence so far has been generally ignored since solid-state diffusion has been considered as the controlling factor of the process. For example, by using the test samples in this research work as a case study, in a situation where IN738 and CMSX-4 SXs are joined together by TLP bonding, the asymmetric microstructure (Figure 4.3) observed in the joint region when isothermal solidification is not fully completed has been conventionally attributed to the mismatch in solid-state diffusion that take place in the substrates.

Recently, Bigvand and Ojo [87] used numerical modeling to show that during TLP bonding, asymmetric eutectic can also be produced by LSD (Figure 4.4). If the asymmetric microstructure is produced by mismatch of solid-state diffusion, then the width of the isothermally solidified zone ahead of the CMSX-4 (ISW (CMSX-4)) as denoted in figure 4.5 will always increase with holding time. However, if the asymmetric microstructure is caused by LSD, then the ISW (CMSX-4) will initially increase and later decrease with holding time

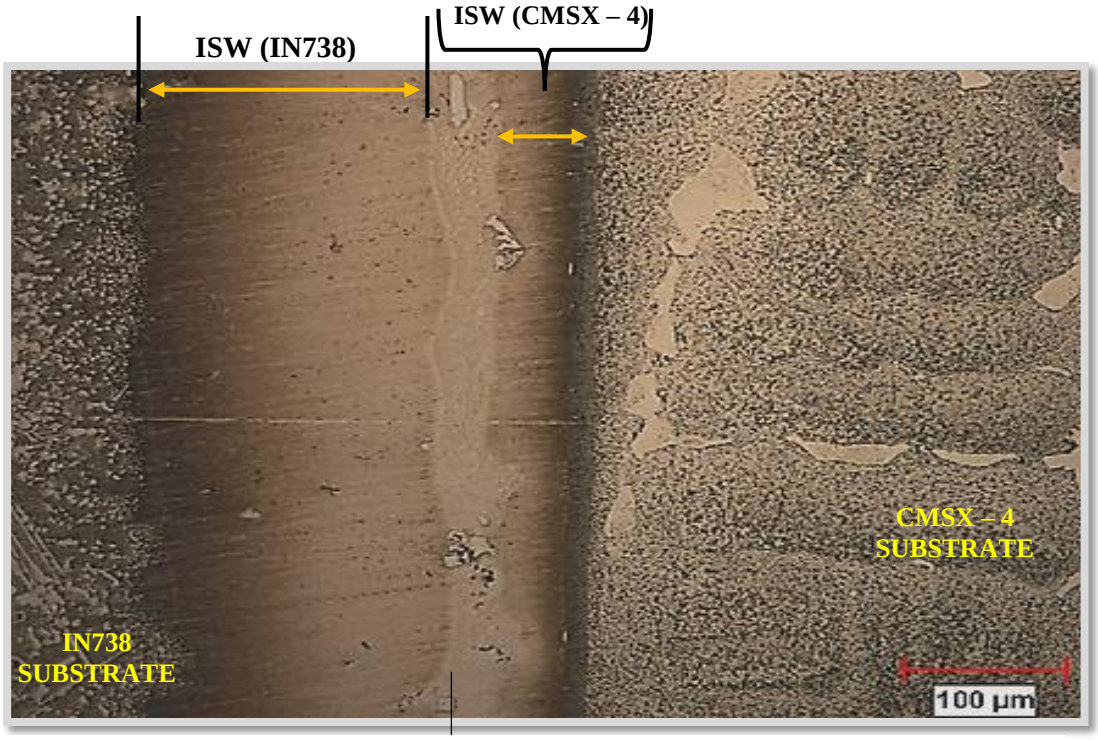

Figure 4.3 - Micrograph of a joint between IN738 & CMSX-4 SX's prepared at 1160^{0}C for 5hrs.

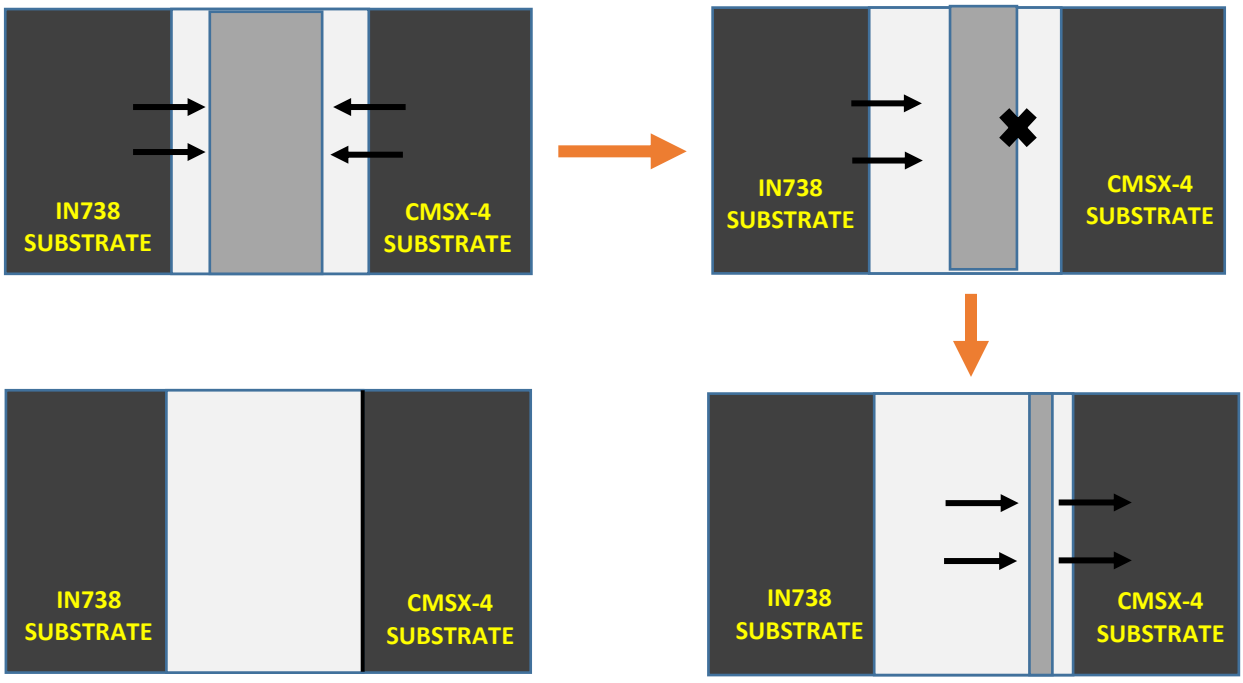

Figure 4.4 - Schematic illustration of the proposed development of asymmetric joint microstructure caused by LSD [87].

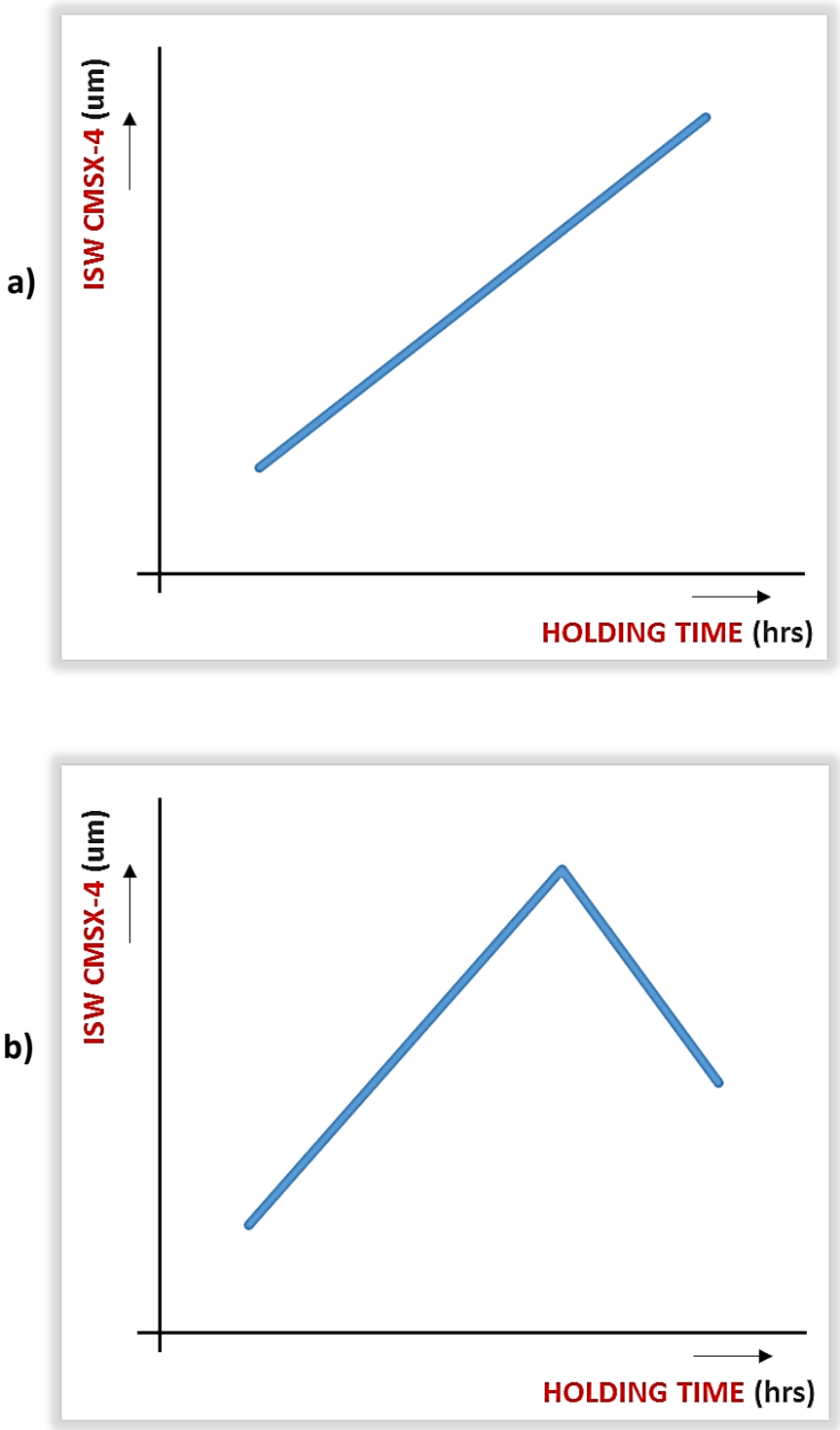

Figure 4.5 - Variation of ISW in the CMSX-4 region with bonding time, due to a) Conventional TLP bonding mechanism (no liquid-phase diffusion) and b) proposed mechanism (presence of liquid-state diffusion).

An experimental work was conducted to investigate which of the two mechanisms, mismatch of solid-state diffusion or LSD, occur during the joining of IN738 and CMSX-4 SX superalloys. Joints fabricated in a vacuum furnace by using a fixed temperature of 1160^0C and different holding times (1 hr, 3 hrs, 5 hrs, 8 hrs and 10 hrs respectively) were used.

The microstructure of the joint region as observed in the transversely sectioned samples after 1 hr, 5 hrs, and 8 hrs of holding time are shown in Figure 4.6. The ISW (CSMX-4) bordered by the eutectic and the CMSX-4 substrate is indicated by **A** in this figure. The variation of this value with holding time is shown in Figure 4.7.

The results show that, the average value of the ISW (CMSX-4) after 1 hr of holding time is 22.76 μm, and the bonded sample that was created with a holding time of 5 hrs subsequently has an increase in the ISW (CMSX-4) value. The average ISW (CMSX-4) was found to be 36 μm after 5 hrs of holding time. This increase in the ISW (CMSX-4) value from 22.76 μm to 36 μm with increase of holding time indicates that the solidification mechanism is attributed to the solid-state diffusion that is taking place in the CMSX-4 and IN738 substrates. However, at a longer exposure time of 8 hrs, the average value of ISW (CMSX-4) is 33.59 μm, and a decrease in this value was observed as the holding time was further increased.

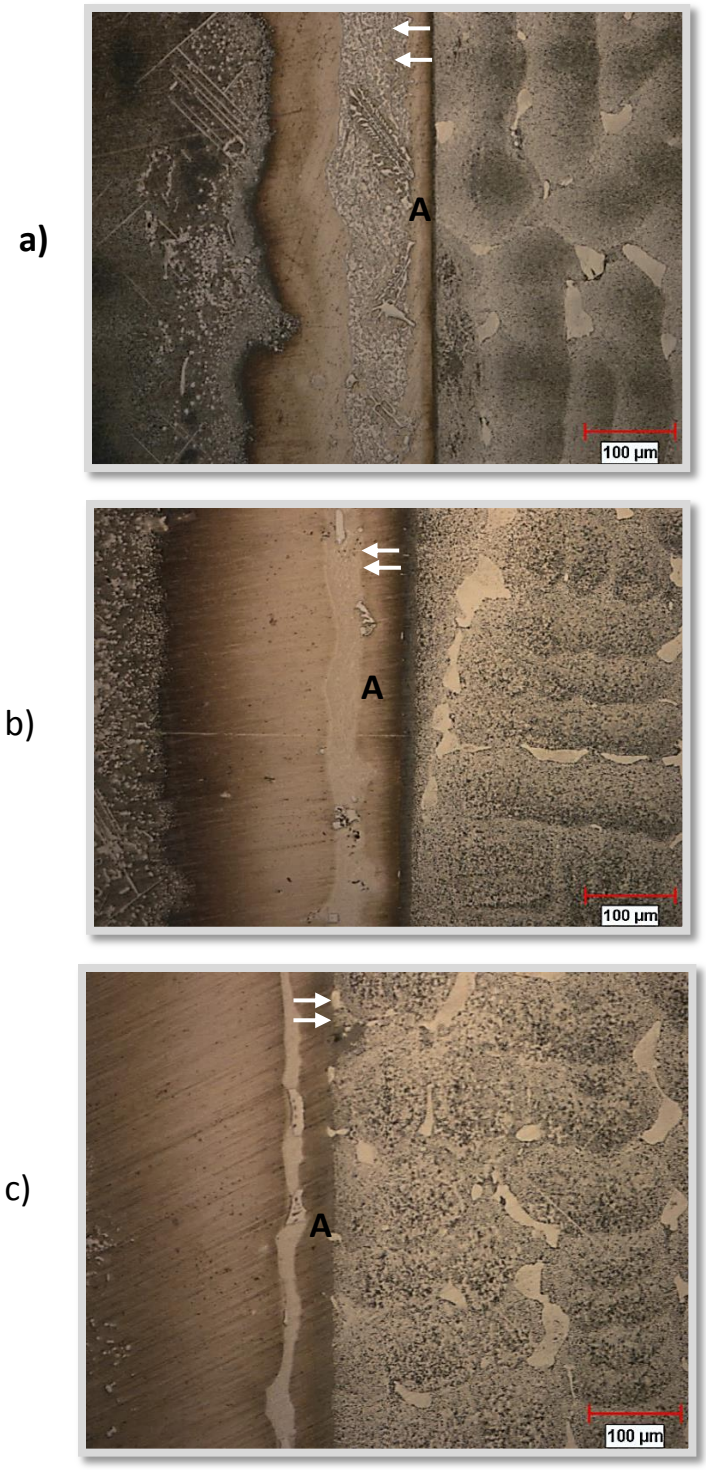

Figure 4.6 - Optical micrographs of 70um IN738/CMSX-4 bonded joints showing the variation of ISW in the CMSX-4 region with holding times of: a) 1hr, b) 5hrs and c) 8hrs respectively; at a bonding temperature of 1160^{0}C.

Holding time (hrs)	ISW (CMSX-4)	Range of ISW (CMSX-4)	A. Joint width (µm)	Eutectic width (µm)
1	22.76µm	17.62µm - 34.47µm	175.9	64.72
4	34.11µm	19.93µm - 44.27µm	209.1	55.92
5	36µm	23.41µm - 52.03µm	204.3	40.21
8	33.59µm	29.11µm - 44.86µm	205.9	23.14
10	25.18µm	5.31µm - 39.11µm	213.1	14.92 (discontinous)

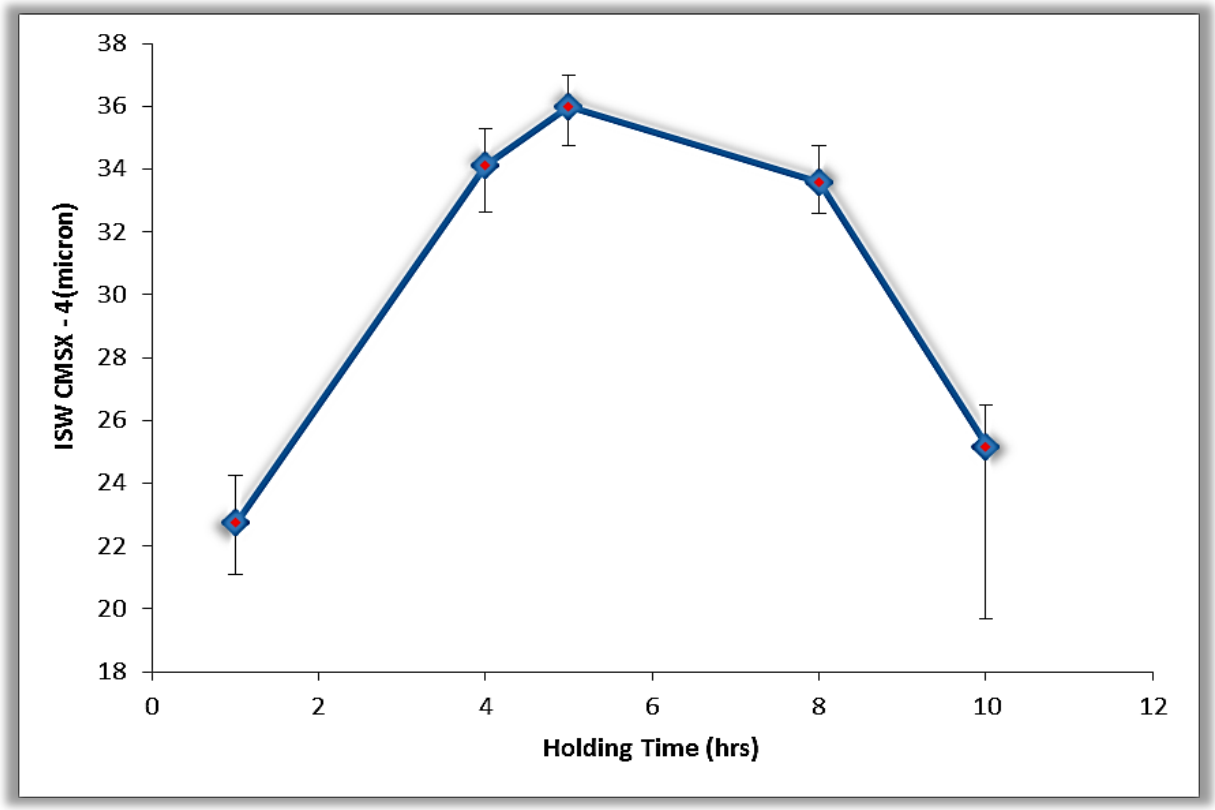

Figure 4.7 - Variation in ISW (CMSX-4) with bonding time for 70µm gap size at 1160^0C

This decrease in ISW (CMSX-4) indicates a unidirectional solidification of the joint with an asymmetric microstructure that is due to the diffusion that took place in the liquid. Therefore, as observed in this work, when joining dissimilar SX superalloys by TLP bonding, the asymmetric microstructure observed in the joint region at short holding times can be attributed to solid-state diffusion, while at longer holding times, the asymmetric microstructure can be attributed to LSD.

Another feature of LSD is that, in the case where two Ni-based SX superalloys with different orientations are bonded, the occurrence of LSD can produce a SX joint. In contrast, without the LSD, a bi-crystal joint will be produced. Figure 4.8 shows the schematic diagram of completely solidified joints with the TLP bonding of IN738 and CMSX-4 substrates following a situation where the influence of liquid state diffusion has been neglected, as well as a situation where its impact is considered.

EBSD by OIM was used to study the crystallographic orientation of the TLP bond between IN738 and CMSX-4 SX, free of the detrimental eutectic in the joint. Figure 4.9 shows that the orientation in the joint region is the same as that in the IN738 substrate, and completely incomparable with the orientation in the CMSX-4 substrate. This suggests that a SX joint was produced. Inverse pole figure (IPF) in Figure 5.0 is used to support this information by randomly choosing two different points in the CMSX-4 substrate, joint region and IN738 substrate. The formation of a SX joint which is not exclusively achievable by solid-state diffusion is confirmed by the stereographic analysis.

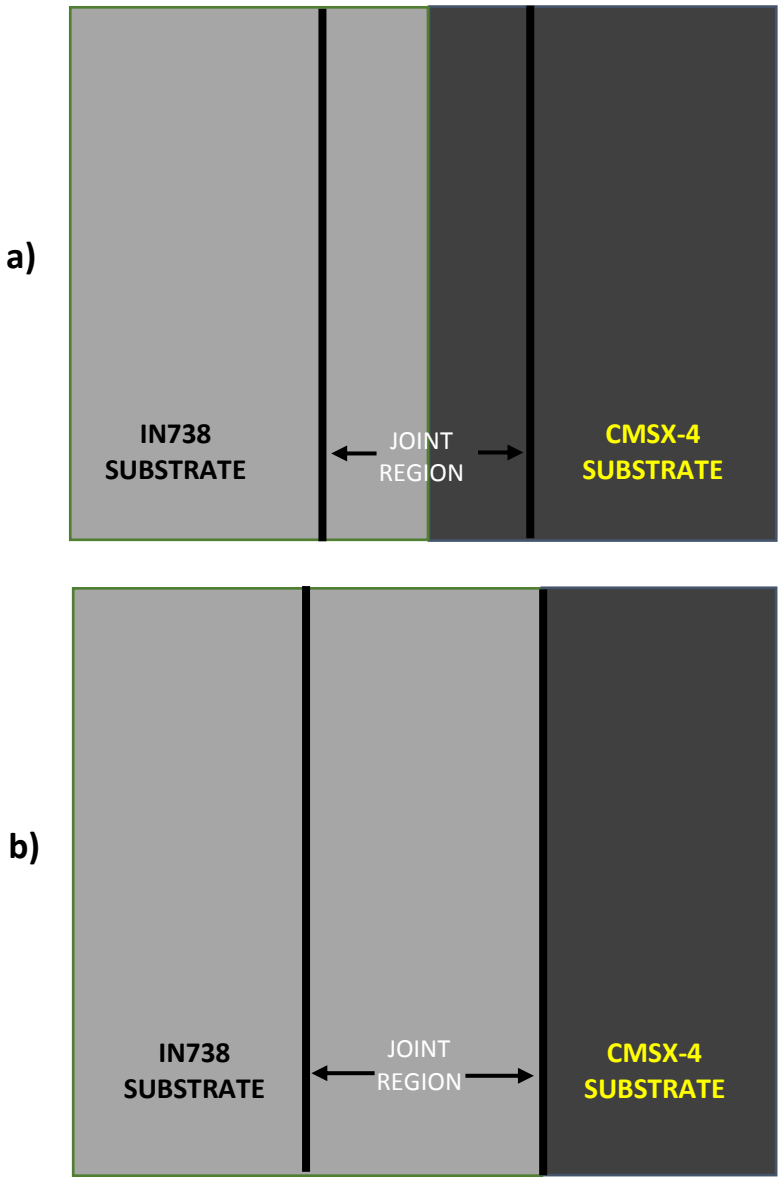

Figure 4.8 - Schematic diagram of completely solidified joints for dissimilar TLP bonded substrates a) With and b) without the influence of liquid-state diffusion.

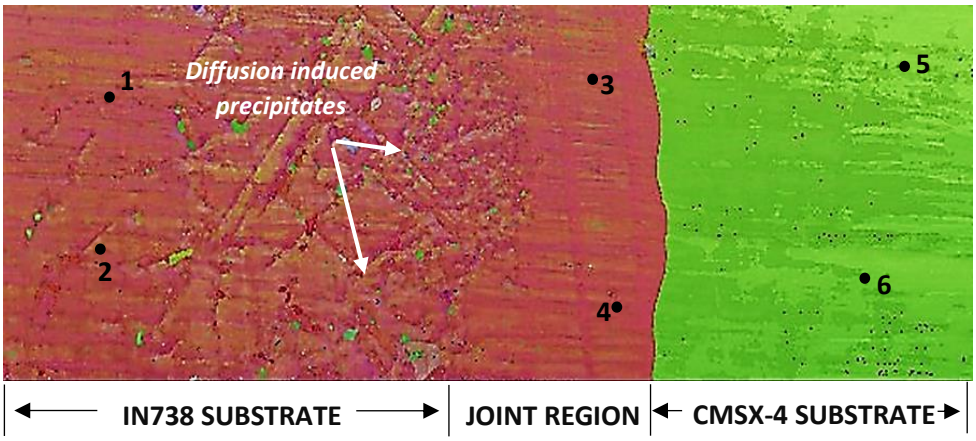

Figure 4.9 - Electron backscattered pattern of an OIM mapped region across a completely solidified CMSX-4/IN738 bonded joint (same color signifies same orientation).

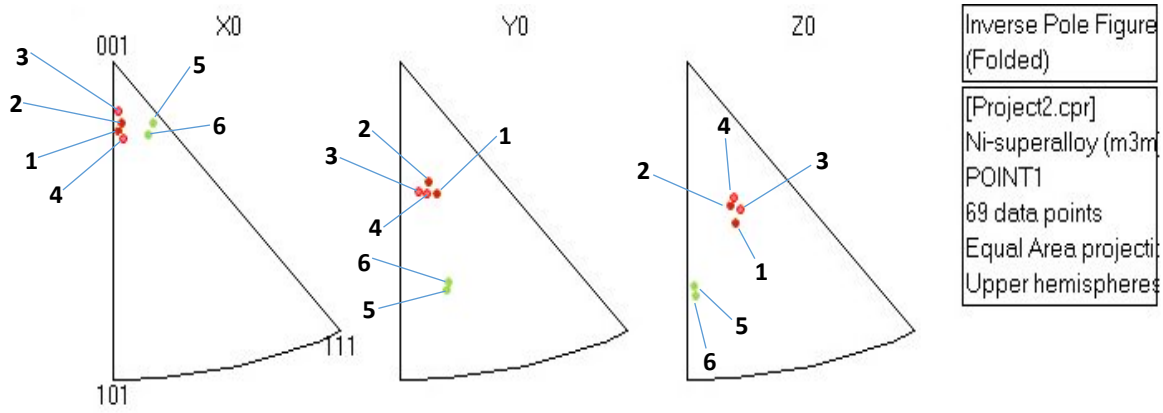

Figure 5.0 - Inverse pole figure of the above OIM mapped region.

Thus, in terms of the joint grain structure, the occurrence of LSD which has been generally ignored in the literature has an essential role during the TLP bonding of dissimilar materials. In the aerospace industry, there are interests in joining SX to polycrystalline materials by TLP bonding. In such a situation, the occurrence of LSD can either produce a SX joint instead of a polycrystalline joint or vice versa, depending on the nature of the materials being joined. In this work, a Ni-based SX superalloy material and a Co-based polycrystalline alloy were bonded at 1160^0C for 20 hrs. Figure 5.1a shows an optical micrograph of the different grains observed in the Co-based alloy. The microstructure of the joint after etching (Figure 5.1b), and EBSD crystallographic orientation analysis (Figure 5.2) reveals the formation of a SX joint instead of a polycrystalline joint. Similarly, the microstructure of the TLP bonded joint between IN738 SX and ATI 718Plus polycrystal substrates as shown in figure 5.3 also produced a SX joint. However, in a situation where IN738 polycrystalline substrate was bonded to CMSX-4 single crystal (figure 5.4), a polycrystalline joint was produced.

a)

b)

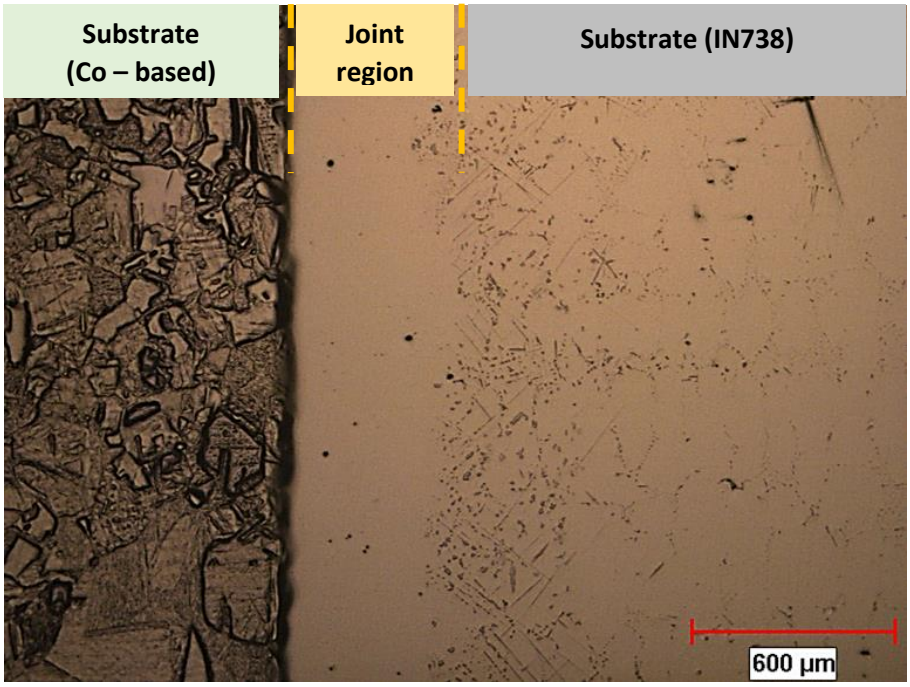

Figure 5.1 - Optical micrograph of a) Co – based alloy showing grain boundaries and b) Co-based/IN738 TLP bonded joint

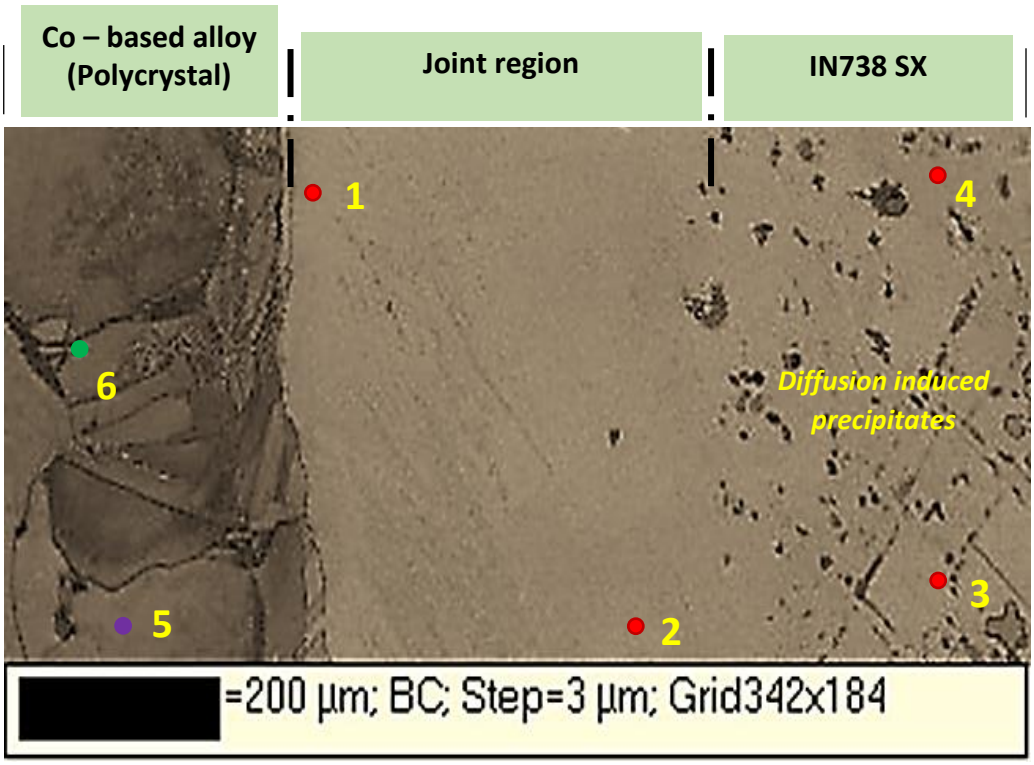

Figure 5.2a – Orientation Image Microscopy (OIM) mapped region across a completely solidified Polycrystalline (Co – based) /Single crystal (IN738) bonded joint.

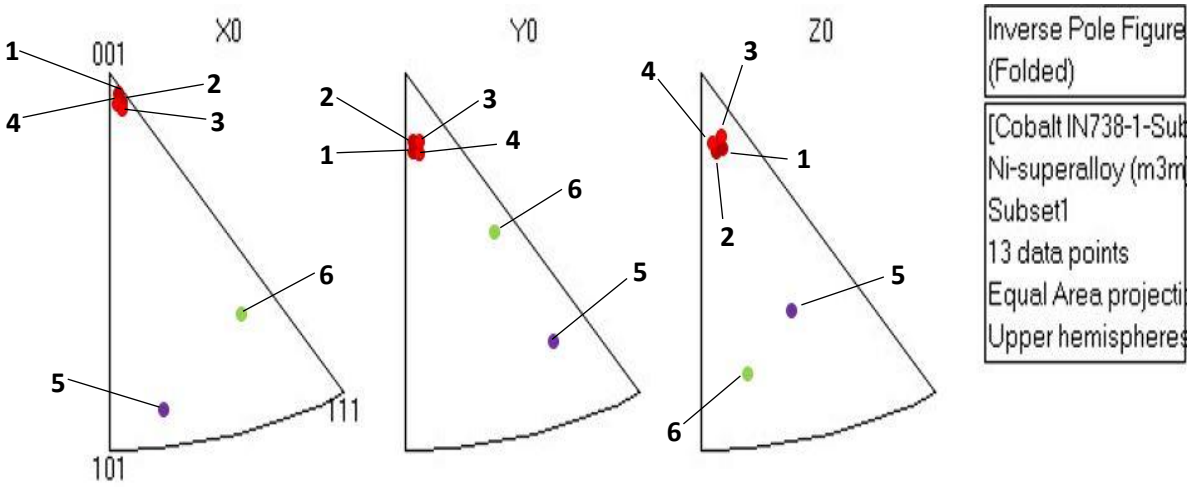

Figure 5.2b - Inverse pole figure of the above OIM mapped region (same color signifies same orientation).

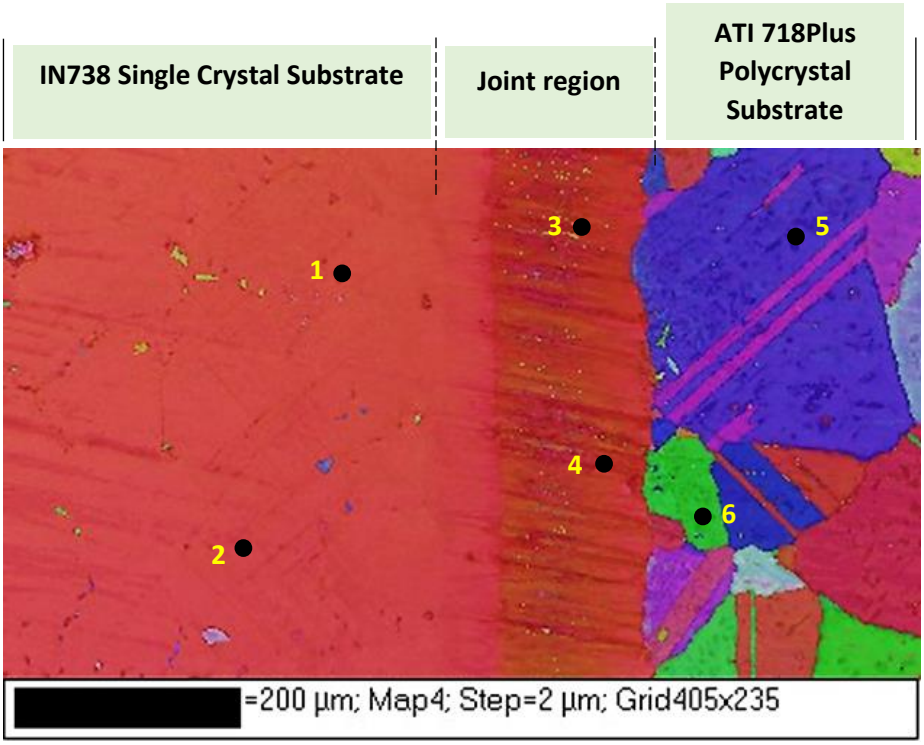

Figure 5.3a – Orientation Image Microscopy (OIM) mapped region across a completely solidified Polycrystalline (ATI 718Plus) /Single crystal (IN738) TLP bonded joint.

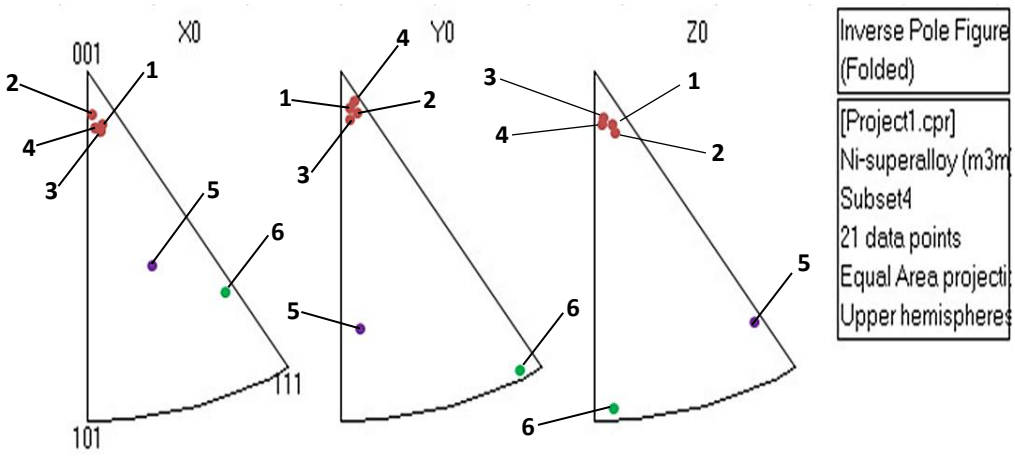

Figure 5.3b - Inverse pole figure of the above OIM mapped region (same color signifies same orientation).

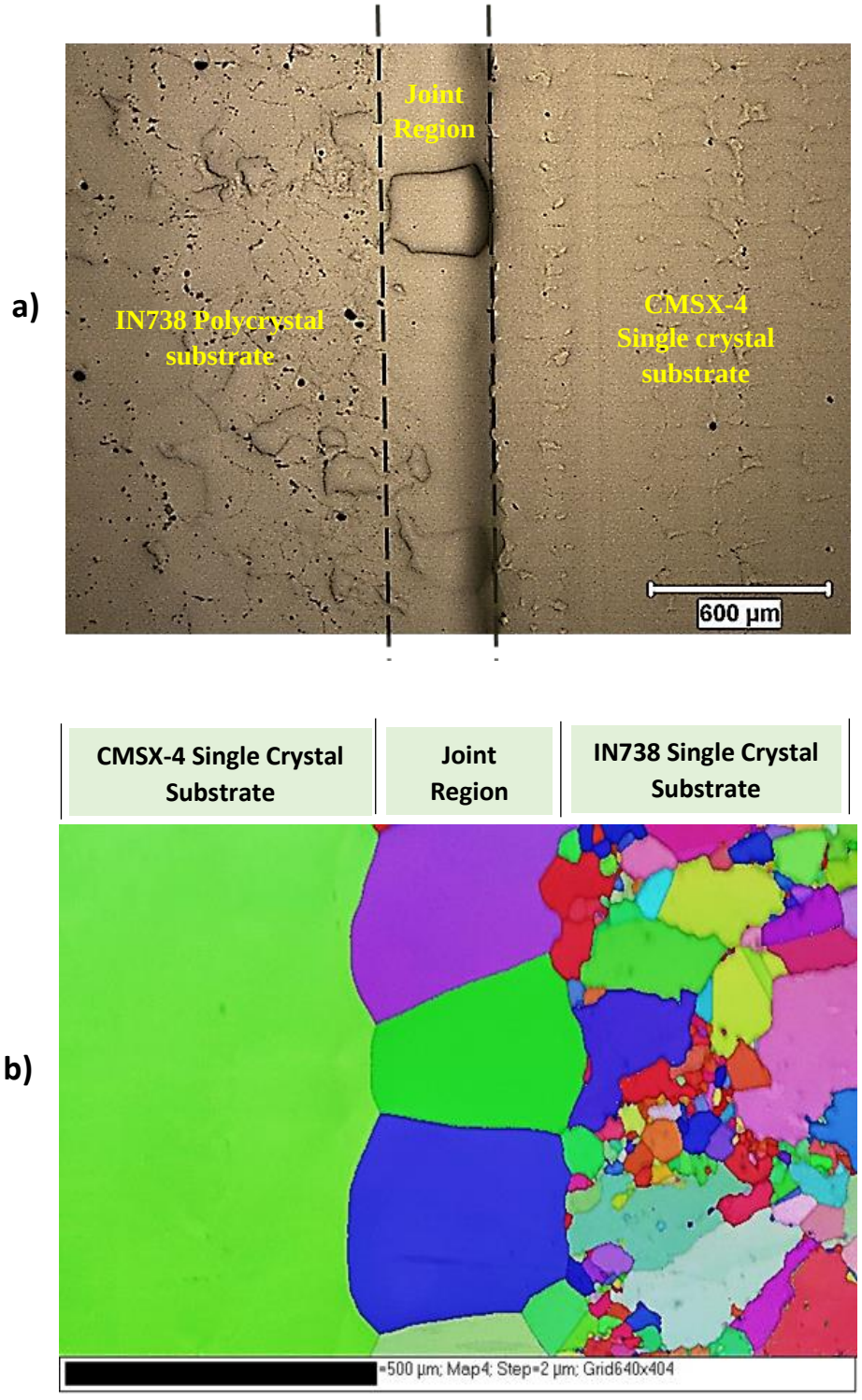

Figure 5.4 – a) Optical micrograph and b) Orientation Image Microscopy (OIM) mapped region, across a completely solidified Polycrystalline (IN738) /Single crystal (CMSX-4) TLP bonded joint.

4.2.8 Influence of liquid-state diffusion on isothermal solidification kinetics

In theory, it has always been stated that when LSD takes place, the rate of isothermal solidification will be controlled by rapid liquid-state diffusion, and that the rate will be faster than that controlled by solid-state diffusion. However, recently, Bigvand and Ojo [88] used a numerical approach to show that, when LSD occurs, the solid-state diffusion can still control the rate of isothermal solidification. In this work, an experimental study of the isothermal solidification rate during the TLP bonding of IN738 and CMSX-4 SX superalloys was carried out by using 100% filler powder as the interlayer material with an initial gap of 127 μm.

Figure 5.5 shows the variation in ISW (CMSX-4) with holding time at the bonding temperature of 1160^0C. By confining the analysis to the domain where ISW (CMSX-4) increased with time (that is, the solid-state diffusion zone), the result shows that the AEW after 1 hr and 11 hrs of holding time are 143.58 μm and 41.78 μm, respectively. This means that within 10 hrs, 102 μm of the residual liquid had completely solidified. In this case, the rate of solidification is 10.2 μm/hr. In the region where LSD occurred, after 13 hrs of holding time, the AEW is 23.96 μm; and after 15 hrs, the AEW is 19.21 μm. As such, within 2 hrs, 4.75 μm of the residual liquid had solidified. Accordingly, the solidification rate is 2.375 μm/hr. Therefore, from the results, the rate of solidification when LSD occurred is not faster than the rate of solidification controlled by solid-state diffusion. Furthermore, the experimental results display a linear relationship between the AEW and the square root of the isothermal solidification holding time during the stages with and without LSD (Figure 5.6). This shows that, the occurrence of LSD does not necessarily mean faster isothermal solidification rate due to rapid diffusion within the liquid.

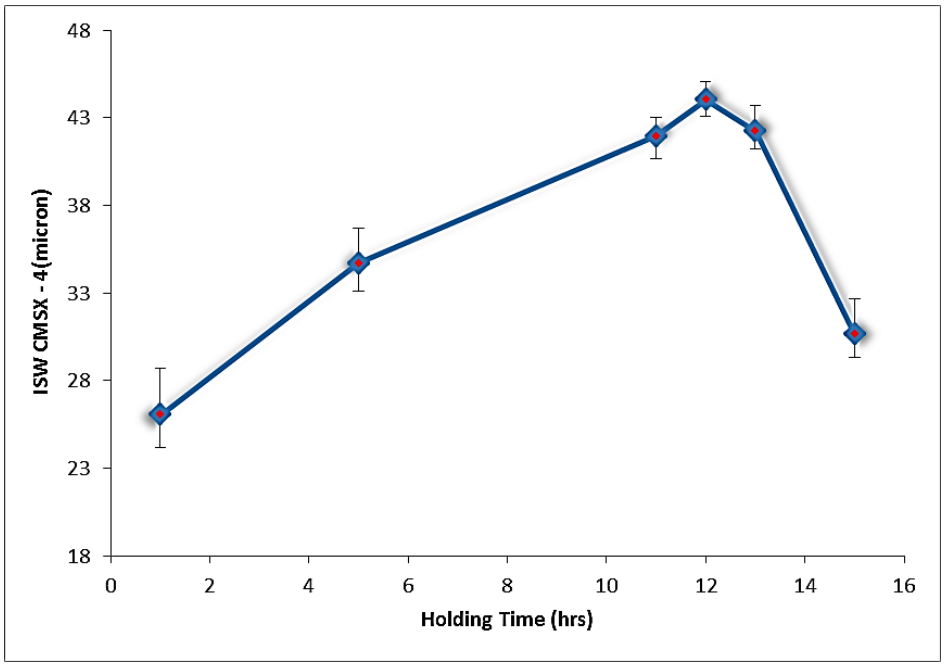

Figure 5.5 - Variation in ISW (CMSX-4) with bonding time for 127µm gap size at 1160^{0}C

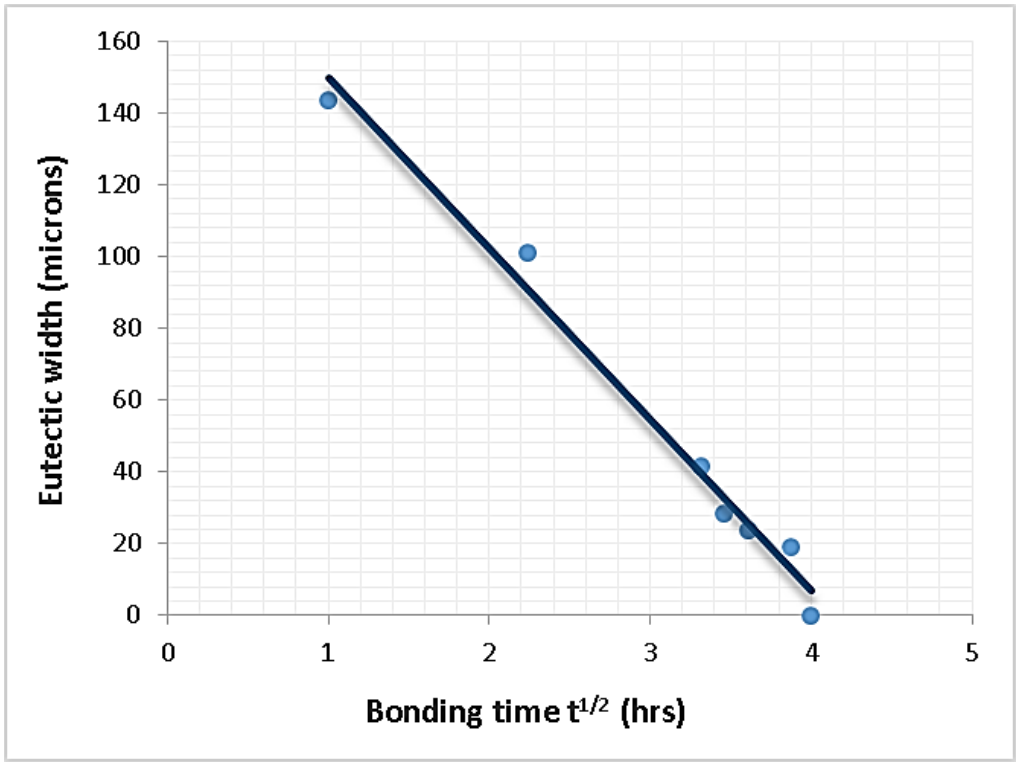

Figure 5.6 - Variation of eutectic width with bonding time for 127µm gap size at 1160^{0}C

CHAPTER 5 – CONCLUSIONS AND SUGESTIONS FOR FUTURE WORK

5.1 Summary and conclusions

A study on the effects of the TG in a vacuum furnace on temperature distribution in TLP bonded specimens have been carried out by using numerical simulation with ANSYS software package and experimental investigation.

1. It is observed that, in spite of presence of TG in a furnace, a symmetric temperature distribution in bonded samples with similar substrates can be obtained anywhere inside the vacuum furnace as long as the diffusion direction is parallel to that of the source of heat emission in the furnace. This implies that a symmetric TLP joint microstructure can be obtained notwithstanding the TG in a furnace.
2. Nevertheless, to minimize the TG in the sample, in order to minimize the residual stress, the best position to place TLP bonded samples inside the vacuum furnace is at the center of the furnace.

Experimental investigations were carried out to examine the effect of the bonding parameters and interlayer characteristics on the microstructure of TLP bonded IN738 and CMSX-4 SX specimens. The results show that:

1. deleterious eutectic micro-constituents form from the residual liquid of the interlayer due to incomplete isothermal solidification during cooling to room temperature,
2. an increase in gap size reduces the time required to achieve complete isothermal solidification of the liquid within the joint,

3. an increase in bonding temperature from 1150^0C to 1160^0C initially increased the rate of isothermal solidification of the liquid within the joint. However, a further increase in the temperature from 1160^0C to 1190^0C caused a decrease in the solidification rate, which can be attributed to the decrease in boron solubility with increase in temperature,
4. the time required to complete isothermal solidification is observed to be longer during the TLP bonding of dissimilar materials (IN738/CMSX-4 SX) than IN738/IN738 SX, when a Ni-Cr-B filler alloy powder was used as the interlayer material,
5. the use of composite powder mixture that comprises a 70% filler and 30% base alloy powder instead of the conventionally used 100% filler alloy powder caused a considerable decrease in isothermal solidification time, and also resulted in the formation of a single crystal joint,
6. aside from what has been generally reported in the literature in that a joint with an asymmetric microstructure during TLP bonding of dissimilar substrates is attributed to the mismatch in solid-state diffusion in the substrates, it has been experimentally confirmed by this study that LSD can also produce a joint with an asymmetric microstructure, as suggested by Bigvand and Ojo [87] who used numerical modeling,
7. it has also been shown that in the case where a SX and polycrsytal substrate are bonded, the occurrence of LSD produced a SX joint instead of a polycrsytal joint. The formation of a SX joint between a SX and polycrsytal substrate, which is not achievable by solid-state diffusion, has not been previously reported in the literature,
8. although it is generally expected that the presence of LSD would imply a faster rate of solidification, the results obtained from the experimental investigation showed that the rate of solidification in the solid-state region is comparable to that in the liquid-state

region. As such, the rate of solidification is still controlled by the diffusion mechanism that is taking place in the solid, as proposed by Arian and Ojo [88] who used a numerical approach.

5.2 Future work.

1. It has been reported that second phase precipitates that form within the DAZ in bonded materials could have damaging effects on high temperature properties of such materials [89]. Further work is therefore recommended to study the influence of post bond heat treatment to remove these precipitates within the DAZ in bonded materials used in this work.
2. The effect of such post-bond heat treatment, on mechanical properties, such as fatigue and creep properties, of bonded materials should be investigated.

REFERNCES

[1] E.F Bradley, "Materials for elevated temperature applications," American Society for Metals, pp. 275-298, 1969.

[2] G.P Sabol and R Strekler., "Microstructure of Ni-based Superalloys," Westling house research laboratories, vol. 35, no. 11, 1969.

[3] E.F Bradley., "Superalloys: A technical guide," ASM International, 1988.

[4] A. K Jena and M. C Chaturvedi, "The role of alloying elements in the design of Nickel base Superalloys," J. Mat Sci, vol. 19, pp. 3121-3139, 1984.

[5] C.T Sims., "Superalloys: Genesis and characteristics in superalloys II," pp. 3-21, 1987.

[6] D.S Duvall, W. Owczarski and D. Paulonis., "TLP bonding: A new method for joining heat resistant alloys," Weld Journal, vol. 53, pp. 203-214, 1974.

[7] http://www.france-metallurgie.com/index.php/2015/07/06/kikuchi-gear-to-supply-titanium-aluminide-blades-to-snecma-us/

[8] J. Matthew Donachie and J. Stephen Donachie., "A Technical Guide of Superalloys", 2nd ed., the Materials Information Society, 2002.

[9] C Sims, N. Stoloff and W. Hagel., "Fundamentals of Strengthening in Superalloys II," John Wiley & Sons, pp. 61-96, 1987.

[10] M. Durand - Charre, "The Microstructure of Superalloys," CRC Press, February 1998.

[11] R. Quigg and H. Collins "Carbide and Intermetallic Instability in Advanced Ni-base Superalloys," Transaction ASME, vol. 61, pp. 139-148, 1968.

[12] T.J Garosshen and G. McCarty, "Low Temperature Carbide Precipitation in a Nickel base Superalloy," Metallurgical Trans, vol. 16A, p. 1213, 1985.

[13] H. Beattie and W. Hagel, "Iron & Steel Institute Special Report," vol. 64, 1959.

[14] Ken Harris, B. Jacqueline, "Improved Single Crystal Superalloys (CMSX-4)," TMS (The Minerals, Metals & Materials Society), pp. 45-52, 2004.

[15] B Geddes, H. Leon and X. Huang, "Superalloys: Alloying and Performance," ASM International.

[16] W. Hagel and C. Sims, "The Superalloys: Vital High Temperature Gas Turbine Materials for Aerospace and Industrial Power", USA, p. 595.

[17] M.C Thomas, "Manufacturing Property and Turbine Engine Performance of CMSX-4 Single Crystal Airfoils," pp. 3-6, October 1994.

[18] P. Burkholder et al, "Allison Engine Testing CMSX-4 Single Crystal Blades and Vanes," in Proceedings of 3rd International Charles Parson Turbines Conference, London (UK), 1995.

[19] K. Fullagar et al, "Aero Engine Test Experience with CMSX-4 Alloy Single Crystal Turbine Blades," Transactions of the ASME, vol. 118, pp. 380-388, April 1996.

[20] A. Mottura and C. Reed, "What is the role of Rhenium in Single Crystal Superalloys," EDP Sciences, pp. 1-6, 2014.

[21] W. Brentnall et al, "Extensive Industrial Gas Turbine Experience with Second Generation Single Crystal Turbine Blades," in International Gas Turbine and Aero engine Congress and Exhibition, Orlando, 1997.

[22] R. Broomfie et al, "Development and Turbine Engine Performance of Three Advanced Rhenium Containing Superalloys for Single Crystal and Directionally Solidified Blades & Vanes," ASME, vol. 120, 1998.

[23] D. Doll, "Competitive Requirements for Refurbishment of Gas Turbine Components," in Gas Turbine Materials Technology Proceedings, Illinois, 1998.

[24] J.W Park, S. Babu, J. Vitek, E. Kenik and S. David, "Stray Grain Formation in Single Crystal Ni-base Superalloy Welds," J. Application Physics, vol. 94, no. 6, pp. 4203-4209, 2003.

[25] M. Gaumann, S. Henry, F. Cleton, J. Wagniere and W. Kurz. "Epitaxial Laser Metal Forming: Analysis of microstructure formation," Mat. Sci ENG, vol. 271A, pp. 232-241, 1999.

[26] M Gaumann, C. Bezencon, P. Canalis and W. Kurz, "Single crystal Laser deposition of superalloys: processing - microstructure maps," Acta mater, vol. 49, pp. 1051-1062, 2001.

[27] W. Brockmann, P. Ludwig, J. Klingen and B. Schroder. “Adhesive Bonding: Materials, Applications and Technology”, 2009.

[28] "Adhesives, Glues and Sealants," [Online]. Available: www.adhesive and glue.com/adhesive.disadvantage.html.

[29] D. Duvall and W. Owczarski, "Further heat affected zone studies in heat resistant nickel alloys," Weld Journal, vol. 46, no. 9, pp. 423s-432s, 1967.

[30] O Ojo, N. Richards and M. Chaturvedi, "Contribution of Constitutional liquation of Gamma prime precipitations to weld HAZ cracking of cast IN738 Superalloy," Sci Mater, vol. 50, pp. 641-646, 2004.

[31] R. Johnson, Brazing: A high technology joining process, Welding and Metal Fabrication, 1999, pp. 433-440.

[32] M. Nicholas, Joining process: Introduction to brazing and diffusion bonding, Boston: Kluwer Academic Publishers.

[33] W. F Gale, D. A Butts. "Overview: Transient Liquid Phase Bonding,” Sci technology weld, vol. 9, no. 4, pp. 283-300, 2004.

[34] M. Schwartz, Brazing, Materials Park, Ohio: ASM International, 1987.

[35] R. Messier, Joining of Advanced Materials, Boston, Butterworth-Heinemann, 1995.

[36] X. Wu, R. Chandel, H. Li "Evaluation of transient Liquid Phase Bonding between Nickel-based Superalloys," J. Materials Sci, vol. 36, pp. 1539-1546, 2001.

[37] J.D Liu, T. Jin and N. Zhou, "Bonding behavior of single crystal and polycrystal superalloys by transient liquid phase method," Sci Technology weld join, vol. 15, pp. 194-199, 2010.

[38] J.D Liu, T. Jin and N. Zhou, "Microstructural study of transient liquid phase bonded DD98 and K465 Superalloys at high temperature," Elsevier Inc., vol. 62, pp. 545-553, 2011.

[39] T. Funamato, H. Wachi, R. Kajiwara, M. Kato., Joining and Welding Society, vol. 6, pp. 23-29, 1988.

[40] Y Komizo, F. Kashimoto, T. Tomori and K. Ogana., Welding & Joining, vol. 8, pp. 197-204, 1990.

[41] R. Loehmann, "Surfaces and Interfaces in ceramic and ceramic metal systems," Plenum press, pp. 701-711, 1980.

[42] T. Momono, S. Jackson and E. Wallach., "Joining of advanced materials," JWES Research Commission on Welding of Special Material, pp. 68-73, 1993.

[43] D. Duvall, W. Owczarski, D. Paulonis, “Diffusion bonding utilizing Transient Liquid Phase Bonding” US Patent, 1971.

[44] R Thanburaj, W. Wallace and J. Goldak., "Post-weld heat treatment cracking superalloys," Int. Mater Rev, vol. 28, no. 1, pp. 1-22, 1983.

[45] M Mahmoudi, A. Ekrami and A. Kokabi., "Effect of solidification mechanism on microstructure and mechanical properties of joints in TLP Bonded AL2024-T0 alloy," Science and technology of welding, vol. 16, no. 2, 2011.

[46] D. MacDonald, T. Eager., "Transient liquid phase bonding process," The minerals, met and mater society, pp. 93-100, 1992.

[47] Y. Zhou and T. N. W.F Gale, "Modeling of Transient Liquid Phase Bonding," Int. Material Rev, vol. 40, no. 5, pp. 181-196, 1995.

[48] C. Cook and C. Sorensen, "Overview of transient liquid phase and partial transient liquid phase bonding," J Mater. Sci, vol. 46, pp. 5305-5323, 2011.

[49] D. Kim and K. Nishimoto, "Creep rupture and fatigue properties of transient liquid phase bonded joints of Ni-base Single Crystal Superalloys," Mat Science and Technology, vol. 19, pp. 456-460, April 2003.

[50] A. Ghoneim, O. Ojo., “Understanding reversed temperature dependence of diffusional solidification time in single crystal superalloy brazement," vol. 91, pp. 3649-3666, 2011.

[51] M. N Wikstrom, M. O Idowu, O. A Ojo, M. C Chaturvedi., "Deviation from conventional TLP bonding models during diffusion brazing of Ni-base superalloys," Brazing and Soldering: Proceedings of the 3rd International Brazing and Soldering Conference (ASM International), no. 6, pp. 6-11, 2006.

[52] M.N Wikstrom, A. T Egbewande, O. A Ojo. "High temperature diffusion induced liquid phase joining of a heat resistant alloy," Journals of alloys and compounds, vol. 46, pp. 379-385, 2008.

[53] O. A Idowu, N. L Richards, M. C. Chaturvedi "Effect of bonding temperature on isothermal solidification rate during TLP bonding of IN738LC Superalloy," Elsevier, vol. 397, no. 1-2, pp. 98-112, April 2005.

[54] M Abdelfattah, O. Ojo., "On the extension of processing time with increase in temperature during TLP bonding," Metallurgical and materials transaction, pp. 377-385, 2009.

[55] D. Manete, Brazing of heat resistant alloys, vol. 6, Ohio: ASM Handbooks, 1993, pp. 924-930.

[56] R. Saha, T. Khan, "Microstructural developments in TLP bonds using thin interlayers based on Ni-B coatings," Mater character, vol. 60, no. 9, pp. 1001-1007, 2009.

[57] W. Gale, Y. Guan, "TLP bonding in the NiAl/Cu/Ni systems - A microstructural investigation," Metal and mater Trans, vol. 27, pp. 3621-3629, November 1996.

[58] G. Cock, C Sorensen "Overview of transient liquid phase and partial transient liquid phase bonding," Journal of materials science, vol. 46, no. 10, pp. 5305-5323, 2011.

[59] E. Lugscheider, S. Humm, "High temperature brazing of superalloys and stainless steels with novel ductile Ni-Hf based filler metals," Advanced engineering materials, vol. 4, no. 3, pp. 138-142, 2002.

[60] O.A Ojo, A. Ghoneim, J. Hunedy., "Transient liquid phase bonding of single crystal Ni3Al - based intermetallic alloy," 2012.

[61] Tuah - Poku, M. Dollar, T. Massalski., "A study of the Transient Liquid Phase Bonding Process Applied to a Ag/Cu/Ag Sandwiched Joint," Metall. Trans, vol. 19A, no. 3, pp. 675-686, 1988.

[62] J. Niemann, R. Garret, "Eutectic bonding of boron-aluminium structural components," Weld J, vol. 52, pp. 175-184, 1974.

[63] W. Gale, T. Eager, "Transient Liquid Phase Bonding Processes," Annual Review of Materials Science, vol. 22, no. 1, pp. 23-46, 1992.

[64] Y Nakao, K. Shinozaki, C. Kang., "Theoretical research on transient liquid insert metal diffusion bonding of nickel base alloys," Trans Jpn Weld Soc, vol. 20, 1996.

[65] S. Liu et al, Weld J, vol. 70, pp. 207s-215s, 1991.

[66] G. Lesoult, "Centre for joining of materials report," Pittsburgh, PA 1976.

[67] P. Danckwerts, "Gas-Liquid Reactions," McGraw-Hill, 1970.

[68] J. Ramirez, S. Liu., "Diffusion brazing in the Nickel-Boron system," Weld J, vol. 71, pp. 365s-375s, 1992.

[69] R. Sekerka, "Physical Metallurgy of Metals Joining," Met - Soc AIME, pp. 1-3, 1980.

[70] J. Jung, C. Kang., Mater Trans JIM, vol. 38, pp. 886-891, 1997.

[71] Z Li, Y. Zhou, T. North., "Canadian Association for Composite Structures and Materials," pp. 1017-1027, 1993.

[72] Y. Zhou, "Analytical Modeling of Isothermal Solidification during Transient Liquid Phase (TLP) Bonding," Journal of Materials Science, vol. 20, pp. 841-844, 2006.

[73] O. Ojo, "On an effective approach for reducing TLP bonding time in SX Superalloys," J Mater Sci, vol. 47, pp. 1598-1602, 2012.

[74] M. Nicholas, "Joining of ceramics," 1990.

[75] A.G Evans, M. Ruhle, M. Turwitt., J Physics, pp. 613-626, 1980.

[76] J.W Park, D.F Mendez, T.W Eager., Acta Mater society, pp. 883-899, 2002.

[77] R.L Williamson, B.H Rabin, J.T Drake., J. Application physics, vol. 74, no. 2, pp. 1310-1320, 1993.

[78] M. Shalz, B. Dalgleish, A. Tomisa, A. Gkeser., "Ceramic joining," Journals of materials science, vol. 28, no. 6, pp. 1673-1684.

[79] J. Liu, T. Jin, R. Zhao, Z. Wang, X. Sun, H. Guan., "Bonding behavior of nickel base single crystal to polycrystal superalloys by transient liquid phase method.," Science and technology of welding and joining, vol. 15, pp. 194-198, 2010.

[80] A. Ghoneim, O. Ojo., "Asymmetric diffusional solidification during transient liquid phase bonding of dissimilar materials," Met and mater transactions, vol. 43A, pp. 900-910, 2011.

[81] M. Pouranvari, A. Ekrami, A. Kokabi., "Microstructure-properties relationship of TLP bonded GTD-111 Ni base superalloy," Materials Science and Engineering, vol. 490, no. 1, pp. 229-234, 2008.

[82] N. Wikstrom, O. Ojo, M. Chaturvedi., "Influence of process parameters on microstructure of transient liquid phase bonded Inconel 738LC superalloy with AMDRY DF-3 Interlayer," vol. 417, no. 1-2, pp. 299-306, 2006.

[83] B. Klee, W. Song, D. Kim, I. Woo, C. Kang., "Effect of bonding temperatures on the transient liquid phase bonding of a directionally solidified Ni-based superalloy GTD-111," Metals and materials international, vol. 13, pp. 59-65, 2007.

[84] E. Lugscheider, V. Dietrich, J. Mittendorff., "Wide joint clearance brazing with nickel base filler metals," Welding Journal, vol. 67, pp. 15-17, 1986.

[85] Maher: Alloy 718 Data Sheet, http://www.maher.com/media/pdfs/718-datasheet.pdf.

[86] W Gale, Y. Xu, X. Wen, Z. Abdo., "Wide-gap transient liquid phase bonding of Ti-48 At. Pct. Al-2 At. Pct. Cr-2 At. Pct. Nb," Metallurgical and materials transactions, vol. 30A, pp. 2723-2726, October 1999.

[87] A Bigvand, O. Ojo., "On asymmetric diffusional solidification during TLP bonding," Metallurgical and Materials Transactions, pp. 1670-1674, 2014.

[88] A. Bigvand, "Numerical Simulation of Transient Liquid Phase Bonding Under Temperature Gradient," M.Sc. Thesis, 2013.

[89] M. Pouranvari, A. Ekrami, A. Kokabi., "Effect of bonding temperature during TLP bonding of a Nickel base superalloy," Journals of alloys and compounds, vol. 469, pp. 270-275, 2009.